AWARD NUMBER: W81XWH-12-1-0320

TITLE: “Cellular Basis for Learning Impairment in Fragile X Syndrome”

PRINCIPAL INVESTIGATOR: John R. Larson

CONTRACTING ORGANIZATION: University of Illinois at Chicago
Chicago, IL 60612

REPORT DATE: August 2014

TYPE OF REPORT: Annual

PREPARED FOR: U.S. Army Medical Research and Materiel Command
Fort Detrick, Maryland 21702-5012

REPORT DOCUMENTATION PAGE

Form Approved
OMB No. 0704-0188

1. REPORT DATE	2. REPORT TYPE	3. DATES COVERED
August 2014	Annual	1 Aug 2013 - 31 Jul 2014

4. TITLE AND SUBTITLE
Cellular Basis for Learning Impairment in Fragile X Syndrome

5a. CONTRACT NUMBER

5b. GRANT NUMBER
W81XWH-12-1-0320

5c. PROGRAM ELEMENT NUMBER

6. AUTHOR(S)
John Larson

E-Mail: jrlarson@uic.edu

5d. PROJECT NUMBER

5e. TASK NUMBER

5f. WORK UNIT NUMBER

7. PERFORMING ORGANIZATION NAME(S) AND ADDRESS(ES)
University of Illinois at Chicago
Chicago, IL 60612-4305

8. PERFORMING ORGANIZATION REPORT NUMBER

9. SPONSORING / MONITORING AGENCY NAME(S) AND ADDRESS(ES)

U.S. Army Medical Research and Materiel Command
Fort Detrick, Maryland 21702-5012

10. SPONSOR/MONITOR'S ACRONYM(S)

11. SPONSOR/MONITOR'S REPORT NUMBER(S)

12. DISTRIBUTION / AVAILABILITY STATEMENT

Approved for Public Release; Distribution Unlimited

13. SUPPLEMENTARY NOTES

14. ABSTRACT
This research combines behavioral, electrophysiological, and molecular approaches to elucidate the cellular basis for learning impairment in Fragile X Syndrome (FXS), using olfactory learning in Fmr1-KO mice as a model system. We hypothesize that FMRP, the protein missing in FXS, participates in two aspects of circuit function that are critical to learning: synaptic plasticity and the generation and survival of new neurons in the adult brain. Efforts in the second year of support were directed toward establishing a method to specifically upregulate neurogenesis in adult fragile X mice, test fragile X mice for learning deficits in hippocampal-independent tasks, and determine if learning affects NMDA receptor trafficking to synapses. Significant advances have been made in the establishment of behavioral paradigms to test both hippocampal -dependent and -independent forms of olfactory learning. Experimental paradigms have also been refined for the study of neurogenesis in the olfactory bulb, glutamate receptor expression as it relates to olfactory learning in olfactory cortex and hippocampus, and the effects of aging on glutamate receptor expression. These studies are likely to advance our understanding of intellectual disability and autism in addition to the specific condition of fragile X syndrome. This knowledge will be necessary for the development of rational strategies for prevention and treatment of cognitive impairments from a variety of causes.

15. SUBJECT TERMS
Fragile X Syndrome, synaptic plasticity, long-term potentiation, glutamate receptors, neurogenesis, olfactory learning

16. SECURITY CLASSIFICATION OF:			17. LIMITATION OF ABSTRACT	18. NUMBER OF PAGES	19a. NAME OF RESPONSIBLE PERSON
a. REPORT	b. ABSTRACT	c. THIS PAGE			USAMRMC
Unclassified	Unclassified	Unclassified	Unclassified	71	19b. TELEPHONE NUMBER *(include area code)*

Table of Contents

Page

INTRODUCTION

Fragile X syndrome is the most common inherited form of intellectual disability. The disorder is caused by mutation in the *FMR1* gene that transcriptionally silences the gene and results in lack of production of the encoded protein, FMRP. A mouse model of the human syndrome (the *Fmr1*-KO mouse) reproduces the protein (FMRP) deficiency and exhibits abnormalities of synaptic structure and function as well as learning impairments. This research combines behavioral, electrophysiological, and molecular approaches to elucidate the cellular basis for learning impairment in *Fmr1*-KO mice using olfactory learning as a model system. We hypothesize that FMRP, the protein missing in FXS, participates in two aspects of circuit function that are critical to learning: synaptic plasticity and the generation and survival of new neurons in the adult brain (neurogenesis). First, we use molecular tools to study the cellular basis for neurogenesis deficits in adult *Fmr1*-KO mice and the signaling pathways by which FMRP regulates neurogenesis in both the olfactory bulb and the hippocampus of the adult brain. We test the hypothesis that selective down-regulation of the pro-apoptotic gene, *Bax*, in neurogenic niches will reverse neurogenic deficits in *Fmr1*-KO mice. Second, electrophysiological, biochemical, and pharmacological methods are used to characterize synaptic dysfunction in the olfactory-hippocampal circuit in *Fmr1*-KO mice. We hypothesize that absence of FMRP disrupts trafficking of NMDA receptors to synapses, resulting in impairments in NMDA-dependent synaptic plasticity mechanisms such as long-term potentiation (LTP). Third, using behavioral analyses, we attempt to determine the contributions of neurogenic and synaptic dysfunction to learning impairments in *Fmr1*-KO mice. Finally, we test the hypothesis that impaired neurogenesis underlies the learning impairment in *Fmr1*-KO mice by experimentally stimulating neurogenesis in the mice. In summary, this project will exploit the advantages of the olfactory system to study the cellular basis for learning impairment in a mouse model for fragile X syndrome. This is likely to also have impact on our understanding of developmental intellectual disability syndromes in general as well as learning impairments in other autism spectrum disorders. This knowledge will be necessary for the development of rational strategies for prevention and treatment of cognitive impairments from a variety of causes.

BODY (OVERALL PROJECT SUMMARY)
Cellular Basis for Learning Impairment in Fragile X Syndrome

Recruitment of research staff: Ms. Patricia Dykas, research assistant. Ms. Dykas was recruited from UIC with a BS with a B.S. in Biological Sciences. She will be completing the behavioral studies of Specific Aims 2 and 3 (re: SOW tasks 4a, 4b, 4c). She is also responsible for genotyping all *Fmr1*-KO mice in the colony.

1) Is olfactory bulb neurogenesis impaired in *Fmr1*-KO mice? (SOW task 2a)
Adult neurogenesis occurs in two areas of the mammalian brain: (i) the subgranular layer (SGL) of the dentate gyrus of the hippocampal formation produces excitatory, glutamatergic granule neurons incorporated into the dentate gyrus and (ii) the subventricular zone (SVZ) produces inhibitory, GABAergic granule and periglomerular cells incorporated into the olfactory bulb. Both of these areas have prominent roles in olfactory learning. We already showed, using molecular markers for dividing cells as well as immature and mature neurons, that proliferation and survival of adult-generated neurons are suppressed in the Fmr1-KO mouse brain, resulting in fewer mature granule cells in the dentate gyrus of one year-old mice (Lazarov et al., 2011). In the past year, we have begun to examine these processes in the SVZ and olfactory bulb. To examine the proliferation history and cell fate of neural progenitor cells (NPCs) in the SVZ of *Fmr1-KO* and *WT* mice, mice were injected with the thymidine analog, bromodeoxyuridine (BrdU) twice a day for three days, one month before sacrifice. Brain sections were processed for immunohistochemistry to identify proliferating cells (labeled with BrdU), immature neurons, mature neurons, and astrocytes. Proliferating cells in an early stage of neuronal differentiation were identified in the subventricular zone (SVZ) and olfactory bulb (OB) using antibodies raised against the early neuronal marker, doublecortin (DCX). For the identification of glia we used antibodies raised against glial fibrillary acidic protein (GFAP). Our preliminary data shows that the number of neuroblasts (DCX+) as well as the number of astrocytes (GFAP+) were not statistically different between *Fmr1*-KO and WT mice (please see **APPENDIX Figure 1**). Ongoing studies are aimed at confirming these preliminary results and determining if any of these processes are differentially affected by age in *Fmr1*-KO mice. In addition, ongoing experiments are aimed at determining the rate of survival of new neurons, their migratory pathway, and functional integration in the olfactory bulb of these mice.

2) Restoration of neurogenesis in *Fmr1*-KO mice by selective down-regulation of Bax in neurogenic niches (SOW task 2c).
It is not clear whether stimulation of neurogenesis is sufficient for the amelioration of cognitive deficits in Fragile X syndrome, and whether enhanced neurogenesis has therapeutic value for these cognitive deficits. In our experimental plan we proposed to use lentiviral vectors to knockdown Bax and enhance neurogenesis. We decided to take a much more advanced and reliable genetic approach (Sahay et al., 2011) by using NestinCreER$^{T2/+}$/Bax$^{f/+}$ mice (obtained from Dr. Rene Hen, Columbia University). This genetic gain-of-function system is based on the observation that 60-80% of young adult-born neurons undergo programmed cell death, for which *Bax* is required (Sun et al., 2004). This approach results in a 2.5-3 fold increase in the number of neuroblasts and immature neurons five weeks after tamoxifen treatment (*Bax* deletion) (Sahay et al., 2011). Preliminary studies conducted in the past year demonstrate that this approach is feasible in our laboratories (please see **APPENDIX Figure 2**) and will be used to generate *Fmr1*-KO mice in which we can selectively stimulate neurogenesis with cell-type specificity and precise temporal control. Preliminary studies also show that mice with stimulated neurogenesis using this approach have enhanced learning and memory function (please see **APPENDIX Figure 3**). Taken together, these results suggest that enhancement of

neurogenesis in mice with cognitive deficits may rescue these deficits. To achieve gain of neurogenic function in *Fmr1-KO* mice, ongoing experiments are following the breeding regimen described above. Specifically *Fmr1*-KO mice are bred with $Bax^{lox/lox}$ followed by breeding of $Bax^{lox/+}$/*Fmr1-KO* mice and NestinCreER$^{T2/+}$/$Bax^{lox/lox}$ to achieve *Fmr1-KO*/nestinCreER$^{T2/+}$/ $Bax^{lox/lox}$ mice.

3) Comparison of synaptic plasticity (LTP) in different components of the olfactory-hippocampal circuit in *Fmr1*-KO and WT mice (re: SOW task 3b).

Since there is increasing evidence that deficits in LTP may only appear in fragile X mice when stimulation conditions do not produce a saturation of synaptic potentiation (Lauterborn et al., 2007; Seese et al., 2014), we have been exploring optimal conditions to use in the different components of the olfactory-hippocampal circuit (piriform cortex, entorhinal cortex, dentate gyrus, CA3, and CA1). A robust deficit in hippocampal LTP in *Fmr1*-KO mice will also be necessary to test for rescue of LTP after stimulation of neurogenesis in *Fmr1*-KO mice (SOW task 3c). One experiment has been completed. In this, we compared a stimulation pattern that produces maximal LTP – theta-burst stimulation (10 high frequency bursts of 4 pulse each at 100 Hz, repeated at 5 Hz) with a submaximal pattern (10 bursts repeated at 1 Hz) on LTP in the final stage of the circuit, field CA1. In WT slices, 5 Hz bursts produced a stable LTP effect of about 30-35%. Similar results were obtained in slices from *Fmr1*-KO mice. We also tested 1 Hz bursts in the same slices and found that submaximal LTP was induced in WT slices (10-15%). Somewhat larger effects were induced in slices from *Fmr1*-KO mice, but the difference between WT and KO mice was not statistically significant (please see **APPENDIX Figure 4**). We are now trying other variations, notably reducing the number of pulses per burst, to further test the idea that LTP may be reduced in hippocampus of *Fmr1*-KO mice.

4) Comparison of olfactory learning in *Fmr1*-KO and WT mice in a successive-cue olfactory discrimination task (re: SOW task 4b).

Experiment 4b calls for the testing of *Fmr1*-KO and WT control mice in a non-hippocampal dependent olfactory discrimination task. We ran several pilot experiments during the first year of this project to optimize a successive-cue discrimination paradigm to compare learning rates in mutant and control mice. The best paradigm (tested with C57Bl/6J control mice) used a series of eight separate odor discrimination problems as follows: Mice (3 months old) were trained on each discrimination problem in 100-trial sessions in which each trial involved presentation of one of the discriminative odors to both sniff ports in our standard discrimination chamber. Each trial was signaled by the extinguishing of a lamp and the presentation of the odor for 5 sec. A nose poke in either port within the 5 sec presentation period constituted a “GO” response; no response in the same period constituted a “NO-GO” response. GO responses to the positive cue (S+) or NO-GO responses to the negative cue (S-) are scored as correct; GO responses to S- or NO-GO responses to S+ are scored as errors. Only Go responses to S+ are rewarded with a drop (.01 ml) of water. The inter-trial interval (ITI) after correct responses was 10 sec and the ITI after errors was 30 sec. In the second year of this award, we tested a cohort of Fmr1-KO and WT littermates at 6-12 months of age on this task. Each mouse was trained to criterion performance of eight consecutive correct responses within a single 100-trial training session. Note that, since no more than three S+ or S- trials can occur consecutively, this criterion requires the mouse to respond correctly to at least two S+ trials and at least two S- trials within the sequence of eight consecutive correct responses. The probability of 8 consecutive correct responses by chance is 1/256 or ~0.4%.) Sessions were repeated on subsequent days if criterion performance was not met.

The main finding was that *Fmr1*-KO mice made significantly more errors while learning the first two-odor discrimination problem. Since other evidence indicates that this successive-

cue olfactory discrimination task does not require participation of the hippocampus, the new results suggest that the learning deficit may be due to impaired synaptic plasticity in the olfactory cortex or defective neurogenesis in the olfactory bulb (SOW task 4c).

These results were presented at the 2014 Annual Meeting of the Society for Neuroscience (please see **APPENDIX 1**) and a manuscript is in preparation for publication (please see **APPENDIX 2**).

5) Comparison of learning rates at different ages in *Fmr1*-KO and WT mice (SOW task 4a). The experiment described immediately above (Section 4) will be repeated in mice ranging in age from 3 to 24 months. Preliminary findings related to this aim were obtained from the animals already tested at 5-12 months of age (please see *Figure 6* of **APPENDIX 2**). In the data collected so far, there is a trend of poorer performance in *Fmr1*-KO mice as they get older; no such trend was evident in the WT mice. If this trend is confirmed, it would strongly suggest that the learning impairment is due to LTP impairment in piriform cortex, since the LTP impairment also does not appear until six months of age (Larson et al., 2005).

6) Analysis of glutamate receptors in olfactory cortex: changes with olfactory discrimination learning (re: SOW task 3a).
The goal of experiments in 3a is to understand how FMRP participates in the trafficking of glutamate (NMDA and AMPA) receptors to synapses in hippocampus and olfactory cortex. We have obtained evidence that olfactory discrimination training selectively stimulates NMDA receptor (GluN1) expression in hippocampus of WT mice. The experiments were run by undergraduate research assistant, Jennifer Sotto and medical student, Allison Kirchner, in collaboration with Drs. Neil Smalheiser and Giovanni Lugli. Mice were trained to criterion (70% correct in a block of 20 trials) on each of four different two-odor discriminations in the simultaneous-cue discrimination task. Samples from olfactory bulb, olfactory cortex, hippocampus, and motor cortex were analyzed for AMPA receptor (GluA1) and NMDA receptor (GluN1) expression by Western blot. Three separate sets of controls were run: (a) home cage (HC) controls were never trained at all; (b) nose poke (NP) controls were trained to nose poke in the same chamber but were not exposed to odors; (c) odor exposed controls (pseudo-trained, PT) were trained to nose poke with the same odors presented as in the discrimination-trained mice, but the odors had no reward significance. The preliminary data (please see **APPENDIX Figure 5**) indicate that odor discrimination training resulted in higher expression of GluN1, but not GluA1 (AMPA-type glutamate receptor), in hippocampus. Analysis of variance yielded a significant effect of group on NMDA receptor expression ($\mathbf{F}_{3,21}$=3.11, p<.05). We are currently attempting to replicate these results in a larger cohort of mice. If the NMDA receptor results are confirmed, it may provide an exciting new way to assess the role of FMRP in regulation of expression and trafficking of NMDA receptors to synapses, particularly when animals are challenged with new learning.

KEY RESEARCH ACCOMPLISHMENTS

- Quantified neuroblasts and astrocytes in the subventricular zone of adult *Fmr1*-KO and WT mice and obtained evidence that neurogenesis is unimpaired in the olfactory bulb of adult *Fmr1*-KO mice.
- Obtained mice in which Bax can be conditionally knocked out in nestin+ cells and showed that conditional ablation of Bax in nestin+ cells of mice with cognitive deficits can rescue learning.
- Obtained further evidence that LTP is selectively impaired in the piriform cortex segment of the olfactory-hippocampal circuit of *Fmr1*-KO mice.
- Demonstrated that *Fmr1*-KO mice are impaired on a hippocampus-independent olfactory learning task.
- Obtained preliminary evidence that olfactory learning impairments in *Fmr1*-KO mice are age-dependent.
- Obtained evidence that NMDA receptor expression is enhanced in hippocampus of mice after extensive olfactory learning.

REPORTABLE OUTCOMES

Publications

1. Gocel, J. & Larson, J. Evidence for loss of synaptic AMPA receptors in anterior piriform cortex of aged mice. *Frontiers in Aging Neuroscience,* **5** (2013) Article 39. (**APPENDIX 3**)
2. Larson, J., Drew, K.L., Folkow, L.P., Milton, S.L., & Park, T.J. No oxygen? No problem! Intrinsic brain tolerance to hypoxia in vertebrates. *Journal of Experimental Biology*, **217** (2014) 1024-1039. (**APPENDIX 4**)
3. Larson, J. Munkácsy, E. Theta-Burst LTP. *Brain Research* (in press). (**APPENDIX 5**)

Abstracts

1. Keil, S.A. & Larson, J. Impaired olfactory discrimination learning in fragile X knockout mice. *Abstracts, Society for Neuroscience* (2014) Program no. 699.10. (**APPENDIX 1**)

Manuscripts

1. Keil, S.A. & Larson, J. Impaired olfactory discrimination learning in fragile X knockout mice. Manuscript in preparation (**APPENDIX 2**)

Degrees obtained with support from this award

1. Patricia Dykas, B.S., with Distinction in Biological Sciences, University of Illinois at Chicago (2014).

Research Opportunities supported by this award

1. Samantha Keil, B.S. was accepted into the UIC Graduate Program in Neuroscience, in part because of research experience obtained working on this project (2013-2014).
2. Tiffany Cheng, UIC undergraduate student, is assisting with the behavioral studies of *Fmr1*-KO mice.

CONCLUSION

Efforts in the second year of support were mainly directed toward the behavioral studies of Specific Aim 3 (SOW tasks 4a and 4b) and establishing a new approach to specifically enhance neurogenesis in Fmr1-KO mice (SOW task 2c). Significant advances have been made in the establishment of behavioral paradigms to test both hippocampal -dependent and -independent forms of olfactory learning. This is important because the electrophysiological impairments of synaptic plasticity that we have observed in the fragile X mouse model occur in olfactory cortex but not hippocampus. We will focus major effort in the coming year (year 3) on the electrophysiological studies of Specific Aim 2 (SOW tasks 3b and 3c) and behavioral studies of Specific Aim 3 (SOW task 4c). Experimental paradigms have also been refined for the study of glutamate receptor expression as it relates to olfactory learning in olfactory cortex and hippocampus. These studies will allow us to establish a cellular basis for certain aspects of the cognitive disability that characterizes the human fragile X syndrome.

REFERENCES

Larson, J., Jessen, R.E., Kim, D., Fine, A.K., and du Hoffmann, J. (2005). Age-dependent and selective impairment of long-term potentiation in the anterior piriform cortex of mice lacking the fragile X mental retardation protein. JNeurosci *25*, 9460-9469.

Lauterborn, J.C., Rex, C.S., Kramar, E., Chen, L.Y., Pandyarajan, V., Lynch, G., and Gall, C.M. (2007). Brain-derived neurotrophic factor rescues synaptic plasticity in a mouse model of fragile X syndrome. J Neurosci *27*, 10685-10694.

Lazarov, O., Demars, M.P., Da Tommy Zhao, K., Ali, H.M., Grauzas, V., Kney, A., and Larson, J. (2011). Impaired survival of neural progenitor cells in dentate gyrus of adult mice lacking FMRP. Hippocampus.

Sahay, A., Scobie, K.N., Hill, A.S., O'Carroll, C.M., Kheirbek, M.A., Burghardt, N.S., Fenton, A.A., Dranovsky, A., and Hen, R. (2011). Increasing adult hippocampal neurogenesis is sufficient to improve pattern separation. Nature *472*, 466-470.

Seese, R.R., Wang, K., Yao, Y.Q., Lynch, G., and Gall, C.M. (2014). Spaced training rescues memory and ERK1/2 signaling in fragile X syndrome model mice. Proc Natl Acad Sci U S A *111*, 16907-16912.

Sun, W., Winseck, A., Vinsant, S., Park, O.H., Kim, H., and Oppenheim, R.W. (2004). Programmed cell death of adult-generated hippocampal neurons is mediated by the proapoptotic gene Bax. J Neurosci *24*, 11205-11213.

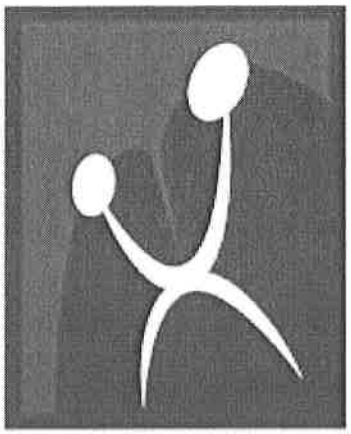

NEUROSCIENCE
2014

Control/Tracking Number: 2014-S-15494-SfN
Activity: Scientific Abstract
Current Date/Time: 5/8/2014 3:32:26 PM

Impaired olfactory discrimination learning in Fragile X knockout mice

AUTHOR BLOCK: S. A. KEIL[1], *J. R. LARSON[2];
[1]Grad. Program in Neurosci., [2]Dept Psychiat, Univ. Illinois Chicago, CHICAGO, IL

Abstract:
Fragile X Syndrome (FXS), caused by mutation of the FMR1 gene, is the leading cause of inherited intellectual disability and is known to cause cognitive impairment, hyperactivity, attention deficits and seizure disorders. Previous studies using a mouse model for FXS (Fmr1-KO) have described impairments in acquisition of simultaneous-cue olfactory discriminations and a specific deficit in LTP in primary olfactory cortex. The present study tested for impaired olfactory discrimination learning in fragile X mice, using a hippocampus-independent successive-cue training procedure.
Male Fmr1-KO and WT littermate mice (C57Bl/6J background; 5-12 months old) were trained to criterion (8 consecutive correct responses) in a fully-automated, successive-cue, go/no-go, two-odor discrimination task. Each mouse was trained in 100-trial sessions on eight separate discrimination problems. Each trial consisted of the presentation of one of two discriminative odors. The eight discrimination problems were presented to half of the mice in each group (randomly chosen) in one order, and in reverse order for the other half. Mice were run blind with respect to genotype.
Fmr1-KO mice made significantly more errors than WT littermates before acquiring the first discrimination problem. Both WT and Fmr1-KO mice made fewer errors on the remaining discrimination problems and did not differ in this regard. Combined with previous work, the present study indicates that Fmr1-KO mice show similar impairments in learning olfactory discriminations, regardless of whether the discriminative cues are present together (simultaneous-cue task) or separately (successive-cue task) on individual trials. Both paradigms depend on the integrity of piriform cortex but are differentially affected by hippocampal damage. This suggests that the impaired learning in Fmr1-KO mice may be a result of LTP impairments in the primary olfactory (piriform) cortex.

Presentation Preference (Complete): Poster Only
Linking Group (Complete): None selected
Nanosymposium Information (Complete):
Theme and Topic (Complete): C.06.g. Fragile X; F.02.k. Learning and memory: Cortical and hippocampal circuits
Keyword (Complete): HIPPOCAMPUS ; FMRP ; piriform cortex
Support (Complete):
Support: Yes
Grant/Other Support: : US Army MRMC #10917352

Special Requests (Complete):
Would you be interested in being considered for a dynamic poster?: No, I am not interested in presenting a Dynamic Poster

Is the first (presenting) author of this abstract a high school or undergraduate student?: None

Religious Conflict?: No Religious Conflict
Additional Conflict?: No

Status: Finalized

APPENDIX 2

Impaired olfactory discrimination learning in Fragile X knockout mice

(DRAFT: manuscript in preparation)

Samantha Keil and John Larson

Psychiatric Institute
Department of Psychiatry
College of Medicine
Graduate Program in Neuroscience
University of Illinois at Chicago
Chicago, Illinois

This work was supported by the Office of the Assistant Secretary of Defense for Health Affairs, through the Peer Reviewed Medical Research Program under Award No. W81XWH-12-1-0320. Opinions, interpretations, conclusions and recommendations are those of the author and are not necessarily endorsed by the Department of Defense.

INTRODUCTION

Fragile X Syndrome (FXS), due to mutation of the *FMR1* gene, is the leading cause of inherited intellectual disability and results in cognitive impairment, hyperactivity, attention deficits, seizure disorders, and autistic features (Bhakar et al., 2012). Neurobiological studies using mouse models of FXS (*Fmr1*-KO mice) have focused on synaptic function, development, and plasticity, since synaptic communication is critical for the cognitive functions affected in the human disorder. Many studies have now identified synaptic plasticity deficits involving both long-term potentiation (LTP) (Larson et al., 2005; Lauterborn et al., 2007; Li et al., 2002; Wilson and Cox, 2007; Zhao et al., 2005) and long-term depression (LTD) (Hou et al., 2006; Huber et al., 2002) in hippocampus and other cortical regions in *Fmr1*-KO mice. However, the molecular mechanisms responsible for these plasticity deficits in mice lacking FMRP are not well understood.

Directly relating cellular dysfunction to cognitive impairments is challenging in mouse models. Olfactory learning has a number of advantages for this type of work. First, the earliest neural processing stages of the olfactory system occur in forebrain networks that are directly connected to systems critical for human cognition, including the hippocampus, amygdala, and prefrontal cortex. Second, the first two stages of the olfactory system, the olfactory bulb and olfactory cortex are telencephalic structures with stratified cell layers and laminated input systems that greatly facilitate electrophysiological studies of synaptic function and plasticity. Third, sophisticated behavioral paradigms (Slotnick, 2001) have exploited the natural tendency of mice to attend to odor cues and demonstrated features of olfactory learning that resemble the human declarative memory system.

Our first behavioral studies used a simultaneous-cue, two-odor, olfactory discrimination task that depends on the integrity of both piriform cortex and hippocampus for optimal learning. In two independent experiments, *Fmr1*-KO mice showed significant impairment of learning rate compared to WT littermate controls (Larson et al., 2008). The deficit was specific for *acquisition* of odor-reward associations since long-term memory for acquired odor-reward associations was unaffected. Tests of olfactory sensory thresholds did not distinguish *Fmr1*-KO mice from WT controls, suggesting that the learning deficit was not simply a failure of odor detection.

Comparisons of LTP induced by theta burst stimulation (TBS), a paradigm that mimics cellular activity in the olfactory-hippocampal circuit during odor sampling behavior (Larson and Munkacsy, in press) were made in anterior piriform cortex (APC) slices prepared from WT and *Fmr1*-KO mice at ages ranging from three to eighteen months (Larson et al., 2005). Input-output curves for ASSN synapses did not reveal any differences in AMPA receptor-mediated basal excitatory synaptic transmission between *Fmr1*-KO and WT mice. In slices from mice 6-18 months old, TBS-induced LTP decayed more rapidly in the *Fmr1*-KO mice than in their age-matched WT controls. The impairment of APC LTP in *Fmr1*-KO mice was age-dependent and progressive: potentiation was normal in mice aged 3-6 months, failed to stabilize in mice aged 6-12 months, and was reduced at all post-TBS time points in 12-18 month-old mice. Given the age-dependence of the LTP deficit in APC, we examined LTP in hippocampal field CA1 from *Fmr1*-KO and littermate WT mice at ages ranging from three to twelve months. LTP was unaffected in *Fmr1*-KO mice at all ages (Larson et al., 2005).

In order to determine if the olfactory learning deficits in *Fmr1*-KO mice are due to impaired LTP in olfactory (piriform) cortex or to disturbance in hippocampal function, the present experiments were designed to assess learning in an olfactory-guided task that depends on

piriform cortex function but does not depend on hippocampal function. A successive-cue, two-odor discrimination task, in which only one discriminative cue is present on each trial and the mouse is required to respond (GO) when the 'positive' cue is present, but not respond (NO GO) when the negative cue is present, is such a task (Eichenbaum et al., 1988). Therefore, we assessed acquisition of a series of two-odor discriminations in *Fmr1*-KO and WT littermates in the successive-cue task.

METHODS

Subjects

Ten male *Fmr1*-KO and ten WT littermate mice (C57BI/6J background; 5-12 months old) were tested. Mice were bred on-site from stock obtained from Jackson Labs (Bar Harbor, ME) and housed in a climate controlled animal colony with a normal 14:10 light-dark cycle. They were maintained on a water deprivation schedule with access to 0.5-2.0mL of water once per day for a week prior to and throughout training. This schedule reduced and sustained the subjects' body weight at 80% of the ad libitum levels. Behavioral experimentation was performed during the light stage.

Apparatus

Four behavior testing chambers were made from black acrylic as described previously (Larson and Sieprawska, 2002). Chambers were constructed with 60 X 10 X 30 cm panels; side panels were set 15º off vertical along the length and vertically at each end. A single small cup in the floor on both the "East" and "West" ends functioned for a water delivery system. Similarly, two cylindrical "sniff ports" at both the East and West end enabled recording of nose poke responses. The sniff ports on the West end were connected to individual air-dilution olfactometers for odor stimulus delivery (Patel and Larson, 2009). Custom software activated and controlled odor and water delivery as well as recording infrared photo beam breaks.

Odor Pairs

Eight odor pairs were utilized throughout experimentation. Odorant was dissolved in a solvent of ddH_2O, propylene glycol or mineral oil. One odor from each pair was randomly chosen as the positive stimulus.

Discrimination	Odor Pair
1	16+ (Banana) / 14- (Strawberry)
2	101+ (Hexyl octanoate) / 102- (Propionic acid)
3	23+ (Root Beer) / 22- (Almond)
4	98+ (Methyl salicylate) / 97- (Ethyl lactate)
5	18+ (Cherry) / 30- (Lemon)
6	107+ (Terpinyl acetate)/ 106- (Anisole)
7	20+ (Vanilla) / 25- (Butter)
8	29+ (Maple) / 17- (Coconut)

Procedure

Shaping

The procedure consisted of daily 40-trial sessions, with 10µL water reinforcement for a nose poke to the sniff port on either end of the chamber. A lamp at each end of the alley was lit

during the inter-trial interval (ITI) and was extinguished over the ports at which the reinforcement was available during the trials. Each trial was a maximum of 120 seconds long, with a 10sec ITI. Mice were required to traverse the chamber repeatedly, as sequential reinforcement was received for a nose poke at the end of the alley opposite the last correct response. Mice were trained to criterion of three sessions in which 90% of the last 20 trials were correct before beginning odor discrimination.

Odor Discrimination

The mice were presented with eight distinct two-odor discrimination problems in 100-trial sessions. Each trial involved presentation of one discriminative odor. Trials were signaled by extinguishing of a lamp and the presentation of the odor for 5 seconds. A nose poke to either port within the presentation period constituted a "GO" response; no response in the same period constituted a "NO-GO" response. GO responses to the positive cue (S+) or NO-GO responses to the negative cue (S-) were scored as correct. Similarly, GO responses to S- or NO-GO responses to S+ were scored as errors. Only GO responses to S+ were rewarded water. The mice were trained to criterion performance of eight consecutive correct responses within a single 100-trial training session, for each of the eight discrimination problems. The eight discrimination problems were presented to half of the mice in each group (randomly chosen) in one order, and in reverse order for the other half.

Memory Retention

The mice were tested on memory retention of their fifth odor discrimination problem. Memory retention was tested after all mice had completed each of the eight odor discriminations and at least one week after finishing this particular odor pair.

Partial Reinforcement

The last odor pair of the original eight discriminations was used. Each mouse was "retrained" to criterion for these odors with a 1:1 reward to response ratio. Once meeting criterion, reward response was changed to 1:2, and 1:4 respectively.

Binary Odor Mixture Discrimination

Two pure chemical odorants, eucalyptol (odor A) and heptanol (odor B), were chosen for mixture discrimination based on previously tested glomerular activation patterns (Johnson and Leon, 2007). Mice were first trained to discriminate the pure odors, i.e., 100% odor A vs. 100% odor B. Whether odor A or B was the rewarded cue (S+) was counter-balanced across mice within each genotype. After reaching learning criterion, mice were trained to discriminate a mixture of 80% A and 20% B from a mixture of 20% A and 80% B. After learning the 80/20 mixture discrimination mice were trained to discriminate mixtures in which there was substantially more overlap between the discriminanda, i.e., 60% A and 40% B vs. 40% A and 60% B (60/40 mixture discrimination).

RESULTS AND DISCUSSION

Odor Discrimination Learning

All mice were trained to a strict behavioral criterion (eight consecutive correct trials) on each of eight two-odor discrimination problems. Fragile X KO mice learned the first discrimination problem more slowly than did WT mice. *Fmr1*-KO mice (n=10) required more trials to reach criterion in the first discrimination than did wild type (n=10) littermates (Figure 1A); however this effect only approached statistical significance (t_{18} = 1.95, p = .07). Total errors for the first discrimination problem (Fig. 1B) were significantly different between WT and KO mice (t_{18} = 2.13, p<.05). Errors were classified as misses or false alarms. The number of misses (Fig. 1C) was significantly higher in *Fmr1*-KO than in WT mice (t_{18} = 2.38, p<.05) but the number of false alarms (Fig. 1D) did not differ (t_{18} = 1.13, p>.25). The average number of errors made during acquisition of all eight discrimination problems in WT and KO mice are shown in Fig. 2. Two-way, repeated measures analysis of variance showed a significant main effect of genotype ($\mathbf{F}_{1,18}$ = 5.94, p<.05) as well as a significant main effect of problem number ($\mathbf{F}_{7,126}$ = 27.57, p<.0001), but no significant interaction between genotype and problem number ($\mathbf{F}_{7,126}$ = 2.04, p>.05). Multiple comparisons tests using the Newman-Keuls method showed that KO mice made significantly more errors (p<.01) before reaching learning criterion only on the first discrimination problem. Both WT and *Fmr1*-KO mice achieved criterion performance on the remaining discrimination problems in fewer trials and with fewer errors, and did not differ in this regard.

These results indicate that *Fmr1*-KO mice are impaired in acquisition of a novel odor discrimination task that does not require normal hippocampal function. The improvement in odor discrimination learning rate across multiple discrimination problems, known as learning set acquisition (Larson and Sieprawska, 2002; Slotnick and Katz, 1974), appeared to be unaffected in *Fmr1*-KO mice. This was also the pattern of results seen in *Fmr1*-KO mice trained using a hippocampal-dependent simultaneous-cue discrimination task (Larson et al., 2008). Together, these results suggest that the learning impairment in *Fmr1*-KO mice may be due to dysfunction in piriform cortex, perhaps because of an LTP impairment (Larson et al., 2005) and/or deficiency of NMDA receptors (Gocel and Larson, 2012).

Memory Retention

The mice were tested on memory retention of the fifth odor discrimination problem, after having learned three additional problems, and at least one week after the last training session for discrimination five. The retention test consisted of a training session with the same odors as in discrimination five, but with the significance (valences) of the odors reversed. If the mice remember the initial significance of the cues, reversal learning should require more trials than the initial learning. As shown in Figure 3, both WT and KO mice required many more trials to meet learning criterion (8 consecutive correct trials) during cue reversal than during initial learning. A difference score was computed for each mouse by subtracting the trials required for initial learning from the trials required for reversal learning, to provide an estimate of the strength of memory for the initial cue valences. WT and KO mice did not differ in memory strength (t_{18} = 1.40, p>.15).

Together with those of the previous study (Larson et al., 2008), these results indicate that *Fmr1*-KO show normal long-term memory for the significance of olfactory cues, provided that they are trained long enough to establish high rates of discriminative responding during training.

Partial Reinforcement

In an effort to test whether or not *Fmr1*-KO mice may be more or less prone to extinction relative to WT mice, both groups were trained using partial reinforcement schedules. After the memory retention test, all mice were retrained to criterion on discrimination eight. As in all previous training, water reinforcement was given after every correct trial (i.e., a fixed ratio 1 reinforcement schedule). After reaching criterion at FR1, the mice were retrained to criterion with a FR2 reinforcement schedule in effect. After criterion was made, mice were trained again with a FR4 (i.e., reinforcement after every fourth correct trial) schedule. The results are shown in Figure 4. Retraining at FR1 and FR2 required about the same number of trials; however, switching to FR4 resulted in increased errors and an increase in trials needed to reach criterion performance. Nevertheless, there were no significant differences in the response of WT and KO mice to partial reinforcement. Two-way, repeated measures ANOVA yielded no significant genotype ($\mathbf{F}_{1,18} = 0.92$, $p>.30$) or reinforcement ratio ($\mathbf{F}_{2,36} = 1.03$, $p>.35$) main effect nor an interaction ($\mathbf{F}_{2,36} = 0.60$, $p>.55$). Since there was a large variance in the data for FR4, due to a few extreme values, a non-parametric test was conducted on these data alone; however, this test was insignificant as well (Mann-Whitney U-test, $p>.05$).

These results suggest that *Fmr1*-KO mice do not differ from WT mice in reponse to changes in cue-reward contingencies.

Binary Odor Mixture Discrimination

Discriminating mixtures of odorants containing overlapping common elements can be a particularly challenging task for the olfactory system (Abraham et al., 2004). In animals that have already been extensively trained using odor cues, discrimination of binary mixtures represents a sensitive test of sensory ability rather than a test of learning *per se*. The same *Fmr1*-KO and WT mice were tested for discrimination of two odors that each contain the same mono-molecular odors in different proportions. Mice were first trained to discriminate the pure odors from each other, that is, to discriminate eucalyptol from heptanol. The mice were then trained to discriminate an 80%/20% mixture (eucalyptol/heptanol) from a 20%/80% mixture of the same two monomolecular odors. Mice were then trained to discriminate 60%/40% mixtures of the two odors. The results are displayed in Figure 5. There was no significant effect of genotype across modes ($\mathbf{F}_{1,18} = 0.56$, $p>.45$) or interaction between genotype and mode ($\mathbf{F}_{2,36} = 0.00$, $p>.95$). There was a highly significant main effect of mode ($\mathbf{F}_{2,36} = 13.58$, $p<.0001$), reflecting the fact that the 60/40 mixture was learned faster than either the pure two-odor discrimination or the 80/20 mixture discrimination.

These results do not support a sensory deficit interpretation of the impairment in odor discrimination learning, at least for well-trained mice. Both *Fmr1*-KO mice seemed to treat the 80/20 mixture as a novel discrimination, requiring about as many trials to reach criterion performance on the 80/20 mixture as for the pure odors. The 60/40 discrimination required many fewer trails to reach criterion performance, as if the significance of the discriminative odors had already been learned.

Effects of Age on Learning of Discrimination Problem One

The mice tested in these experiments were between 5.5 and 11.5 months old at the outset of training. Since the only significant learning impairment in *Fmr1*-KO mice was on the first discrimination problem, we examined the number of errors on this problem as a function of age

(Fig. 6). WT mice at different ages showed no obvious trends in error scores across ages. However, the KO mice showed increases in error scores as age increased. Although the sample sizes are too small for these trends to be statistically significant, if confirmed they would suggest that the age-dependent LTP impairment in these mice may play an important role in the initial learning deficit.

CONCLUSIONS

Combined with previous work, the present study indicates that *Fmr1*-KO mice show similar impairments in learning olfactory discriminations, regardless of whether the discriminative cues are present together (simultaneous-cue task) or separately (successive-cue task) on individual trials. Both paradigms depend on the integrity of the piriform cortex but are differentially affected by hippocampal damage. This suggests that the impaired learning in *Fmr1*-KO mice may be a result of LTP impairments in the primary olfactory (piriform) cortex. Learning set formation (Larson and Sieprawska, 2002; Slotnick, 2001) or "rule learning" (Quinlan et al., 2004) appears to be unaffected in *Fmr1*-KO mice trained in either paradigm. Long-term memory for the significance of odors also appears to be normal in *Fmr1*-KO mice. Finally, we obtained no evidence that the ability to detect odors (Larson et al., 2008) or to process odor mixtures is impaired in the *Fmr1*-KO mice, suggesting that the learning deficit is not sensory in nature. An extensive study of the effect of age on olfactory learning will be necessary to determine if this learning impairment is due to a deficiency of NMDA receptors in piriform cortex or to possibly related disturbances in synaptic plasticity such as LTP at synapses in this structure.

Figure 1

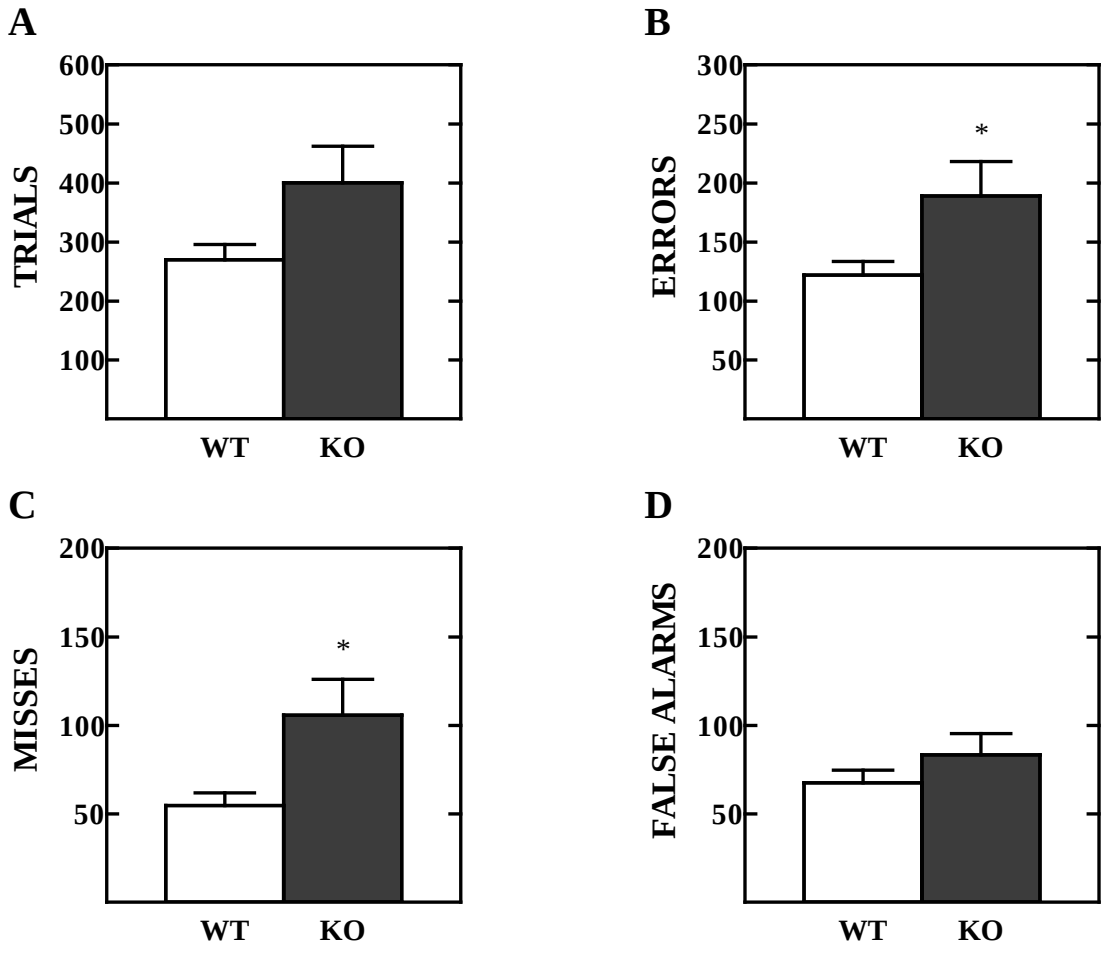

Figure 1. *Fmr1*-KO mice show impaired learning of an appetitively-motivated, successive-cue, two-odor discrimination task. A) The total trials (mean + s.e.m.) required to achieve criterion performance on discrimination 1 were higher in *Fmr1*-KO (n = 10) than in WT (N = 10) mice, although the difference only approached statistical significance. B) The number of errors made during acquisition of the first discrimination problem were significantly higher in KO than in WT mice (*: $p<.05$). C) Misses (failure to respond to presentation of the positive cue, S+) were significantly higher in KO than in WT mice (*: $p<.05$). D) False alarms (Responding to the negative, unreinforced S- cue) were not different between KO and WT mice.

Figure 2

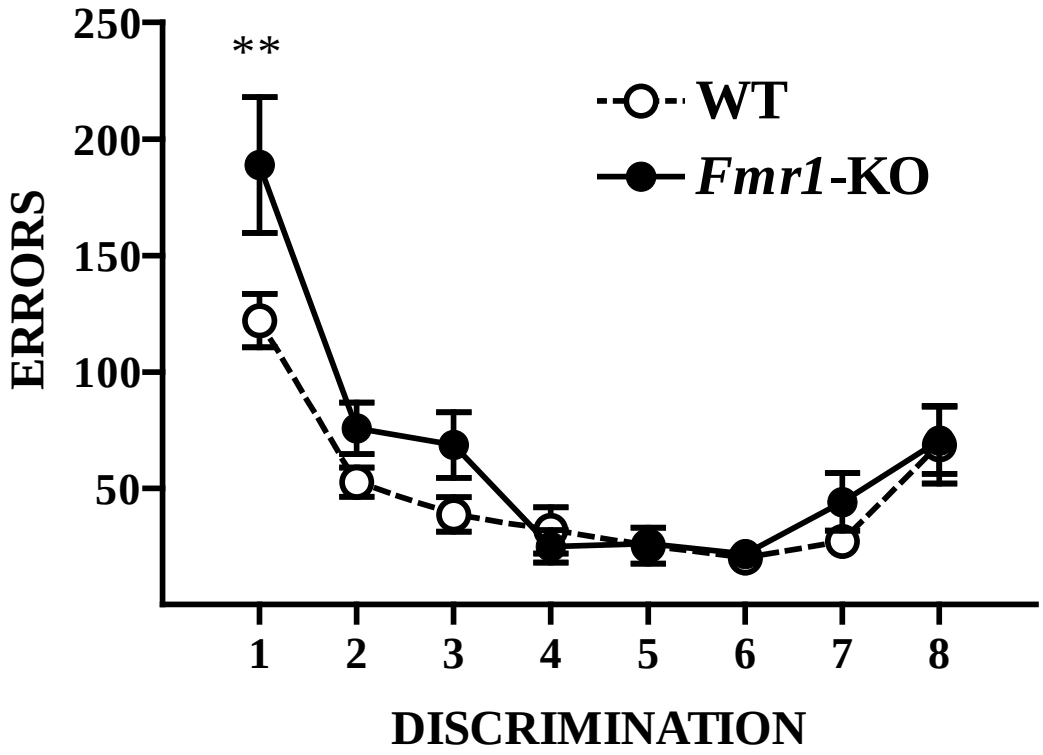

Figure 2. Learning curve for successive-cue olfactory discrimination acquisition in WT (C57Bl/6, n = 10) and *Fmr1*-KO (n = 10) mice. Mice were trained on eight distinct two-odor discrimination problems. The graph plots the average number of errors made before reaching the learning criterion for each problem. **: $p<.01$

Figure 3

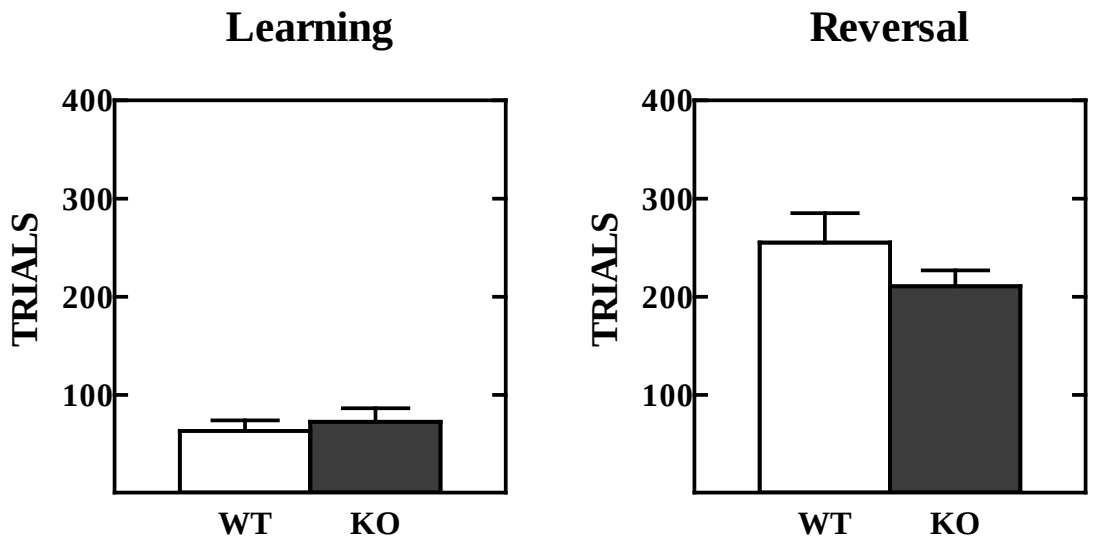

Figure 3. Mice were tested for long-term memory by retraining on one of the odor discrimination problems and comparing the trials needed to acquire the reversal (right) with the trials needed for initial learning (left). WT (n = 10) mice showed a significant increase in trials needed for reversal, relative to initial learning (paired $t_9 = 5.78$, $p<.001$), as did *Fmr1*-KO (n = 10) mice (paired $t_9 = 7.18$, $p<.0001$). The relative increase in trials necessary to learn the reversal compared to initial learning did not differ between *Fmr1*-KO and WT mice ($t_{18} = 1.40$, $p>.15$).

Figure 4

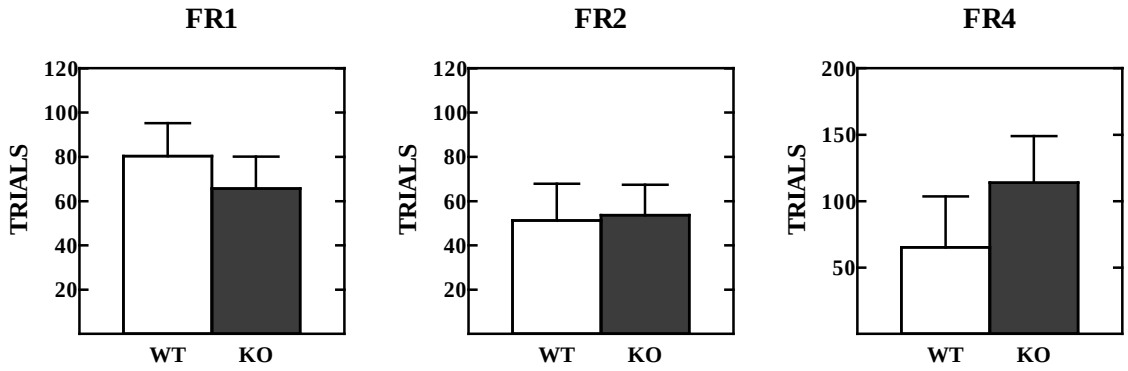

Figure 4. Response to partial reinforcement in WT (n = 10) and *Fmr1*-KO (n = 10) mice. Mice were first tested for performance of a familiar discrimination problem (#8) on a FR1 reinforcement schedule; after performing at criterion (8 consecutive correct trials), the next session was conducted with a FR2 reinforcement session(s) until criterion was again reached, followed by sessions at FR4. Shown are the means (+s.e.m.) trials to criterion for each reinforcement contingency. Although, the *Fmr1*-KO mice tended to require more trials at FR4, this effect was not statistically significant.

Figure 5

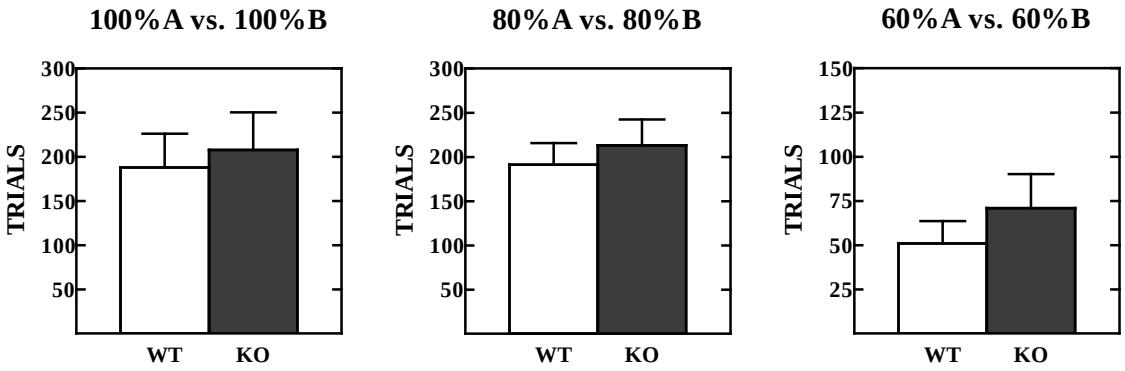

Figure 5. Odor mixture discrimination in *Fmr1*-KO (n = 10) and WT (n = 10) mice. Histograms display mean (+ s.e.m.) trials required to reach criterion on discriminations involving pure eucalyptol and heptanol (100% A vs. 100% B; left panel), the two odors in a mixture of either 80% eucalyptol and 20% heptanol versus 20% eucalyptol and 80% heptanol (middle panel) or the two odors in 60%/40% mixtures (right panel). There were no statistically significant differences between KO and WT mice on any of these discriminations.

Figure 6

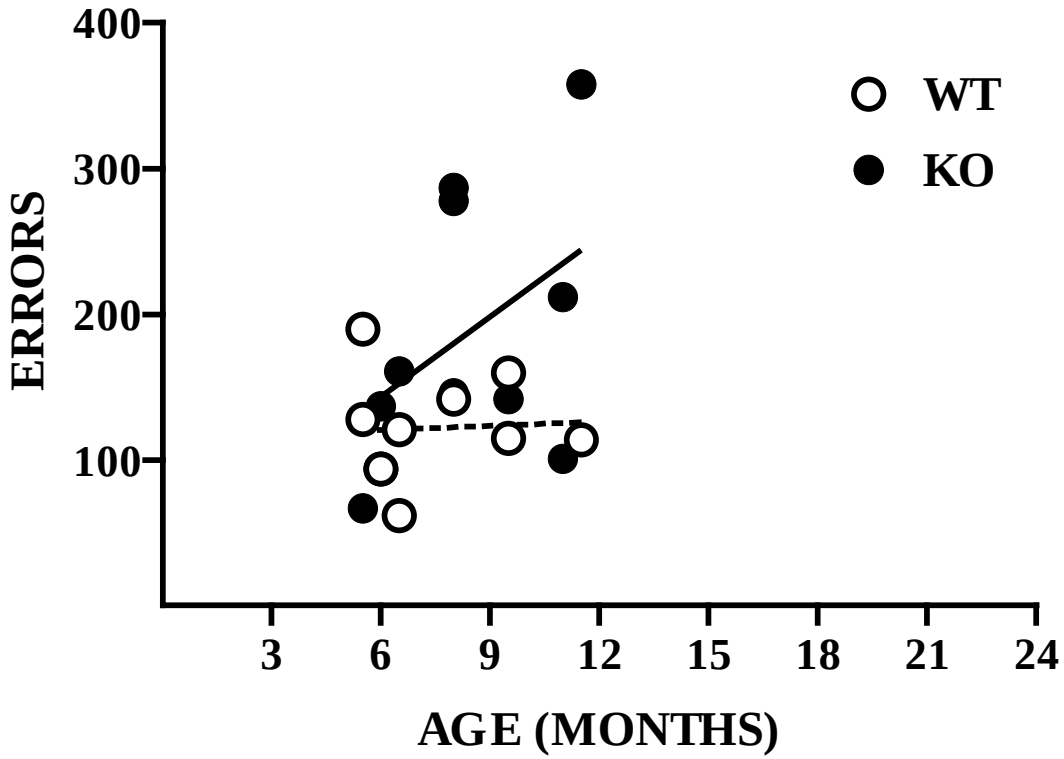

Figure 6. Effect of age on discrimination learning in WT (n = 10) and *Fmr1*-KO (n = 10) mice. Scatter plot shows the number of errors committed before acquiring criterion performance on discrimination problem #1 for individual mice. The dotted line shows the best-fitting regression line for WT subjects whereas the solid line shows the best-fitting regression line for KO subjects.

REFERENCES

Abraham, N.M., Spors, H., Carleton, A., Margrie, T.W., Kuner, T., and Schaefer, A.T. (2004). Maintaining accuracy at the expense of speed: stimulus similarity defines odor discrimination time in mice. Neuron *44*, 865-876.

Bhakar, A.L., Dolen, G., and Bear, M.F. (2012). The pathophysiology of fragile X (and what it teaches us about synapses). Annual review of neuroscience *35*, 417-443.

Eichenbaum, H., Fagan, A., Mathews, P., and Cohen, N.J. (1988). Hippocampal system dysfunction and odor discrimination learning in rats: impairment or facilitation depending on representational demands. BehavNeurosci *102*, 331-339.

Gocel, J., and Larson, J. (2012). Synaptic NMDA receptor-mediated currents in anterior piriform cortex are reduced in the adult fragile X mouse. Neuroscience *221*, 170-181.

Hou, L., Antion, M.D., Hu, D., Spencer, C.M., Paylor, R., and Klann, E. (2006). Dynamic translational and proteasomal regulation of fragile X mental retardation protein controls mGluR-dependent long-term depression. Neuron *51*, 441-454.

Huber, K.M., Gallagher, S.M., Warren, S.T., and Bear, M.F. (2002). Altered synaptic plasticity in a mouse model of fragile X mental retardation. ProcNatlAcadSciUSA *99*, 7746-7750.

Johnson, B.A., and Leon, M. (2007). Chemotopic odorant coding in a mammalian olfactory system. J Comp Neurol *503*, 1-34.

Larson, J., Jessen, R.E., Kim, D., Fine, A.K., and du Hoffmann, J. (2005). Age-dependent and selective impairment of long-term potentiation in the anterior piriform cortex of mice lacking the fragile X mental retardation protein. JNeurosci *25*, 9460-9469.

Larson, J., Kim, D., Patel, R.C., and Floreani, C. (2008). Olfactory discrimination learning in mice lacking the fragile X mental retardation protein. NeurobiolLearnMem *90*, 90-102.

Larson, J., and Munkacsy, E. (in press). Theta-Burst LTP. Brain research.

Larson, J., and Sieprawska, D. (2002). Automated study of simultaneous-cue olfactory discrimination learning in adult mice. BehavNeurosci *116*, 588-599.

Lauterborn, J.C., Rex, C.S., Kramar, E., Chen, L.Y., Pandyarajan, V., Lynch, G., and Gall, C.M. (2007). Brain-derived neurotrophic factor rescues synaptic plasticity in a mouse model of fragile X syndrome. J Neurosci *27*, 10685-10694.

Li, J., Pelletier, M.R., Perez Velazquez, J.L., and Carlen, P.L. (2002). Reduced cortical synaptic plasticity and GluR1 expression associated with fragile X mental retardation protein deficiency. MolCell Neurosci *19*, 138-151.

Patel, R.C., and Larson, J. (2009). Impaired olfactory discrimination learning and decreased olfactory sensitivity in aged C57Bl/6 mice. Neurobiology of Aging *30*, 829-837.

Quinlan, E.M., Lebel, D., Brosh, I., and Barkai, E. (2004). A molecular mechanism for stabilization of learning-induced synaptic modifications. Neuron *41*, 185-192.

Slotnick, B. (2001). Animal cognition and the rat olfactory system. Trends Cogn Sci *5*, 216-222.

Slotnick, B.M., and Katz, H.M. (1974). Olfactory learning-set formation in rats. Science *185*, 796-798.

Wilson, B.M., and Cox, C.L. (2007). Absence of metabotropic glutamate receptor-mediated plasticity in the neocortex of fragile X mice. ProcNatlAcadSciUSA *104*, 2454-2459.

Zhao, M.G., Toyoda, H., Ko, S.W., Ding, H.K., Wu, L.J., and Zhuo, M. (2005). Deficits in trace fear memory and long-term potentiation in a mouse model for fragile X syndrome. JNeurosci *25*, 7385-7392.

frontiers in
AGING NEUROSCIENCE

APPENDIX 3

ORIGINAL RESEARCH ARTICLE
published: 06 August 2013
doi: 10.3389/fnagi.2013.00039

Evidence for loss of synaptic AMPA receptors in anterior piriform cortex of aged mice

James Gocel and John Larson*

Psychiatric Institute (M/C 912), Department of Psychiatry, College of Medicine, University of Illinois at Chicago, Chicago, IL, USA

Edited by:
Orly Lazarov, The University of Illinois at Chicago, USA

Reviewed by:
Eric Blalock, University of Kentucky, USA
Junming Wang, University of Mississippi Medical Center, USA

****Correspondence:***
John Larson, Psychiatric Institute (M/C 912), Department of Psychiatry, College of Medicine, University of Illinois at Chicago, 1601 West Taylor Street, Chicago, IL 60612, USA
e-mail: jrlarson@uic.edu

It has been suggested that age-related impairments in learning and memory may be due to age-related deficits in long-term potentiation of glutamatergic synaptic transmission. For example, olfactory discrimination learning is significantly affected by aging in mice and this may be due, in part, to diminished synaptic plasticity in piriform cortex. In the present study, we tested for alterations in electrophysiological properties and synaptic transmission in this simple cortical network. Whole-cell recordings were made from principal neurons in slices of anterior piriform cortex from young (3–6 months old) and old (24–28 months) C57Bl/6 mice. Miniature excitatory postsynaptic currents (mEPSCs) mediated by AMPA receptors were collected from cells in presence of tetrodotoxin (TTX) and held at −80 mV in voltage-clamp. Amplitudes of mEPSCs were significantly reduced in aged mice, suggesting that synaptic AMPA receptor expression is decreased during aging. In a second set of experiments, spontaneous excitatory postsynaptic currents (s/mEPSCs) were recorded in slices from different cohorts of young and old mice, in the absence of TTX. These currents resembled mEPSCs and were similarly reduced in amplitude in old mice. The results represent the first electrophysiological evidence for age-related declines in glutamatergic synaptic function in the mammalian olfactory system.

Keywords: piriform cortex, mEPSC, LTP, AMPA, aging, mouse, olfaction

INTRODUCTION

Changes in the nervous system with aging are profound and mysterious. The brain exhibits subtle alterations in cellular morphology, synaptic structure, gene expression patterns, and electrophysiological characteristics as it ages; less subtle, perhaps, are the sensory, motor, and cognitive declines that accompany the aging process. Understanding the relationships between neurobiological changes and functional outcomes is one of the fundamental challenges of aging neuroscience. Considerable progress has been made in correlating age-dependent changes in hippocampal circuitry to spatial learning and memory deficits in aging animals. Two general principles have emerged from studies of hippocampal long-term potentiation (LTP) in aged animals (Burke and Barnes, 2010): first, age-dependent effects on synaptic function are regionally heterogeneous. For example, synaptic density declines in the dentate gyrus, but not field CA1, of old rats. Electrophysiological studies using minimal stimulation suggest that "basal" synaptic potency, the average size of the postsynaptic response to a presynaptic release event (Stevens and Wang, 1994), declines with extreme age in CA1 but not dentate. Second, LTP induction mechanisms are typically only impaired when stimulation is close to the induction threshold; LTP expression, provided that induction conditions are suprathreshold, appears normal (Burke and Barnes, 2010).

The olfactory system has a number of advantages for neurobiological studies of sensory and cognitive functions in aging. Olfactory discrimination ability declines markedly in human aging (Doty et al., 1984; Cain and Stevens, 1989) and appears to be particularly vulnerable to age-related neurodegenerative disease (Serby et al., 1985; Kesslak et al., 1988). Olfactory dysfunction has also been reported for aging rodents (Roman et al., 1996; Frick et al., 2000; Schoenbaum et al., 2002; Enwere et al., 2004; Prediger et al., 2005; LaSarge et al., 2007). For instance, a recent study from our laboratory found that old mice took more trials to learn two-odor discrimination problems for positive reinforcement and failed to show improvement across multiple discrimination problems when compared to young mice (Patel and Larson, 2009). However, the neurobiological bases for these deficits are largely unexplored.

The primary olfactory (piriform) cortex receives monosynaptic input from the mitral (and tufted) cells of the olfactory bulb, which themselves receive monosynaptic input from primary sensory neurons in the olfactory epithelium. Layer II pyramidal neurons of piriform cortex appear to be situated to form combinatorial representations of the different olfactory bulb glomeruli that respond to distinct molecular features of the chemicals comprising an odor (Wilson and Sullivan, 2011). Piriform neurons project monosynaptically to the lateral entorhinal cortex, providing olfactory input to the hippocampal formation, as well as to parts of the amygdalar complex and the prefrontal cortex (Shipley et al., 1995). Both the afferent synapses made by the mitral cells onto layer II pyramidal cells and the associational feedback system generated by neighboring pyramidal cells are glutamatergic and exhibit LTP (Jung et al., 1990a,b; Kanter and Haberly, 1990), possibly to strengthen representations of learned odors or to participate in odor–reward associations. The present studies were directed to test for synaptic functional changes in anterior piriform cortex (APC) of aged mice. The results provide the first

direct evidence that aging results in decreases in synaptic currents mediated by AMPA-type glutamate receptors in a simple cortical network.

MATERIALS AND METHODS

ANIMALS

C57Bl/6J mice were bred in the Psychiatric Institute vivarium from breeding stock obtained from Jackson Laboratories (Bar Harbor, ME, USA). Mice were weaned at 21 days of age and males were separated and housed in groups of two to four per cage until sacrificed for experiments. Food and water were available *ad libitum* and routine veterinary visits ensured that animals were in good health prior to experimentation. Any animals that displayed physical ailments or lethargy were excluded from this study. Electrophysiological experiments were conducted on brain slices obtained from mice aged 3–6 months ("young"; $n = 16$) or 24–28 months ("old"; $n = 12$). All procedures were in accordance with NIH guidelines and protocols were approved by the Animal Care Committee of the University of Illinois at Chicago (UIC ACC #09-232).

ELECTROPHYSIOLOGY

In vitro slice preparation and electrophysiology

Parasagittal slices (300 μm) of APC were prepared in the usual method. Mice were decapitated and brains removed in oxygenated artificial cerebral spinal fluid (aCSF) containing (in mM): NaCl (120), KCl (3.1), K_2HPO_4 (1.25), $NaHCO_3$ (26), dextrose (5.0), L-ascorbate (2), $MgCl_2$ (1.0), $CaCl_2$ (2.0) at ∼4°C. The brain was then sectioned into blocks (2–3 mm thick), mounted on a cutting stage, and sliced on a vibrating cutter (Vibratome, St. Louis, MO, USA). The slices were incubated at 32°C for 1 h and then allowed to cool to room temperature (∼25–27°C). Slices were then transferred to a submerged recording chamber and perfused with aCSF. Recordings were obtained from principal cells in layer II at room temperature, as described previously (Gocel and Larson, 2012). Patch electrodes (1.8–3 MΩ) contained (in mM): cesium methanesulfonate (145), $MgCl_2$ (1), HEPES (10), BAPTA (1.1), MgATP (5), and phosphocreatine (20) adjusted to pH 7.2 with CsOH, 290 mOsm. Cells were visualized with differential interference contrast (DIC) optics on a Nikon Eclipse E600FN "PhysioStation" (Nikon, Melville, NY, USA). Twisted bipolar electrodes (custom made) with a tip diameter ∼50 μm were positioned in layer Ia and Ib 150–200 μm rostral from the recorded cell. Stimulation (0.1 ms pulses 1–200 μA) in these layers activate afferent lateral olfactory tract (LOT) and intrinsic association (ASSN) fibers synapsing onto principal cells in layer II. Responses at ASSN synapses display paired-pulse depression whereas stimulation of afferent LOT fibers in layer Ia exhibit facilitation (Bower and Haberly, 1986). Therefore, stimulation of ASSN fibers in layer Ib was confirmed after obtaining whole-cell recording by non-facilitating responses to paired-pulse stimulation at a 200 ms inter-pulse interval (IPI). Evoked excitatory postsynaptic currents (EPSCs), miniature EPSCs (mEPSCs) and spontaneous EPSCs (s/mEPSCs) were recorded with an Axopatch-1D amplifier and pClamp software (Molecular Devices, Sunnyvale, CA, USA), filtered at 1 kHz, digitized at 10 kHz, and stored on the computer hard drive. Cells were immediately rejected if series resistance exceeded 15 MΩ upon obtaining whole-cell recording configuration. Series and whole-cell capacitance compensation and junction potential correction were not used.

PHARMACOLOGY

All drugs and chemicals were applied via the perfusate by a solenoid-controlled gravity-feed system (ValveLink 8, AutoMate Scientific, Inc., Berkeley, CA, USA). The rate of flow of all drug perfusates was equilibrated to 2 mL/min prior to the inception of experimentation. $GABA_A$ mediated transmission was blocked by 25 μM 1(S),9(R)-(−)-bicuculline methiodide (BMI) in all experiments in order to isolate postsynaptic excitatory currents. The NMDA receptor antagonist, 3-[(R)-2-carboxypiperazin-4-yl]-prop-2-enyl-1-phosphonic acid (CPP, 20 μM)) was used to isolate AMPA receptor-mediated currents. 1 μM tetrodotoxin (TTX) was added to the perfusate in order to eliminate spontaneous action potential-dependent events. Some experiments used 6-cyano-7-nitroquinoxaline-2,3-dione (CNQX) to block AMPA receptors (20 μM). All drugs were taken from stock solutions dissolved in H_2O and diluted in aCSF as needed.

EVOKED SYNAPTIC CURRENTS

In experiments using synaptic stimulation under voltage-clamp, the following stimulation protocol was used: each trial began with a baseline recording period of 300 ms, followed by paired-pulse stimulation of the LOT (50 ms IPI), a one-second delay, and paired-pulse stimulation of the ASSN fibers (50 ms IPI). Stimulation current levels were set to yield a reliable response with the least amount of stimulation in order to avoid polysynaptic activity or synaptic population crosstalk. Stimulation intensities were the following: LOT: 3–6 months, 40.61 ± 12.12 μA; 24–28 months, 120.00 ± 47.97 μA and ASSN: 3–6 months, 26.17 ± 3.02 μA, 24–28 months, 60.89 ± 11.17 μA. Any recordings demonstrating polysynaptic activity were excluded from analysis. Measurements of averaged (50–100 trials) current attributes were performed in Clampfit.

mEPSC AND s/mEPSC ANALYSIS

For analysis of mEPSCs, slices were perfused with TTX (1 μM) until whole-cell currents evoked by LOT and ASSN fiber stimulation were abolished. Cells were maintained at a holding potential of −80 mV throughout recordings and bicuculline and CPP were used to prevent activation of $GABA_A$ and NMDA receptors, respectively. Spontaneous synaptic currents were recorded for 200 s of continuous recording from every cell. mEPSCs were identified as follows: A single 50 ms variable amplitude template was constructed (Clements and Bekkers, 1997) from >20 visually-identified events in a randomly-selected cell and served as a search criterion for collecting and aligning mEPSCs and s/mEPSCs for all cells. Cells were excluded from analysis if the baseline drifted more than 50 pA or if access resistance changed more than 20% throughout the 200 s of continuous recording. All compound events were excluded from analysis. Measurements of the current waveforms (kinetics) were obtained from an average of all events (>100) that met analysis criteria in each cell. Decay time constants were fit to averaged mEPSCs with the standard exponential equation

$I(t) = I \times \exp(-t/\tau)$, where I is the peak amplitude and τ is a the decay time constant.

Spontaneous EPSCs (s/mEPSCs) were recorded and quantified as for mEPSCs, except that TTX was not used.

HISTOLOGY

Some cells used for electrophysiology were also filled with a 4% Lucifer yellow solution passively during the recordings. Brain sections were then immediately fixed in 4% paraformaldehyde overnight, whole mounted on glass slides and coverslipped. Additional physiological slices fixed in 4% paraformaldehyde were cryoprotected in 30% sucrose in PBS. These slices were then resectioned at 30 μm, processed, and stained with 0.1% cresyl violet. Filled cells were visualized under a fluorescein isothiocyanate (FITC) filter and stained slices were visualized under bright field illumination on an Axioskop 2 microscope. Images were acquired through Axiovision software (Zeiss, Thornwood, NY, USA) and edited in GNU image manipulation program (GIMP, open source).

STATISTICS

All data are based on cells as individual sample units and are presented as means ± SEM. Statistical differences between two groups were evaluated using Student's unpaired *t*-test. Analysis of variance was used for comparisons involving more than two groups.

RESULTS

A subset of the cells chosen for electrophysiological study were filled with Lucifer yellow to confirm that they were layer II pyramidal cells (**Figure 1**). Filled cells from mice at all ages showed multiple, spiny apical dendrites which projected toward the pial surface. Other slices stained with cresyl violet were examined for cytoarchitecture. There were no obvious differences in soma morphology, cortical lamination, or cell density of APC of 3–6 months old and 24–28 months old mice.

AMPA RECEPTOR-MEDIATED mEPSCs ARE SMALLER IN THE AGED MOUSE

As described previously (Gocel and Larson, 2012), superficial pyramidal (SP) neurons held at −80 mV under voltage clamp in the presence of BMI, CPP, and TTX showed spontaneous inward currents with the characteristics of mEPSCs, in slices from both young and old mice (**Figure 2A**). These events were abolished by perfusion with CNQX, confirming that they were mediated by AMPA receptors (data not shown). Synaptic events were collected from continuous 200 s recording epochs, aligned, averaged, and analyzed. Amplitude distributions were positively skewed in both young (**Figure 2B**) and old mice (**Figure 2C**). The mean amplitudes of mEPSCs recorded in slices from old mice were significantly smaller than those from young mice (**Figure 2D**). Since the amplitude distributions were skewed, the median mEPSC amplitude was also calculated for each cell and compared between age groups. These measures were also significantly smaller in the aged mice (young: 12.31 ± 0.51 pA; old: 9.95 ± 0.53 pA; $p < 0.01$). The average frequency of detected mEPSCs did not significantly differ between age groups (**Figure 2E**). Cumulative amplitude distributions (**Figure 2F**) also illustrate the shift in amplitude toward smaller mEPSCs in the neurons from old mice. Possible age-related changes in the kinetics of AMPA receptors mediating mEPSCs were calculated by fitting a single exponential function to the decay phase of averaged mEPSCs in each cell. The decay time constants tended to be longer in cells from old mice, although this difference only approached statistical significance (young: 4.22 ± 0.16 ms, $n = 24$; old: 4.72 ± 0.18 ms, $n = 14$; $t_{36} = 1.95$, $p = 0.06$).

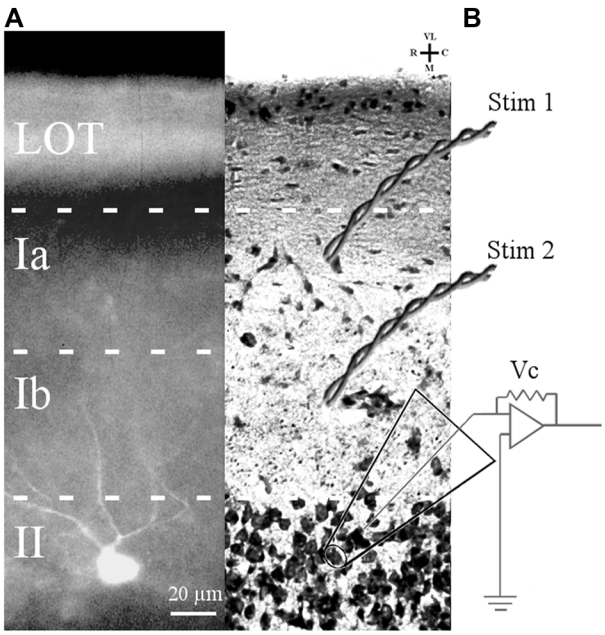

FIGURE 1 | Slice preparation of APC and arrangement of stimulation and recording electrodes. (A) A Lucifer yellow-filled cell in APC slice is shown. The soma is located in layer II and primary dendrites (only partially in the focal plane) ascend through layer I. **(B)** Cresyl violet-stained APC section showing position of bipolar electrodes to stimulate LOT fibers (Stim 1) and ASSN fibers (Stim 2). Patch clamp recordings were obtained in the whole cell configuration from somata of layer II principal cells visually identified under DIC optics.

PAIRED-PULSE RESPONSES ARE UNAFFECTED BY AGING

The vast majority of glutamatergic synapses on SP neurons in APC are generated by either afferents from the olfactory bulb (LOT), terminating in the outer molecular layer (Ia) or the intrinsic associational (ASSN) system generated by the SP neurons themselves and terminating in the inner molecular layer (Ib). To test whether or not changes in the potency of individual synapses (mEPSCs) with aging were accompanied by presynaptic changes in release characteristics at either or both of these systems, paired-pulse stimulation (50 ms IPI) was applied to each pathway while recording from cells held at −80 mV in slices from young and old mice. Cells were only included in analysis if responses were present from both synaptic pathways. All traces collected for a given cell which met criteria were averaged and the percent potentiation or depression of the second response was calculated relative to that of the first response (**Figure 3**). The robust facilitation of responses to LOT stimulation was not significantly altered by

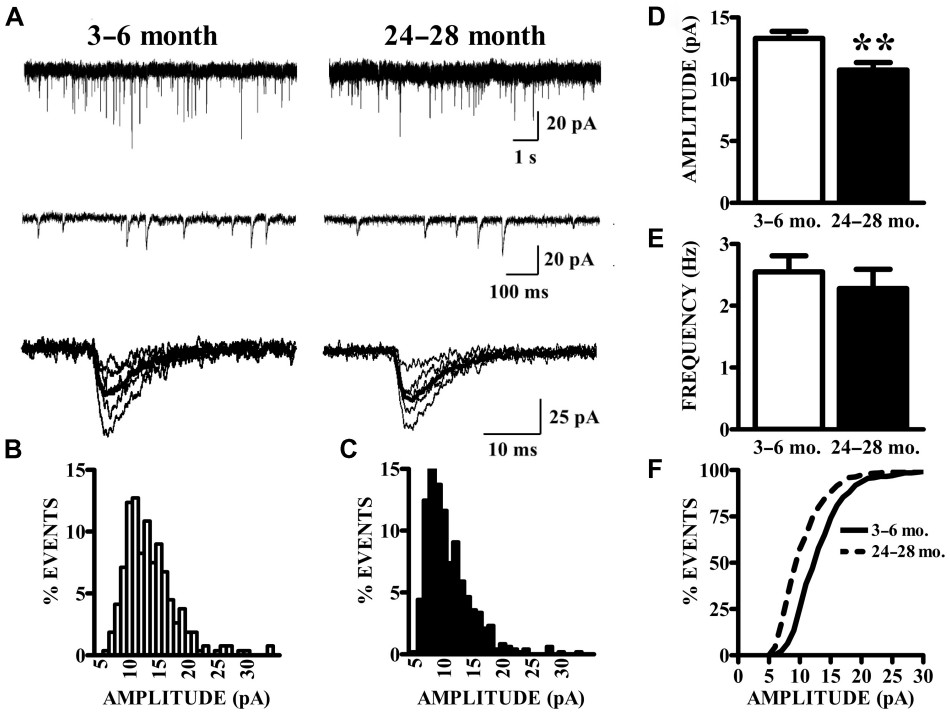

FIGURE 2 | AMPA receptor-mediated currents at single synapses are reduced in aged mice. (A) mEPSCs were collected in the presence of TTX. Top raw traces were extracted from 200 s recording epochs from which spontaneous currents were collected. Middle traces are expanded sections of the top traces; a template algorithm was used to search for individual currents. Bottom traces are selected individual mEPSCs aligned according to onset of the current. **(B,C)** All currents collected during the 200 s epochs were binned according to amplitude. As demonstrated by these representative histograms, AMPA mEPSC amplitude histograms in old (24–28 months) animals **(C)** demonstrated a leftward shift in distribution as compared to young (3–6 months) animals **(B)**. **(D)** Mean amplitudes (shown) of AMPA mEPSCs were significantly decreased in old relative to young mice ($t_{36} = 2.87$, $p < 0.01$). Comparison of both age groups according to the median amplitude (not shown) also demonstrated a reduction. **(E)** The frequency of mEPSCs was comparable between age groups. Frequency was determined by counting the events that occurred during the entire 200-s recording epochs. **(F)** Cumulative distributions illustrate the shift in the mEPSC amplitudes.

age. ASSN responses showed neither facilitation nor depression at the interval tested; normalized responses were also unaffected by age.

SPONTANEOUS SYNAPTIC CURRENTS (s/mEPSCs) ARE REDUCED IN THE AGED MOUSE

Spontaneous currents in the absence of stimulation were obtained from the same cells in which evoked paired-pulse responses were obtained. Experiments were performed in the absence of TTX in order to obtain evoked responses; therefore, the spontaneous currents collected are presumed to be a mixture of action potential-dependent (sEPSCs) and independent (mEPSCs) events. The manner of analysis was identical to the method of analyzing mEPSC data. Aged animals exhibited a significant reduction in mean (**Figure 4**) and median (young: 12.78 ± 0.53 pA; old: 10.69 ± 0.41 pA; $p < 0.01$) s/mEPSC amplitude. The similar size of mEPSCs recorded in the presence of TTX (**Figure 2**) and s/mEPSCs recorded in the absence of TTX (**Figure 4**) suggests either (1) that action potential-dependent and -independent release events evoke similar postsynaptic responses or (2) that the action potential-dependent (TTX-sensitive) events are a small fraction of spontaneous release events in these cells. Frequency distributions of s/mEPSC amplitudes also did not reveal any obvious differences with those of mEPSCs. In any case, it bears noting that the s/mEPSC (**Figure 4**) and mEPSC (**Figure 2**) recordings were made from completely different sets of young and old animals.

DISCUSSION

There is compelling evidence that olfaction-mediated sensory and cognitive functions decline with aging in humans (Doty et al., 1984; Cain and Stevens, 1989; Wysocki and Gilbert, 1989; Larsson et al., 2000, 2006; Gilbert et al., 2008) and experimental animals (Roman et al., 1996; Frick et al., 2000; Enwere et al., 2004; Prediger et al., 2005; LaSarge et al., 2007; Dardou et al., 2008; Luu et al., 2008; Patel and Larson, 2009). The piriform cortex occupies a strategic position in the neural processing of odors: (i) it is the largest target of efferents from the olfactory bulb (Neville and Haberly, 2004); (ii) its internal wiring suggests a combinatorial mechanism for synthetic integration of odor percepts from multiple chemical constituents that activate distinct odorant receptor proteins and corresponding glomeruli in the olfactory bulb (Haberly, 2001; Franks and Isaacson, 2006; Stettler and Axel, 2009; Wilson and Sullivan, 2011); (iii) odor discrimination and olfactory learning are disrupted by piriform lesions (Staubli et al., 1987); (iv) olfactory training modifies synaptic structure and function in

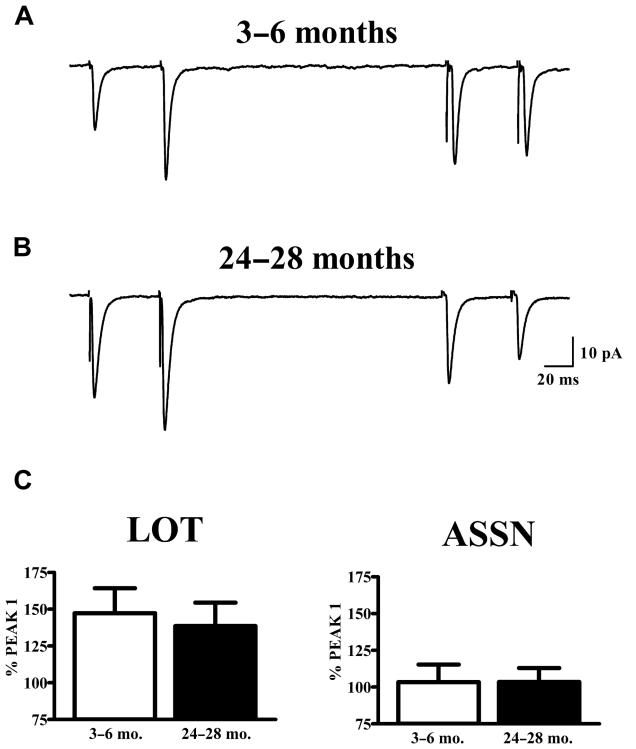

FIGURE 3 | Paired-pulse characteristics in APC at LOT and ASSN synapses are unaffected by aging. (A,B) Evoked LOT (left traces) and ASSN (right traces) paired pulse responses from principal cells in layer II of APC were collected from young (3–6 months, $n = 18$) and old (24–28 months, $n = 11$) mice at –80 mV. Cells were only included in analysis if recordings were obtained from both LOT and ASSN inputs. Paired-pulse stimulation (50 ms ISI) was presented to LOT fibers followed by the same stimulation to ASSN fibers one second later. Currents were collected every 20 s and the representative traces illustrated are an average of 50–100 stimulations. **(C)** Normalized averages of the second response were generated by calculating the response amplitude relative to that of the first response. No differences in paired-pulse response at either LOT or ASSN synapses were detected between age groups.

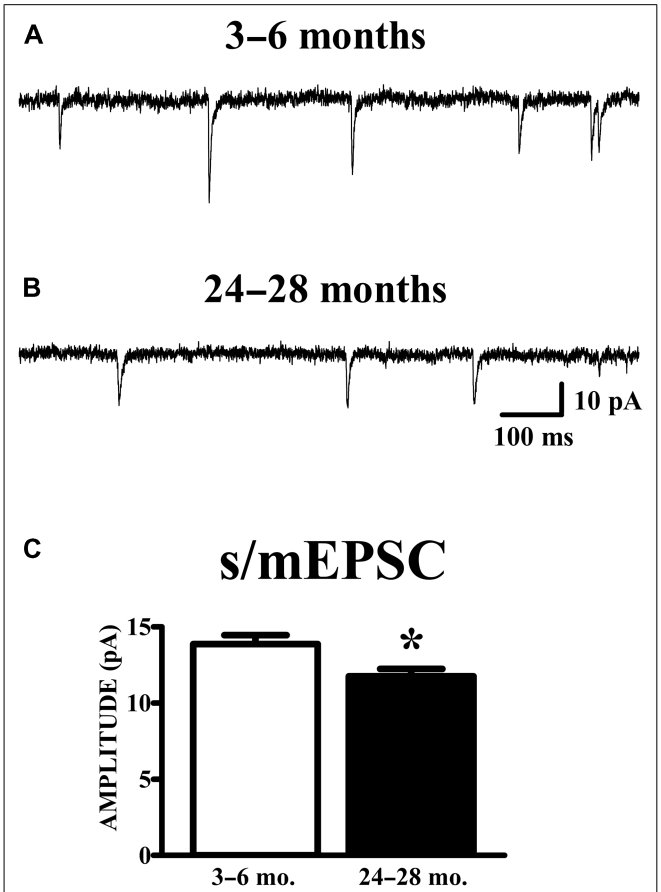

FIGURE 4 | AMPA s/mEPSC amplitudes are reduced in APC of old mice. (A,B) Raw traces illustrated include events collected during recording periods where no stimulation was presented in the same cells shown in **Figure 3**. Spontaneous currents (s/mEPSCs) in these recordings are presumed to emanate from action potential-mediated and -independent events since TTX was not present in the perfusate. **(C)** The mean amplitude of s/mEPSCs was calculated and averaged across cells. Events collected from aged (24–28 months, $n = 11$) mice demonstrated a decrease in amplitude compared to those from young (3–6 months, $n = 18$) mice ($t_{27} = 2.48$, $p < 0.05$).

piriform cortex (Barkai and Saar, 2001); and (v) it is the primary pathway by which olfactory information reaches the hippocampus, amygdala, and prefrontal cortex (Shipley et al., 1995). However, this structure has received very little attention in neurobiological studies of aging. The present study represents an initial step in a comprehensive analysis of the brain substrate for olfactory dysfunction in aging.

We recorded from principal neurons in primary olfactory cortex from young adult and aged mice. The main finding of the experiments described here is a decrease in the amplitude of synaptic currents mediated by AMPA receptors on these cells in aged mice. TTX-resistant spontaneous synaptic currents (mEPSCs) are thought to be evoked by stochastic release of single glutamate quanta at individual synapses. Assuming that synaptic vesicles are the physical basis for quantal release, there are two main ways to alter quantal size: a change in glutamate loading of vesicles or a change in postsynaptic receptors in the synaptic zone. There is little precedent for changes in vesicle loading but considerable evidence that postsynaptic AMPA receptor numbers can be altered in an experience-dependent manner (Lynch and Baudry, 1984; Bredt and Nicoll, 2003) or in certain disease models (Li et al., 2002). Therefore the most parsimonious interpretation of a decrease in mEPSC size is a reduction in the number of functional AMPA receptors activated by synaptic glutamate release in the aged mice. In theory, a postsynaptic mechanism could be confirmed or ruled out by measuring NMDA receptor-mediated mEPSCs; however, this was impractical due to the voltage-dependence and slow kinetics of NMDA receptor-mediated currents. On the other hand, there are numerous reports of decreases in AMPA receptor expression, measured by mRNA or protein expression or ligand binding, in various brain regions of aged rodents (Bahr et al., 1992; Magnusson and Cotman, 1993; Nicoletti et al., 1995; Nicolle et al., 1996; Magnusson, 1998; Wenk and Barnes, 2000; Majdi et al., 2009).

It is important to note that spontaneous EPSCs (sEPSCs) were also recorded from APC cells in slices from completely

independent cohorts of young and old mice, in the absence of TTX. The amplitude distributions of these events were almost identical to the events (mEPSCs) recorded in slices exposed to TTX. This suggests that the sEPSCs and mEPSCs are the same events; the lack of TTX sensitivity may be attributed to the high resting membrane potentials and low spontaneous firing of piriform pyramidal cells *in vitro* (Scholfield, 1978; Tseng and Haberly, 1988; Suzuki and Bekkers, 2006). In any case, the smaller amplitude of spontaneously-occurring synaptic AMPA currents in cells from old mice was replicated for both mEPSCs and "sEPSCs," in different cohorts of mice.

The frequency of mEPSCs was not altered in the aged mice, suggesting that either (i) no change in the number of synapses contributing to these synapses with aging or (ii) that any such changes are accompanied by compensatory changes in spontaneous release probability. The synaptic origin of the mEPSCs could not be determined in these experiments. However, it is worth noting that the paired-pulse experiments did not reveal any differences that would be indicative of changes in release probability in either the LOT or ASSN pathways in young versus old mice. It is also worth noting that paired-pulse ratios may not be very sensitive measures of release kinetics.

In toto, the results of the present study point to the conclusion that aging results in a loss of functional AMPA receptors at synapses on layer II pyramidal cells in piriform cortex. These losses may occur at LOT synapses, ASSN synapses, or both. Further studies will be necessary to establish whether these AMPA receptor losses are due to alterations in receptor subunit transcription, translation, trafficking, post-translational modification, or receptor assembly, as well as whether or not synaptic NMDA receptors are similarly effecting by aging. The decrease in synaptic potency with aging observed in the present study is in contrast to studies using minimal stimulation in rat hippocampal formation where the results suggest that dentate synapses increase in potency (larger unitary EPSPs) while CA1 synapses remain unchanged in old age (Barnes and McNaughton, 1980; Foster et al., 1991; Barnes et al., 1992).

A loss of synaptic AMPA receptors would not be expected to be without effect on LTP in the APC. Although the effects of aging on LTP have not been studied in piriform cortex, activation of more synapses with fewer AMPA receptors would be needed to trigger LTP in aged mice, in order to overcome the voltage-dependent block of NMDA receptors during high frequency stimulation. A disturbance of LTP might not be evident with supramaximal stimulation paradigms but may appear with near threshold stimulation, as observed in hippocampal field CA1. In this scenario, enhancement of AMPA receptor function might compensate for loss of synaptic AMPA receptors. Drugs that act in this way are known to facilitate olfactory learning in young animals (Larson et al., 1995) and may alleviate some of the learning deficits shown by aged mice.

ACKNOWLEDGMENTS

The research was supported by grants from the National Institutes of Health (DC5793) and the U.S. Army Medical Research and Materiel Command (#10917352).

REFERENCES

Bahr, B. A., Godshall, A. C., Hall, R. A., and Lynch, G. (1992). Mouse telencephalon exhibits an age-related decrease in glutamate (AMPA) receptors but no change in nerve terminal markers. *Brain Res.* 589, 320–326. doi: 10.1016/0006-8993(92)91293-N

Barkai, E., and Saar, D. (2001). Cellular correlates of olfactory learning in the rat piriform cortex. *Rev. Neurosci.* 12, 111–120. doi: 10.1515/REVNEURO.2001.12.2.111

Barnes, C. A., and McNaughton, B. L. (1980). Physiological compensation for loss of afferent synapses in rat hippocampal granule cells during senescence. *J. Physiol.* 309, 473–485.

Barnes, C. A., Rao, G., Foster, T. C., and McNaughton, B. L. (1992). Region-specific age effects on AMPA sensitivity: electrophysiological evidence for loss of synaptic contacts in hippocampal field CA1. *Hippocampus* 2, 457–468. doi: 10.1002/hipo.450020413

Bower, J. M., and Haberly, L. B. (1986). Facilitating and nonfacilitating synapses on pyramidal cells: a correlation between physiology and morphology. *Proc. Natl. Acad. Sci. U.S.A.* 83, 1115–1119. doi: 10.1073/pnas.83.4.1115

Bredt, D. S., and Nicoll, R. A. (2003). AMPA receptor trafficking at excitatory synapses. *Neuron* 40, 361–379. doi: 10.1016/S0896-6273(03)00640-8

Burke, S. N., and Barnes, C. A. (2010). Senescent synapses and hippocampal circuit dynamics. *Trends Neurosci.* 33, 153–161. doi: 10.1016/j.tins.2009.12.003

Cain, W. S., and Stevens, J. C. (1989). Uniformity of olfactory loss in aging. *Ann. N. Y. Acad. Sci.* 561, 29–38. doi: 10.1111/j.1749-6632.1989.tb20967.x

Clements, J. D., and Bekkers, J. M. (1997). Detection of spontaneous synaptic events with an optimally scaled template. *Biophys. J.* 73, 220–229. doi: 10.1016/S0006-3495(97)78062-7

Dardou, D., Datiche, F., and Cattarelli, M. (2008). Memory is differently impaired during aging according to the learning tasks in the rat. *Behav. Brain Res.* 194, 193–200. doi: 10.1016/j.bbr.2008.07.007

Doty, R. L., Shaman, P., Applebaum, S. L., Giberson, R., Siksorski, L., and Rosenberg, L. (1984). Smell identification ability: changes with age. *Science* 226, 1441–1443. doi: 10.1126/science.6505700

Enwere, E., Shingo, T., Gregg, C., Fujikawa, H., Ohta, S., and Weiss, S. (2004). Aging results in reduced epidermal growth factor receptor signaling, diminished olfactory neurogenesis, and deficits in fine olfactory discrimination. *J. Neurosci.* 24, 8354–8365. doi: 10.1523/JNEUROSCI.2751-04.2004

Foster, T. C., Barnes, C. A., Rao, G., and McNaughton, B. L. (1991). Increase in perforant path quantal size in aged F-344 rats. *Neurobiol. Aging* 12, 441–448. doi: 10.1016/0197-4580(91)90071-Q

Franks, K. M., and Isaacson, J. S. (2006). Strong single-fiber sensory inputs to olfactory cortex: implications for olfactory coding. *Neuron* 49, 357–363. doi: 10.1016/j.neuron.2005.12.026

Frick, K. M., Burlingame, L. A., Arters, J. A., and Berger-Sweeney, J. (2000). Reference memory, anxiety and estrous cyclicity in C57BL/6NIA mice are affected by age and sex. *Neuroscience* 95, 293–307. doi: 10.1016/S0306-4522(99)00418-2

Gilbert, P. E., Pirogovsky, E., Ferdon, S., Brushfield, A. M., and Murphy, C. (2008). Differential effects of normal aging on memory for odor-place and object-place associations. *Exp. Aging Res.* 34, 437–452. doi: 10.1080/03610730802271914

Gocel, J., and Larson, J. (2012). Synaptic NMDA receptor-mediated currents in anterior piriform cortex are reduced in the adult fragile X mouse. *Neuroscience* 221, 170–181. doi: 10.1016/j.neuroscience.2012.06.052

Haberly, L. B. (2001). Parallel-distributed processing in olfactory cortex: new insights from morphological and physiological analysis of neuronal circuitry. *Chem. Senses* 26, 551–576. doi: 10.1093/chemse/26.5.551

Jung, M. W., Larson, J., and Lynch, G. (1990a). Long-term potentiation of monosynaptic EPSPs in rat piriform cortex in vitro. *Synapse* 6, 279–283. doi: 10.1002/syn.890060307

Jung, M. W., Larson, J., and Lynch, G. (1990b). Role of NMDA and non-NMDA receptors in synaptic transmission in rat piriform cortex. *Exp. Brain Res.* 82, 451–455. doi: 10.1007/BF00231264

Kanter, E. D., and Haberly, L. B. (1990). NMDA-dependent induction of long-term potentiation in afferent and association fiber systems of piriform cortex in vitro. *Brain Res.* 525, 175–179. doi: 10.1016/0006-8993(90)91337-G

Kesslak, J. P., Cotman, C. W., Chui, H. C., Van den Noort, S., Fang, H., Pfeffer, R., et al. (1988). Olfactory tests as possible probes for detecting and monitoring Alzheimer's disease. *Neurobiol. Aging* 9, 399–403. doi: 10.1016/S0197-4580(88)80087-3

Larson, J., Lieu, T., Petchpradub, V., LeDuc, B., Ngo, H., Rogers, G. A., et al. (1995). Facilitation of olfactory learning by a modulator of AMPA receptors. *J. Neurosci.* 15, 8023–8030.

Larsson, M., Finkel, D., and Pedersen, N. L. (2000). Odor identification: influences of age, gender, cognition, and personality. *J. Gerontol. B Psychol. Sci. Soc. Sci.* 55, 304–310. doi: 10.1093/geronb/55.5.P304

Larsson, M., Oberg, C., and Backman, L. (2006). Recollective experience in odor recognition: influences of adult age and familiarity. *Psychol. Res.* 70, 68–75. doi: 10.1007/s00426-004-0190-9

LaSarge, C. L., Montgomery, K. S., Tucker, C., Slaton, G. S., Griffith, W. H., Setlow, B., et al. (2007). Deficits across multiple cognitive domains in a subset of aged Fischer 344 rats. *Neurobiol. Aging* 28, 928–936. doi: 10.1016/j.neurobiolaging.2006.04.010

Li, J., Pelletier, M. R., Perez Velazquez, J. L., and Carlen, P. L. (2002). Reduced cortical synaptic plasticity and GluR1 expression associated with fragile × mental retardation protein deficiency. *Mol. Cell. Neurosci.* 19, 138–151. doi: 10.1006/mcne.2001.1085

Luu, T. T., Pirogovsky, E., and Gilbert, P. E. (2008). Age-related changes in contextual associative learning. *Neurobiol. Learn. Mem.* 89, 81–85. doi: 10.1016/j.nlm.2007.09.006

Lynch, G., and Baudry, M. (1984). The biochemistry of memory: a new and specific hypothesis. *Science* 224, 1057–1063. doi: 10.1126/science.6144182

Magnusson, K. R. (1998). Aging of glutamate receptors: correlations between binding and spatial memory performance in mice. *Mech. Ageing Dev.* 104, 227–248. doi: 10.1016/S0047-6374(98)00076-1

Magnusson, K. R., and Cotman, C. W. (1993). Age-related changes in excitatory amino acid receptors in two mouse strains. *Neurobiol. Aging* 14, 197–206. doi: 10.1016/0197-4580(93)90001-R

Majdi, M., Ribeiro-da-Silva, A., and Cuello, A. C. (2009). Variations in excitatory and inhibitory postsynaptic protein content in rat cerebral cortex with respect to aging and cognitive status. *Neuroscience* 159, 896–907. doi: 10.1016/j.neuroscience.2008.11.034

Neville, K. R., and Haberly, L. B. (2004). "Olfactory cortex," in *The Synaptic Organization of the Brain*, Vol. 5, ed. G. M. Shepherd (New York: Oxford University Press), 415–454. doi: 10.1093/acprof:oso/9780195159561.003.0010

Nicoletti, V. G., Condorelli, D. F., Dell'Albani, P., Ragusa, N., and Giuffrida Stella, A. M. (1995). AMPA-selective glutamate receptor subunits in the rat hippocampus during aging. *J. Neurosci. Res.* 40, 220–224. doi: 10.1002/jnr.490400210

Nicolle, M. M., Bizon, J. L., and Gallagher, M. (1996). In vitro autoradiography of ionotropic glutamate receptors in hippocampus and striatum of aged Long-Evans rats: relationship to spatial learning. *Neuroscience* 74, 741–756. doi: 10.1016/0306-4522(96)00147-9

Patel, R. C., and Larson, J. (2009). Impaired olfactory discrimination learning and decreased olfactory sensitivity in aged C57Bl/6 mice. *Neurobiol. Aging* 30, 829–837. doi: 10.1016/j.neurobiolaging.2007.08.007

Prediger, R. D., Batista, L. C., and Takahashi, R. N. (2005). Caffeine reverses age-related deficits in olfactory discrimination and social recognition memory in rats. Involvement of adenosine A1 and A2A receptors. *Neurobiol. Aging* 26, 957–964. doi: 10.1016/j.neurobiolaging.2004.08.012

Roman, F. S., Alescio-Lautier, B., and Soumireu-Mourat, B. (1996). Age-related learning and memory deficits in odor–reward association in rats. *Neurobiol. Aging* 17, 31–40. doi: 10.1016/0197-4580(95)02030-6

Schoenbaum, G., Nugent, S., Saddoris, M. P., and Gallagher, M. (2002). Teaching old rats new tricks: age-related impairments in olfactory reversal learning. *Neurobiol. Aging* 23, 555–564. doi: 10.1016/S0197-4580(01)00343-8

Scholfield, C. N. (1978). Electrical properties of neurones in the olfactory cortex slice in vitro. *J. Physiol.* 275, 535–546.

Serby, M., Corwin, J., Conrad, P., and Rotrosen, J. (1985). Olfactory dysfunction in Alzheimer's disease and Parkinson's disease. *Am. J. Psychiatry* 142, 781–782. doi: 10.1038/nrneurol.2012.80

Shipley, M. T., McLean, J. H., and Ennis, M. (1995). "Olfactory system," in *The Rat Nervous System*, Vol. 2, ed. G. Paxinos (San Diego: Academic Press), 899–926.

Staubli, U., Schottler, F., and Nejat-Bina, D. (1987). Role of dorsomedial thalamic nucleus and piriform cortex in processing olfactory information. *Behav. Brain Res.* 25, 117–129. doi: 10.1016/0166-4328(87)90005-2

Stettler, D. D., and Axel, R. (2009). Representations of odor in the piriform cortex. *Neuron* 63, 854–864. doi: 10.1016/j.neuron.2009.09.005

Stevens, C. F., and Wang, Y. (1994). Changes in reliability of synaptic function as a mechanism for plasticity. *Nature* 371, 704–707. doi: 10.1038/371704a0

Suzuki, N., and Bekkers, J. M. (2006). Neural coding by two classes of principal cells in the mouse piriform cortex. *J. Neurosci.* 26, 11938–11947. doi: 10.1523/JNEUROSCI.3473-06.2006

Tseng, G. F., and Haberly, L. B. (1988). Characterization of synaptically mediated fast and slow inhibitory processes in piriform cortex in an in vitro slice preparation. *J. Neurophysiol.* 59, 1352–1376.

Wenk, G. L., and Barnes, C. A. (2000). Regional changes in the hippocampal density of AMPA and NMDA receptors across the lifespan of the rat. *Brain Res.* 885, 1–5. doi: 10.1016/S0006-8993(00)02792-X

Wilson, D. A., and Sullivan, R. M. (2011). Cortical processing of odor objects. *Neuron* 72, 506–519. doi: 10.1016/j.neuron.2011.10.027

Wysocki, C. J., and Gilbert, A. N. (1989). National Geographic Smell Survey. Effects of age are heterogenous. *Ann. N. Y. Acad. Sci.* 561, 12–28. doi: 10.1111/j.1749-6632.1989.tb20966.x

Conflict of Interest Statement: The authors declare that the research was conducted in the absence of any commercial or financial relationships that could be construed as a potential conflict of interest.

Received: 06 May 2013; accepted: 17 July 2013; published online: 06 August 2013.
*Citation: Gocel J and Larson J (2013) Evidence for loss of synaptic AMPA receptors in anterior piriform cortex of aged mice. Front. Aging Neurosci. **5**:39. doi: 10.3389/fnagi.2013.00039*

© 2014. Published by The Company of Biologists Ltd | The Journal of Experimental Biology (2014) 217, 1024-1039 doi:10.1242/jeb.085381

REVIEW

No oxygen? No problem! Intrinsic brain tolerance to hypoxia in vertebrates

John Larson[1,*], Kelly L. Drew[2], Lars P. Folkow[3], Sarah L. Milton[4] and Thomas J. Park[5]

ABSTRACT

Many vertebrates are challenged by either chronic or acute episodes of low oxygen availability in their natural environments. Brain function is especially vulnerable to the effects of hypoxia and can be irreversibly impaired by even brief periods of low oxygen supply. This review describes recent research on physiological mechanisms that have evolved in certain vertebrate species to cope with brain hypoxia. Four model systems are considered: freshwater turtles that can survive for months trapped in frozen-over lakes, arctic ground squirrels that respire at extremely low rates during winter hibernation, seals and whales that undertake breath-hold dives lasting minutes to hours, and naked mole-rats that live in crowded burrows completely underground for their entire lives. These species exhibit remarkable specializations of brain physiology that adapt them for acute or chronic episodes of hypoxia. These specializations may be reactive in nature, involving modifications to the catastrophic sequelae of oxygen deprivation that occur in non-tolerant species, or preparatory in nature, preventing the activation of those sequelae altogether. Better understanding of the mechanisms used by these hypoxia-tolerant vertebrates will increase appreciation of how nervous systems are adapted for life in specific ecological niches as well as inform advances in therapy for neurological conditions such as stroke and epilepsy.

KEY WORDS: Arctic ground squirrel, Cetacean, Hypoxia, Naked mole-rat, Seal, Turtle

Introduction

Environmental conditions vary enormously for vertebrates, both with respect to the extreme conditions tolerated by a given species at different times and with respect to average living conditions tolerated by different species. Temperature is perhaps the most obvious example: from the poles to the equator, average ambient temperatures vary widely and have been accompanied by physiological adaptations appropriate to resident species; seasonal variations in temperature and resource variability can induce dramatic changes in physiological and/or behavioral patterns including migration and hibernation. Oxygen levels also vary widely, with animals adapted to sea level, high-altitude, underground and aquatic habitats. Oxygen levels can also change dramatically on a shorter-term basis, as can occur in tidal pools or in breath-hold divers.

[1]Psychiatric Institute, Department of Psychiatry and Laboratory of Integrative Neuroscience, Department of Biological Sciences, University of Illinois, Chicago, IL 60612, USA. [2]Institute of Arctic Biology, Alaska Neuroscience Program, University of Alaska, Fairbanks, AK 99775-7000, USA. [3]Department of Arctic and Marine Biology, University of Tromsø – The Arctic University of Norway, Tromsø NO-9037, Norway. [4]Department of Biological Sciences, Florida Atlantic University, Boca Raton, FL 33431-0991, USA. [5]Laboratory of Integrative Neuroscience, Department of Biological Sciences, University of Illinois, Chicago, IL 60607, USA.

*Author for correspondence (jlarson@uic.edu)

Approximately 20% of the oxygen consumed by the human body is used by the brain. The greater part of this oxygen is used to produce the ATP required to maintain the membrane potentials necessary for electrical signaling with synaptic and action potentials (Harris et al., 2012). In many vertebrates, including adult humans, interruption of the oxygen supply to the brain for more than a few minutes leads to irreversible neurological damage, including neuronal death. Without oxidative phosphorylation, ATP-dependent neuronal processes including ion transport and neurotransmitter re-uptake decline sharply. Without pumping, ion gradients fail and neurons depolarize, releasing excessive levels of excitotoxic neurotransmitters such as glutamate and dopamine. The overstimulation of glutamate [*N*-methyl-D-aspartate (NMDA) and alpha-amino-3-hydroxy-5-methyl-4-isoxazolepropionic acid (AMPA)] receptors increases intracellular calcium levels and triggers multiple internal cascades that result in cell damage and death, including activation of lipases, endonucleases and proteases, and mitochondrial-dependent apoptosis (Lipton, 1999). Not all vertebrates, however, are equally susceptible to brain damage resulting from periods of low oxygen. Specializations of brain physiology that have evolved in certain vertebrate species to cope with oxygen deprivation (hypoxia) were the subject of a symposium held during the 10th International Congress of Neuroethology in August 2012. Much has been learned about the catastrophic sequelae of hypoxia that lead to neuronal death; the study of hypoxia-tolerant species has played a major role in advancing this understanding, although significant gaps still remain.

This review focuses on specialized mechanisms in certain vertebrate brains to tolerate either chronic or acute hypoxic challenges imposed directly by extreme environmental conditions or indirectly by physiological/behavioral responses to those conditions. The brains of the particular species that are discussed here are all robustly and intrinsically tolerant to hypoxic challenge but differ markedly in the circumstances in which hypoxia occurs as a normal consequence of habitat and lifestyle. It may be present chronically, during the animal's entire life (naked mole-rats), on a seasonal basis (fresh-water turtles, hibernating ground squirrels) or during execution of particular behaviors necessary for survival (diving seals). It is hoped that consideration of the similarities and differences in how the brains of these different vertebrates cope with hypoxia will increase our appreciation of how nervous systems are adapted for life in specific ecological niches as well as inform advances in therapy for neurological conditions such as stroke and epilepsy.

Down for the count: hypoxia tolerance in the freshwater turtle brain

Among the most robust of hypoxia-tolerant vertebrates is the freshwater turtle *Trachemys scripta*, which can withstand complete anoxia for days at room temperature to weeks in winter hibernation (Jackson and Ultsch, 2010); even at room temperature, 24 h of anoxia and re-oxygenation results in no evident loss of neurons

The Journal of Experimental Biology

The Journal of Experimental Biology (2014) doi:10.1242/jeb.085381

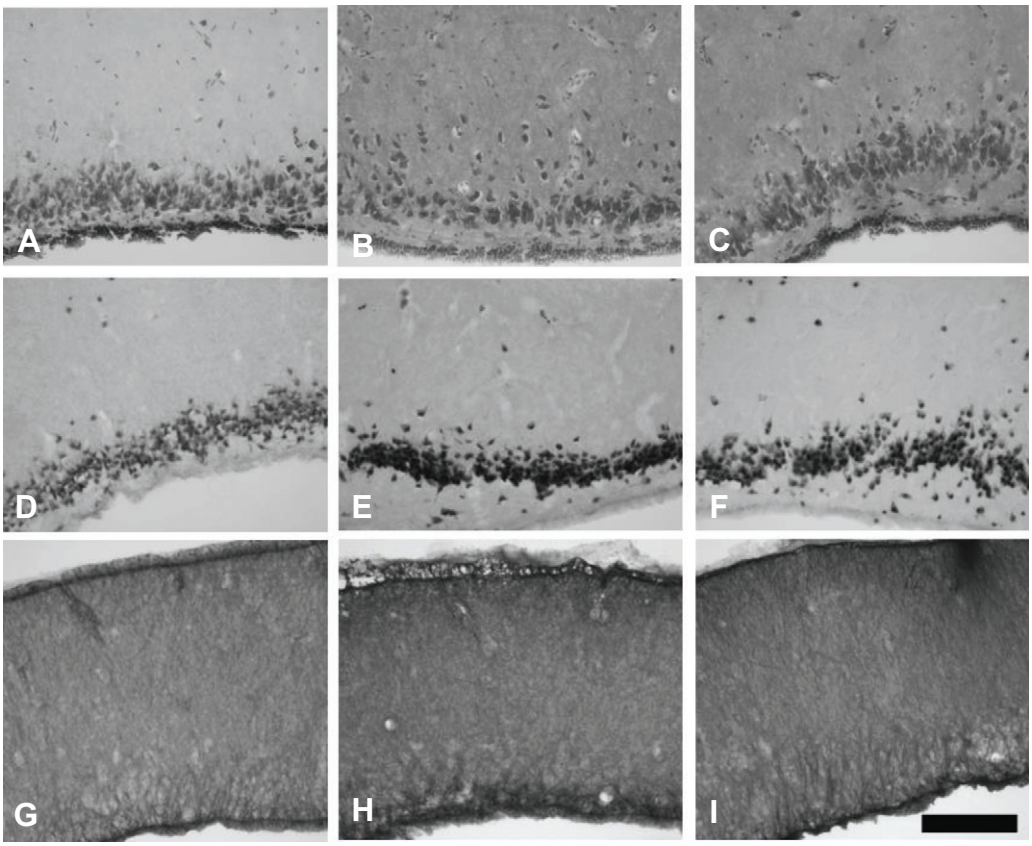

Fig. 1. Analysis of the cortex of the turtle for neuronal damage. (A–C) Cresyl Violet staining. (D–I) Immunolabeling for the neuronal marker NeuN (D–F), and the glial marker GFAP (G–I). Sections of tissue were examined from animals treated as follows: (A,D,G) Control; (B,E,H) anoxia; (C,F,I) anoxia followed by 3 days of survival. Note preservation of neuronal cell band at all time points in Cresyl Violet stained and NeuN-immunolabeled samples. GFAP signals were not increased at 3 days. Scale bar: 200 µm for all. [Figure reprinted from Kesaraju et al. (Kesaraju et al., 2009), with permission.]

(Fig. 1). Hypoxia tolerance in turtle species is not a matter of ectothermy per se, but is due to specific adaptations related to habitat: aquatic turtles with far northern ranges are more anoxia tolerant than southern animals even within a single species (probably because of the need to survive potentially long periods under ice or in hypoxic mud) (Ultsch, 2006). Interestingly, although hatchlings of many turtle species survive in the nest in their first winter through freeze tolerance (Storey, 2006) or super-cooling (Packard and Packard, 2003), in general hatchlings are far less able to tolerate anoxic submergence than adults (Reese et al., 2004). It has been suggested that this is because of their incomplete shell development, as the shell is important for lactate buffering (Ultsch, 2006). However, the development of anoxia tolerance is unknown, as only the hatchling and adult stages have been studied.

As with some of the other models discussed in this review, one mechanism to extend anoxic survival is entrance into a state of deep reversible hypo-metabolism; energy demand is reduced to meet the energy supplied by anaerobic glycolysis. Energy demanding processes are greatly suppressed; in the turtle brain these include decreases in excitatory neurotransmitter release (Milton and Lutz, 1998; Milton et al., 2002; Thompson et al., 2007), and increased neural inhibition (Lutz and Manuel, 1999; Nilsson and Lutz, 1991; Nilsson and Lutz, 1992). Decreased ion permeability (channel arrest), and the suppression of action potentials (spike arrest) also contribute to significant energy savings. Together, the reductions in ion flow and neurotransmitter release result in a reversible ‘coma’ of very reduced brain electrical activity (Fernandes et al., 1997). Protein synthesis is inhibited (Fraser et al., 2001), perhaps through epigenetic mechanisms (Biggar and Storey, 2012; Krivoruchko and Storey, 2010a), the phosphorylation–dephosphorylation of regulatory proteins (Rider et al., 2009) or through cell cycle arrest (Zhang et al., 2013).

Ion channels and neurotransmitters

Recent work has shown that many of these adaptations are intertwined, especially the interactions between neurotransmitter balance and various ion channels, with multiple and apparently redundant effects. For example, gamma-aminobutyric acid (GABA) induces anoxia-like decreases in excitatory post-synaptic potential (EPSP) activity in the normoxic turtle brain, apparently by the pre-synaptic inhibition of glutamate release. GABA also decreases ion current through glutamatergic NMDA and AMPA receptors (Pamenter et al., 2012), such that the stimulus required to generate an action potential increases more than 20-fold (Fig. 2). However, NMDA-receptor (NMDAR)-dependent excitotoxicity is also suppressed by δ-opioid receptors (Pamenter and Buck, 2008) which exist at surprisingly high density in the turtle brain (Xia and Haddad, 2001), and aid resistance to glutamate and hypoxic stress in mammals (Zhang et al., 2000). AMPA receptor currents, meanwhile, are also reduced by activation of mitochondrial ATP-dependent K^+ channels (Zivkovic and Buck, 2010), which in turn also reduce glutamate and dopamine release in early anoxia (Milton and Lutz, 2005; Milton et al., 2002). In longer anoxic exposures, glutamate release is suppressed by adenosine and GABA (Thompson et al., 2007). Adenosine in turn affects channel arrest (Pék and Lutz, 1997; Pérez-Pinzón et al., 1993), dopamine release (Milton and Lutz, 2005; Milton et al., 2002), NMDAR currents (Buck and Bickler, 1998) and cerebral blood flow (Hylland et al., 1994).

Neuroprotection at the molecular level

Despite the many pathways aimed at metabolic suppression, recent work has shown that a variety of protective mechanisms are instead activated at the molecular level in anoxic turtle brain. These include increases in heat shock proteins, anti-apoptotic factors, the MAP kinases, antioxidants and modulation of the p53 pathway.

The Journal of Experimental Biology (2014) doi:10.1242/jeb.085381

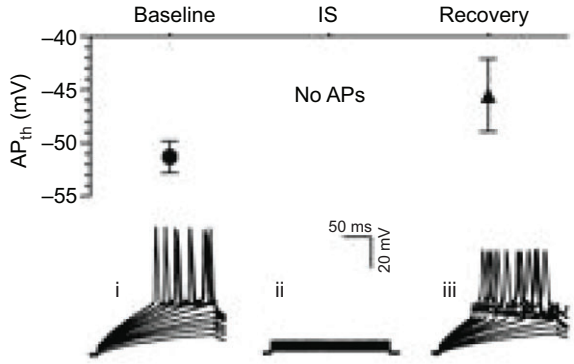

Fig. 2. Cortical neuronal membrane potential (mV) treated with an ischemic mimicking solution depolarizes to E_{GABA}. Top panel: summary of action potential (AP) threshold (AP_{th}) from stimulated neurons treated as indicated. APs could not be elicited during IS (ischemic solution) treatment. Bottom panel: sample recordings of evoked APs recorded during baseline control (i), IS perfusion (ii) and normoxic reperfusion (iii). [Adapted from Pamenter et al. (Pamenter et al., 2012); reprinted with permission from Macmillan Publishers Ltd.]

Interestingly, many of these factors may not only protect against damage under anoxic conditions, but also ameliorate oxidative stress when oxygen is restored.

Induction of the heat shock proteins (HSPs) is one of the first lines of defense against physiological stress, shifting cellular equilibrium away from apoptosis and towards survival (Lanneau et al., 2008; Obrenovitch, 2008). Although their specific roles in anoxia tolerance in the turtle are yet unknown, HSPs increase in a number of organs. Krivoruchko and Storey reported twofold to threefold elevations in several HSPs in skeletal muscle along with increases in both heat shock transcription factor 1 (HSF1) and the nuclear translocation of HSF1 in the heart and muscle (Krivoruchko and Storey, 2010b). In the brain, increases in both Hsp72 and Hsc73 were first reported by Prentice et al. (Prentice et al., 2004). The increase in the heat shock cognate Hsc73 was a novel finding, as this is one of the most abundant intracellular proteins in mammals but is considered unresponsive to stress (Snoeckx et al., 2001). Also surprising was the readily detectable normoxic levels of Hsp72, because in mammals it is essentially undetectable under control conditions (Snoeckx et al., 2001). Additional work has shown high basal levels of numerous HSPs in the brain (Kesaraju et al., 2009) and other organs (Stecyk et al., 2012) and their rapid upregulation in anoxia. Some HSPs continue to increase over 24 h anoxia in the brain; in mammals these are associated primarily with glia, leading to the speculation that in the turtle brain astrocytes may play a significant role throughout anoxia even if neurons shut down much of their function (Kesaraju et al., 2009).

The high normoxic levels of HSPs and rapid increase in response to low oxygen led to the suggestion that turtles essentially show ‘constitutive preconditioning’ in the face of anoxia, with high basal protein levels able to respond immediately to cellular stress (Prentice et al., 2004). Interestingly, Stecyk et al. reported HSP levels are also enhanced by cold temperatures, hypothesizing that turtles will experience winter temperatures before their ponds freeze over, and thus cold may further prepare them for anoxia before oxygen levels are fully depleted (Stecyk et al., 2012).

Hsp72 cytoprotection may occur through inhibition of apoptotic and necrotic cell death pathways (Giffard et al., 2008), with cell fate decided by the equilibrium between stress proteins and the apoptotic pathway (Beere, 2001), especially Bcl-2 and Bax levels. In the turtle brain, the Bcl-2:Bax ratio is maintained (Kesaraju et al., 2009) or slightly elevated (Nayak et al., 2011), in contrast to mammalian hypoxia and ischemia where increases in Bax and decreases in Bcl-2 tip the cell towards apoptosis (Feldenberg et al., 1999). In the turtle brain the balance of pro-death and survival pathways may also be affected by such factors as p53 and the MAP kinases.

The p53 transcription factor regulates the cell cycle, energy metabolism, DNA damage repair and apoptosis (Zhang et al., 2010), and is responsive to cellular stress. p53 is activated by metabolic stress, in part through AMP-activated protein kinase (AMPK) (Vousden and Ryan, 2009; Zhang et al., 2010), which increases in anoxic turtle white muscle (Rider et al., 2009). In addition, a recent study of the p53 target Tp53-induced glycolysis and apoptosis regulator (TIGAR) showed that activation reduced the generation of reactive oxygen species (ROS) and elevated levels of reduced glutathione (Wanka et al., 2012). Because the downregulation of energy pathways and protection against cell death and oxidative stress are hallmarks of anoxia tolerance, it is not surprising to find evidence of p53 activation in the turtle (Zhang et al., 2013). Interestingly, there is also cross-talk between p53 and the phosphoinositide 3-kinase–protein kinase B (PI3K/AKT) pathway (Ladelfa et al., 2011), which is upregulated in the anoxic turtle brain (Milton et al., 2008; Nayak et al., 2011).

Activated PI3K/AKT and extracellular regulated kinase (ERK1/2), generally considered to be cytoprotective, increase in turtle neurons *in vivo* (Milton et al., 2008) and *in vitro* (Nayak et al., 2011), as does Bcl-2. AKT is thought to work in part through interactions with the Bcl-2 family of proteins (Wang et al., 2007), and as with other components of anoxic survival, these pathways are linked to increases in adenosine. Blockade of the adenosine A1 receptor (A1R) prevents their upregulation, and increases levels of the pro-apoptotic factors JNK, p38MAPK and Bax (Nayak et al., 2011).

Anoxic survival mechanisms also reduce ROS damage

Unlike the mammalian brain, which shows an overproduction of reactive oxygen species (ROS) following hypoxia or ischemia/reperfusion (Hashimoto et al., 2003), the turtle brain appears to suppress ROS production upon re-oxygenation (Milton et al., 2007; Pamenter et al., 2007). As with other protective mechanisms, adenosine also impacts the production of ROS upon re-oxygenation (Fig. 3). Blockade of A1 adenosine receptors increases ROS release and cell death (Milton et al., 2007) despite high levels of antioxidants (Pérez-Pinzón and Rice, 1995; Rice et al., 1995; Willmore and Storey, 1997; Willmore and Storey, 2007). Adenosine effects on ROS may occur in part through Bcl-2, as overexpression decreases cell death during oxidative stress by enhancing antioxidant levels and suppressing free radicals (Lee et al., 2001). Recent work in the Milton laboratory has also shown that Hsp72 is involved in the reduction of ROS production (unpublished data). By affecting parts of the apoptotic pathway and possibly mitochondrial stability, then, the increases in Bcl-2, ERK1/2, AKT and certain HSPs are also likely to decrease oxidative stress during the recovery period, when ROS production might otherwise overwhelm even the high antioxidant levels of the turtle brain.

One recently discovered potential antioxidant in the turtle is neuroglobin (Burmester et al., 2000), which has also been studied in other models of hypoxia tolerance (Avivi et al., 2010; Mitz et al., 2009; Roesner et al., 2008; Schneuer et al., 2012). Neuroglobin is strongly upregulated in both hypoxia and upon re-oxygenation in the turtle (Milton et al., 2006; Nayak et al., 2009), and decreasing neuroglobin expression with turtle-specific siRNA doubles ROS

The Journal of Experimental Biology (2014) doi:10.1242/jeb.085381

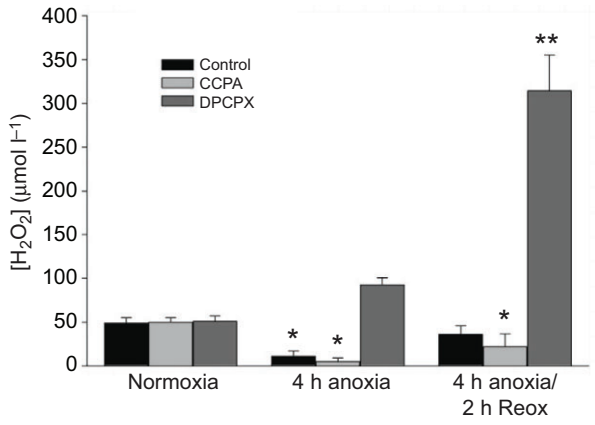

Fig. 3. H_2O_2 concentration in the medium of neuronally enriched primary cell cultures treated with either the adenosine agonist 2-chloro-N6-cyclopentyladenosine (CCPA) or antagonist 8-cyclopentyl-1,3-dipropylxanthine (DPCPX). Anoxia for 4 h significantly decreased ROS production except in DPCPX-treated cells. Re-oxygenation increased ROS production only to normoxic levels in controls, whereas CCPA reduced and DPCPX increased ROS production. Asterisks indicate a signficant difference from normoxic cells, **P*<0.05, ***P*<0.01. Data are means ± s.e.m., *N*=3 independent experiments/group. [Figure adapted from Milton et al. (Milton et al., 2007), with permission.]

release upon re-oxygenation. However, this does not increase cell death, so it appears that turtle neurons are sufficiently protected by other mechanisms to withstand a twofold increase in ROS (Nayak et al., 2009); additional roles for neuroglobin in the turtle brain have not been investigated.

And finally, despite their remarkable tolerance to anoxia, histological examination of *T. scripta* brains that had not been exposed to anoxia in the lab showed some evidence of brain lesions, suggestive of prior damage probably occurring during long periods of anoxia during winter hibernation (S.L.M., unpublished observation). This led us to investigate the possibility of neuronal regeneration as a long-term mechanism of anoxia tolerance. When heavily damaged by global ischemia, *T. scripta* showed evidence of neuronal reproduction within 3 weeks (Kesaraju and Milton, 2009), adding yet another strategy to the toolbox of anoxic survival in these remarkable animals.

Raising the 'dead': mechanisms of hypoxia tolerance in a hibernating species

Hibernation – prolonged periods of suspended blood flow and metabolism

Like the metabolic suppression seen in turtles, certain mammals enter periods of metabolic suppression known as hibernation. Hibernation was initially proposed as a model of resistance to ischemic brain injury because cerebral blood flow declines to levels that would produce ischemic injury in humans (Frerichs et al., 1994). It was subsequently found that brain and other organs of hibernating species resist ischemic injury better than classic rodent models even when animals are not hibernating (Dave et al., 2006; Kurtz et al., 2006) and the same is true for hypoxic injury (Bullard et al., 1960; Drew et al., 2004). Interestingly, because of metabolic suppression during hibernation, arterial partial pressure of oxygen (P_{aO_2}) is similar to other mammals. However, P_{aO_2} falls significantly during arousal from hibernation (Ma et al., 2005). Whether resistance to ischemic or hypoxic injury depends on the hibernation season, and thus seasonal expression of a hibernation phenotype, remains a matter of debate and may depend on the tissue and species studied (Christian et al., 2008; Kurtz et al., 2006). Here we provide a brief overview of hibernation and review evidence for resistance to ischemia/reperfusion (I/R) injury in hibernating species with emphasis on the arctic ground squirrel (AGS), *Urocitellus parryii*.

Hibernation is a means of systemic energy conservation that involves an orchestration of behavioral, physiological and molecular adaptations or specializations that defies the need for resources such as food and water as well as processes such as blood flow. Diverse mammalian species, including one species of primate (Dausmann et al., 2004), hibernate with similar characteristics, such as a decrease in body temperature (T_b) and metabolic rate with a minimum torpid metabolic rate that is on average 5–30% of basal metabolic rate (Geiser, 2004) and inter-bout arousals (Dausmann et al., 2004). When hibernating, animals may spend from a few days to several weeks at a time in a highly regulated and reversible state of prolonged torpor during which whole body metabolic rate, core T_b, heart rate and blood flow plummet to levels seemingly inconsistent with life support. When T_b falls below 30°C, prolonged periods of torpor are interrupted by brief intervals of euthermy during which animals spontaneously return to high, euthermic T_b of 35–37°C (Dausmann et al., 2004; Geiser and Ruf, 1995) and blood flow returns to vital organs in a heterogeneous manner (Osborne et al., 2005).

Tolerance to hypoxia, cerebral ischemia and brain injury during hibernation

During hibernation, metabolic rate drops to a minimum, which in the AGS is 1–2% of resting metabolic rate. While metabolic rate declines, cerebral blood flow decreases as much as 10-fold. Mass-weighted cerebral blood flow in hibernating animals is 7±4 ml 100 g^{-1} min^{-1} compared with 62±18 ml 100 g^{-1} min^{-1} in active, euthermic, animals (Frerichs et al., 1994). Despite prolonged ischemic-like levels in local cerebral blood flow and reperfusion-like return of cerebral blood flow upon arousal, ground squirrels show no evidence of ischemic injury (Frerichs et al., 1994; Ma et al., 2005), and some restorative processes (von der Ohe et al., 2006; Weltzin et al., 2006). In addition to hypo-metabolism, other aspects of the hibernation phenotype may contribute to ischemia tolerance in the hibernating state including cold tissue temperature, immunosuppression, anticoagulant properties of the blood and increased antioxidant defenses (Drew et al., 2001; Zhou et al., 2001).

Resistance to cerebral ischemia/reperfusion injury when euthermic

Even when not hibernating, however, AGS and other species of ground squirrels tolerate hypoxia (D'Alecy et al., 1990) and ischemic-like conditions better than ischemia-vulnerable species such as rat (Christian et al., 2008; Dave et al., 2006; Frerichs and Hallenbeck, 1998). Marked tolerance to hypoxia in fossorial species such as the naked mole rat (Larson and Park, 2009) suggests that tolerance in AGS may be the result of the fossorial nature of ground squirrels. Indeed, ground squirrels and hamsters, both semi-fossorial species, tolerate hypoxia better than other rodent species (Bullard et al., 1960; D'Alecy et al., 1990). Evidence also suggests that the AGS experiences hypoxemia regularly during emergence from hibernation and that hypoxemia and ischemia tolerance may be related to selective pressures associated with transitions into and out of torpor (Ma et al., 2005) (Fig. 4). During rewarming and in some cases, during euthermy MAPK stress pathways are activated and nitric oxide synthase (iNOS), another indicator of cellular stress, is increased (Zhu et al., 2006). Moreover, Hypoxia-inducible factor 1-alpha (HIF-1α) increases after rewarming and remains elevated

The Journal of Experimental Biology (2014) doi:10.1242/jeb.085381

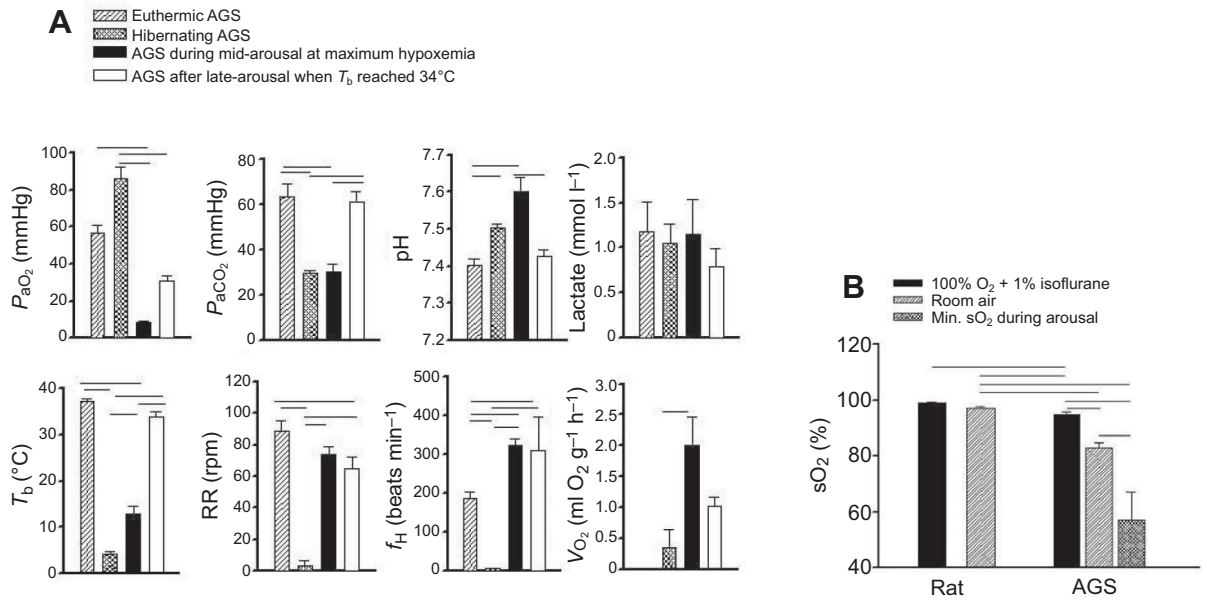

Fig. 4. P_{aO_2} and oxygen saturation during torpor and arousal in arctic ground squirrel (AGS) shows evidence of hypoxemia during arousal. Note also that in euthermic AGSs (i.e. those that are not hibernating) P_{aO_2} and oxygen saturation (sO_2) are lower than in the hibernating state or in rat. (A) Mean blood gas values, and other parameters during arousal at maximum hypoxemia (mid arousal) and during late arousal in AGS compared with euthermic (n=8) and hibernating AGS (n=7) during torpor and arousal, at the time when P_{aO_2} was minimal, and after T_b reached 34°C. (B) Hemoglobin sO_2 in euthermic AGS (n=9) and rats (n=8) under light anesthesia (100% O_2 with isoflurane, 1%) and while breathing room air. sO_2 was monitored in another group of AGS during arousal from hibernation and the minimum sO_2 recorded during arousal is shown for comparison with euthermic levels. Horizontal lines indicate significant difference between groups. T_b, core body temperature; RR, respiratory rate; f_H, heart rate; V_{O_2}, rate of O_2 consumption. [From Ma et al. (Ma et al., 2005).]

during euthermy (Ma et al., 2005). Marked synaptogenesis and activation of proliferative stress activated signaling pathways following rewarming from hibernation suggest that AGSs may benefit from restorative processes during periods of inter-bout euthermy (Drew et al., 2004; von der Ohe et al., 2006; Weltzin et al., 2006), and like turtles, restorative processes may contribute to tolerance to ischemia and anoxia (Drew et al., 2011; McGee et al., 2008; Popov et al., 2011).

Studies designed to tease out the influence of the hibernation state on protection from hypoxia and I/R in isolated brain tissue found that cold tissue temperature alone could account for enhanced protection in the hibernating state. When hippocampal slices from AGS are exposed to oxygen and glucose deprivation (OGD) at 36–37°C, resistance to injury is similar regardless of the torpid state of the animal (Christian et al., 2008; Ross et al., 2006). Tolerance to OGD *in vitro* suggested that AGSs would tolerate global cerebral ischemia *in vivo*. Dave et al. challenged summer active AGSs and rats with 8 min of asphyxia leading to cardiac arrest (Dave et al., 2006). Although asphyxia induced an immediate bradycardia and cardiac arrest in both species, only rats showed significant cell death in hippocampus, striatum and cortex 7 days after restoration of spontaneous circulation (Dave et al., 2006) (Fig. 5). In a subsequent study, summer active AGSs challenged with 10 min of asphyxia showed no significant loss of healthy neurons in the vulnerable CA1

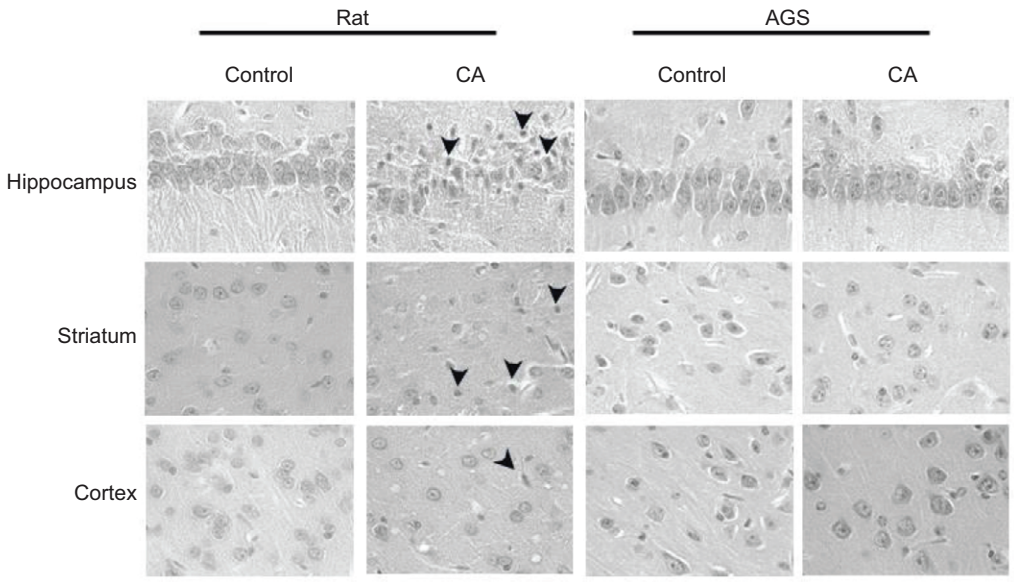

Fig. 5. Arctic ground squirrels (AGSs) resist injury in all regions studied including the hippocampus, striatum and cortex following cardiac arrest. Representative histological images of the hippocampal CA1 region of AGSs and rats subjected to sham or 8 min of asphyxia leading to cardiac arrest. Spontaneous circulation was restored within 120 s and tissues were collected for histopathology 7 days later. Sections were stained with Hematoxylin and Eosin. Arrowheads indicate ischemic neurons. All images were captured at 40× magnification. [From Dave et al. (Dave et al., 2006).]

region of the hippocampus when compared with naïve AGSs (Dave et al., 2009).

Resistance to cerebral ischemia/reperfusion injury in the arctic ground squirrel does not require preparation for the hibernation season or the hibernation state

Resistance to brain injury following cardiac arrest in summer active (euthermic) AGSs led to doubt about how much of the tolerance to I/R noted in AGSs was due to the hibernation season and how much was intrinsic to the species. Liver and intestine isolated from the thirteen-lined ground squirrel during inter-bout arousal resist I/R injury; however, tolerance is lost or decreased when tissue is obtained from animals during the summer season (Kurtz et al., 2006; Lindell et al., 2005). By contrast, in AGS, tolerance to cerebral I/R in acute hippocampal slices is actually greater during the summer season than during winter inter-bout euthermy; where, only during inter-bout euthermy is any difference noted between active and hibernating ground squirrels (Christian et al., 2008). In other species, the state of hibernation seems to enhance tolerance relative to active (euthermic) animals and rats, although, as bath temperature is decreased, tolerance of brain slices from active animals approaches the degree of tolerance observed in slices from hibernating animals (Frerichs and Hallenbeck, 1998). In future studies better distinction between summer euthermic, winter inter-bout euthermy, and winter season animals that do not show signs of hibernation might clarify if or when the hibernating state contributes to ischemia tolerance. Importantly, cooler temperatures clearly increase tolerance and are expected to play a primary role in neuroprotection in hibernating AGS *in vivo* (Zhou et al., 2001).

Resistance to ischemia/reperfusion in the euthermic state involves events downstream of loss of ATP and NMDAR activation

Tolerance to OGD in euthermic AGSs involves aspects of enhanced ion homeostasis and events downstream of NMDAR activation. OGD leads to a loss of ATP in brain slices from AGSs as it does in brain slices from rats (Christian et al., 2008). Despite a loss of ATP, ionic homeostasis persists longer in AGSs than in rats both *in vitro* and *in vivo*, and preservation of ionic homeostasis in AGSs depends upon protein kinase C epsilon (εPKC) signaling. Dave et al. monitored ischemic depolarization (ID) in cerebral cortex during cardiac arrest *in vivo* and during OGD *in vitro* in acutely prepared hippocampal slices from AGS and rat (Dave et al., 2009). In both the *in vitro* and *in vivo* models of global cerebral ischemia, the onset of ID was significantly delayed in AGS compared with rat. During cardiac arrest, ID occurred on average at 1.9 min in rat and at 3.1 min in AGS. During OGD in hippocampal slices, ID occurred at 2.8 min in rat and at 6.6 min in AGS. The selective peptide inhibitor of εPKC (eV1-2) shortened the time to ID in brain slices from AGSs but not in rats even though εV1-2 decreased activation of εPKC in brain slices from both species. Activation of εPKC inhibits Na^+/K^+ATPase and voltage-gated sodium channels (Chen et al., 2005; Nowak et al., 2004), both of which contribute to the collapse of ion homeostasis during ischemia and may be targets of εPKC during cerebral ischemia in AGSs (Dave et al., 2009). Blocking or delaying the ID can significantly improve recovery (Anderson et al., 2005; Takeda et al., 2003).

Other mechanisms downstream of delayed ID may also contribute to cerebral ischemia tolerance in AGS. During cerebral ischemia, the loss of neuronal membrane potential that leads to ID results in the massive release of neurotransmitters, including the excitatory neurotransmitter glutamate (Lipton, 1999). Glutamate efflux into the extracellular space activates NMDA and AMPA receptors, causing excitotoxic calcium influx (Lipton, 1999).

Although ID is delayed in AGS, once it occurs glutamate efflux approximates efflux seen in rat hippocampal slices, but with minimal evidence of cell death in AGS (Drew et al., 2012). Thus, glutamate released during OGD in AGS hippocampal slices is not excitotoxic. Attenuated excitotoxicity in AGS is further supported by evidence in the semi-acute slice preparation developed by Ross et al. in which 500 μmol l^{-1} NMDA plus 20 mmol l^{-1} KCl fails to induce cell death in AGS (Ross et al., 2006). By contrast, the same concentrations of NMDA and KCl applied to slices from rat produces a significant increase in cell death (Ross et al., 2006). Protective mechanisms downstream to glutamate efflux may be related to differences in the effects of glutamate receptor activation in AGS compared with rat.

Lower levels of functional NMDA receptors located in the plasma membrane and less glutamate-induced increases in intracellular calcium are associated with ischemia tolerance in euthermic AGS. Membrane expression of NR1, an obligatory subunit of the NMDA receptor, is lower in AGS (both active and hibernating) than in rat (Zhao et al., 2006). Moreover, intracellular calcium increased by bath-applied glutamate does not exceed 400 nmol l^{-1} in hippocampal slices prepared from euthermic or hibernating AGS, whereas in rats intracellular calcium increased by bath-applied glutamate exceeds 500 nmol l^{-1} (Fig. 6) (Zhao et al., 2006). Evidence of blunted excitotoxicity and blunted calcium responses to glutamate is consistent with similar phenomena in the naked mole-rat (Peterson et al., 2012a; Peterson et al., 2012b).

AGSs do not rely on glycogen or oxidative phosphorylation for energy needs during OGD

Many organisms tolerant of low oxygen levels possess large stores of glycogen and pH buffering mechanisms that fuel and protect against pH shifts resulting from anaerobic glycolysis (Jackson, 2004; Lutz and Milton, 2004). Indeed, AGSs demonstrate enhanced pH buffering capacity because blood pH remains around 7.4 despite arterial P_{CO_2} levels of 60 mmHg (Ma et al., 2005) and arterial HCO_3^- concentrations tend to be higher in AGS than in rat. However, ischemia tolerance cannot be explained by enhanced peripheral stores of glycogen. Firstly, glucose derived from glycogen is not expected to reach ischemic tissue when blood flow is stopped during cardiac arrest. Secondly, addition of iodoacetate, an inhibitor

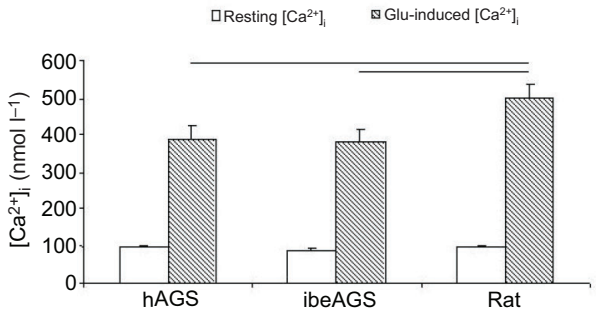

Fig. 6. Hibernating arctic ground squirrel (hAGS), AGS in the inter-bout euthermic state between bouts of torpor (ibeAGS) and rats display similar resting internal calcium concentrations $[Ca^{2+}]_i$. Glutamate induces a significant increase in $[Ca^{2+}]_i$ in all groups, however, both ibeAGS and hAGS show less glutamate-induced $[Ca^{2+}]_i$ increase compared with rat. Organotypic hippocampal slices were loaded with fura-2AM for calcium imaging under control conditions and after treatment with glutamate. Horizontal bars indicate significant difference between groups, $P<0.05$, n=12–17 slices per group. [From Zhao et al. (Zhao et al., 2006).]

of glycolysis, which would negate any benefit from glycogen, as well as the addition of NaCN, an inhibitor of cellular respiration, which would prevent use of residual oxygen in the bath, during OGD fails to increase cell death in an acute slice preparation (Christian et al., 2008).

In summary, arctic ground squirrels, similar to other hibernating rodents, experience periods of prolonged torpor when oxidative metabolism and other life-supporting processes are suspended for weeks at a time. For unknown reasons torpor is interrupted by brief, albeit regular periods of euthermy. During regular arousal to euthermy AGSs experience hypoxemia with less than 60% O_2 saturation in arterial blood (Ma et al., 2005). Despite these periods of hypoxemia, AGSs and other rodent species recover from hibernation without injury and show signs of restorative processes including synaptogenesis (von der Ohe et al., 2006) and cognitive enhancement (Weltzin et al., 2006). Similarly, when challenged by a number of experimental models of I/R, hibernating species including AGS resist injury to the brain as well as other organs. Studies show that resistance to I/R injury in the brain is independent of the hibernation season or the hibernation state (Christian et al., 2008; Dave et al., 2006; Dave et al., 2009). In hippocampal slices from AGS, oxygen and glucose deprivation produces an overflow of glutamate but dramatically less cell death than in slices from rat (Drew et al., 2012). AGS hippocampal slices also resist NMDA-induced excitotoxicity and demonstrate smaller increases in intracellular calcium following bath application of glutamate (Ross et al., 2006; Zhao et al., 2006). Taken together evidence points to species-dependent differences in NMDAR function that contributes to resistance to I/R injury in AGS brain.

When the brain goes diving: adaptations for hypoxia tolerance in diving mammals

Although in diving mammals periods of hypoxia exposure are shorter than those seen in the hibernating turtle or ground squirrel, their aquatic lifestyles, involving both breath-hold diving and exercise, may still induce severely hypoxic conditions. During diving, these animals rely on large endogenous stores of O_2 – either bound to hemoglobin in their blood or to myoglobin in their skeletal muscles – to support oxidative metabolic processes (Burns et al., 2007; Lenfant et al., 1970; Scholander, 1940). Such adaptations, along with cardiovascular and metabolic adjustments (Blix and Folkow, 1983; Folkow and Blix, 2010; Ponganis et al., 2011; Scholander, 1940), enable some seals and whales to remain submerged for a staggering 2 h (Hindell et al., 1991; Watkins et al., 1985). But towards the end of dives, arterial blood O_2 tension may still drop to only 12–20 mmHg, even during routine free diving (Meir et al., 2009; Qvist et al., 1986; Scholander, 1940), and encephalographic recordings made during simulated diving in seals have shown that cerebral integrity is maintained down to 7–10 mmHg (Elsner et al., 1970; Kerem and Elsner, 1973). These levels are lower than ‘the critical arterial O_2 tension’ of 25–40 mmHg, at which impairments from limitations in ATP production are first seen in brains of non-diving mammals (Erecińska and Silver, 2001), which begs the question: how does the brain of diving mammals cope with repeated and extreme hypoxemia during diving?

Cerebral substrate supply

Cerebral blood flow is generally well maintained during prolonged simulated diving in seals, despite the otherwise widespread vasoconstrictor response (Blix et al., 1983; Zapol et al., 1979), and the challenge encountered by the diving brain therefore is different from that of the ischemic brain. However, blood-borne glucose will be delivered in steadily declining amounts (Guppy et al., 1986), particularly during long dives, because glucose then cannot be readily replenished from the liver due to its much reduced blood supply (Blix et al., 1983; Zapol et al., 1979). However, data from freely diving seals suggest that blood glucose depletion does not limit diving capacity (Guppy et al., 1986), which in part is related to the favorably low brain-mass-to-blood-volume ratio of seals (Hochachka, 1981). Brain metabolism may also be further supported by endogenous stores of glycogen, which are larger in divers than in non-divers by a factor of two to three but still quite small compared with those of skeletal and cardiac muscles (Kerem et al., 1973). Thus, the steadily declining blood O_2 content remains the major challenge to the diving brain.

O_2 diffusion and possible roles of neuroglobin

One possible compensatory adaptation to the hypoxemic challenge would be to maintain a high cerebral capillary density, which would reduce the diffusion distance and thereby improve the flow of O_2 to neurons. Indeed, two studies suggest that the brain capillary density of seals and whales is higher than in typical non-diving species (Glezer et al., 1987; Kerem and Elsner, 1973).

Downstream, cellular O_2 flow might be enhanced by means of facilitated intracellular diffusion, i.e. as achieved by myoglobin in skeletal muscle cells (Wittenberg and Wittenberg, 2003). Diving mammals maintain high levels of both myoglobin and hemoglobin and might therefore be expected to also carry higher loads of the neurally based neuroglobin. This globin, discovered about a decade ago (Burmester et al., 2000), is thought to play a key role for maintenance of aerobic metabolism in neural tissue, possibly by facilitating O_2 diffusion (Burmester and Hankeln, 2009). However, neuroglobin may also have other functions related to hypoxia defense, such as the detoxification of reactive oxygen species (ROS) (Burmester and Hankeln, 2009) that are generated during and after diving (Zenteno-Savín et al., 2002). Interestingly, studies in the deep-diving hooded seal (*Cystophora cristata*) have revealed that their cerebral neuroglobin levels are not higher than those of rodents or man (Mitz et al., 2009). Instead, the protein has an unusual cellular distribution, with higher levels in glial cells (astrocytes) than in neurons. This distribution, which contrasts with that in terrestrial mammals (Mitz et al., 2009), was later confirmed in other seal species (Fig. 7A) (Schneuer et al., 2012). Because neuroglobin has repeatedly been shown to be closely associated with mitochondria, thereby implying a key role in oxidative metabolism (Burmester and Hankeln, 2009; Mitz et al., 2009), these findings suggest that in the seal brain, glial cells are more involved in aerobic metabolism than are neurons. This further implies that seal brain neurons depend more heavily on anaerobic metabolic pathways, whereas glial cells/astrocytes may remove and metabolize the lactate that thereby is produced, and that seal brains may have a reversed lactate shuttle system compared with non-diving mammals (Mitz et al., 2009; Schneuer et al., 2012), a hypothesis that is currently under investigation. Whales, in contrast, have recently been shown to have a typical mammalian neuroglobin distribution, with higher levels in neurons than in astrocytes (Fig. 7B), but in whales neuroglobin mRNA expression levels are 4 to 15 times higher than in seal, cow (*Bos taurus*) and ferret (*Mustela putorius furo*) brains (Fig. 7C) (Schneuer et al., 2012). This finding is consistent with a possible role for neuroglobin in facilitated diffusion and local storage of O_2 within whale neurons. It, thus, appears that neuroglobin may convey brain hypoxia tolerance in both seals and whales, but that its role is quite different in the two orders.

The Journal of Experimental Biology (2014) doi:10.1242/jeb.085381

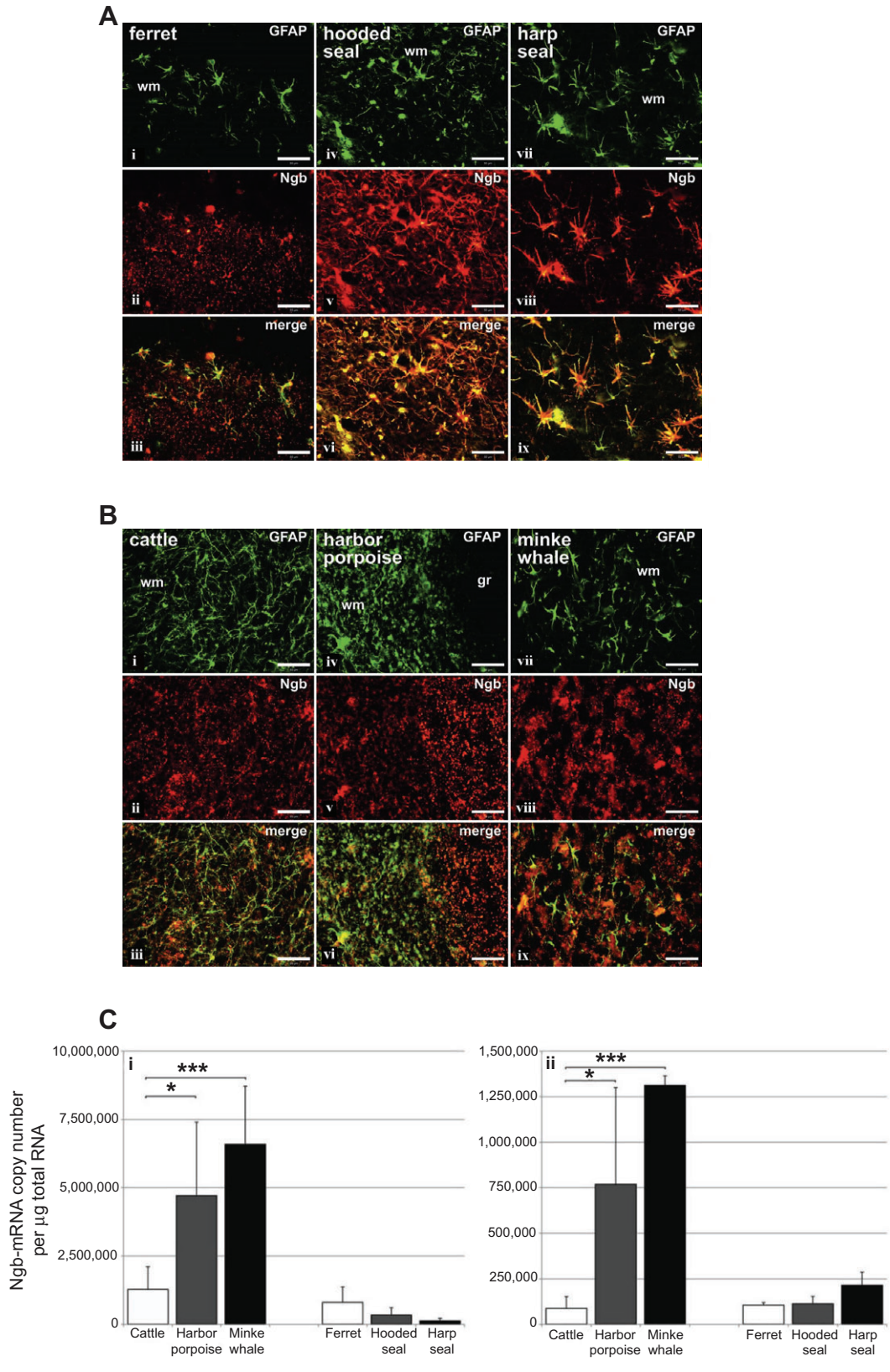

Fig. 7. Neuroglobin distribution. (A) Immunofluorescence of the glial marker glial fibrillary acidic protein (GFAP; green) and neuroglobin (Ngb; red) in the cerebrum of ferret, *Mustela putorius furo* (i–iii), hooded seal, *Cystophora cristata* (iv–vi) and harp seal, *Pagophilus groenlandicus* (vii–ix), showing colocalization of GFAP and Ngb (merge; yellow) in astrocytes in hooded and harp seals (vi,ix), but to a much lesser extent in ferrets (iii), in which Ngb immunoreactivity was observed in cortical neurons (c). (B) Immunofluorescence of GFAP (green) and Ngb (red) in the cerebrum of cattle, *Bos taurus* (i–iii), the odontocete harbor porpoise, *Phocoena phocoena* (iv–vi) and the mysticete minke whale, *Balaenoptera acutorostrata* (vii–ix), showing Ngb immunoreactivity in neurons of the cerebral cortex in all species (ii,v,viii) and only marginal colocalization of GFAP and Ngb (merge; yellow) in astrocytes (iii,vi,ix). (C) Quantification of Ngb mRNA expression in (i) the cerebral cortex and (ii) the cerebellum of whales and seals compared with cattle and ferret. In both brain regions, whales show significantly higher Ngb mRNA levels compared with cattle, ferret and seals (***P≤0.001, *P≤0.05). wm, white matter; gr, gray matter. Scale bars: 50 µm. [Reprinted and modified from Schneuer et al. (Schneuer et al., 2012), with permission from Elsevier.]

Enhanced cerebral anaerobic capacity

Cerebral tolerance towards extreme diving hypoxia may, thus, depend on a high anaerobic capacity. Earlier studies in seals subjected to simulated diving have shown that lactate levels rise in the venous effluent from their heads (which presumably is dominated by cerebral venous drainage), but only towards the end of long dives, when arterial blood O_2 tension drops below 25 mmHg and the difference in arterio-venous blood oxygen content starts to decrease (Hochachka, 1981; Kerem and Elsner, 1973). This suggests that the brain's dependence on anaerobic metabolism rises as the animal becomes

severely hypoxemic. The maintained blood glucose supply (Guppy et al., 1986) in combination with fairly large endogenous glycogen stores (Kerem et al., 1973) and a high enzymatic capacity for anaerobic glycolysis in brains of divers (Messelt and Blix, 1976; Murphy et al., 1980; Shoubridge et al., 1976) all indicate enhanced cerebral anaerobic capacity, although not likely to be sufficient to support normal resting brain function (Hochachka, 1981). However, *in vitro* recordings from spontaneously active isolated neocortical slices from hooded seals have shown that these may maintain a high spiking activity for up to 60 min in severe hypoxia (Ramirez et al., 2011), and hooded seal cerebellar slices may even maintain a high spontaneous activity for durations of 10–15 min in chemical anoxia (2 mN NaCN) (L.P.F., S. Ludvigsen and S. Geiseler, unpublished observations), as also previously demonstrated in eider ducks, *Somateria mollissima* (Ludvigsen and Folkow, 2009). The ATP required to maintain neural integrity and activity under the latter conditions must have been derived through anaerobic pathways, because CN^- effectively blocks oxidative phosphorylation.

Evidence of cerebral hypometabolic responses

Regardless of mode of ATP production, the diving brain would benefit if its metabolic activity was depressed during the asphyxic challenge. Some depression is likely to result from the Q_{10} effect of the up to 3–4°C drop in brain temperature that has been documented in harp seals (*Pagophilus groenlandicus*) and hooded seals during simulated diving (Fig. 8) (Blix et al., 2010; Odden et al., 1999). Such brain cooling probably also protects neurons by limiting both primary and secondary injury through its other known effects on metabolic, molecular and cellular events (Yenari and Han, 2012). Also, data from harbor seals (*Phoca vitulina*) that were subjected to simulated dives in the laboratory suggest that cerebral O_2 uptake does decrease towards the end of long dives, but a simultaneous rise in lactate release implies that this drop – at least in part – reflects insufficient oxygen supply, rather than metabolic depression (Kerem and Elsner, 1973). However, evidence for direct intrinsic hypometabolic responses to hypoxia and/or chemical anoxia have been derived from other tissues: in *in vitro* studies of both seal liver (Hochachka et al., 1988) and kidney slices (Hong et al., 1982), which seem to display both metabolic arrest (depressed ATP production rates) and channel arrest (reduced ion permeability) in response to O_2 deprivation (Hochachka et al., 1988; Murphy et al., 1980). A similar (pilot) study using seal brain slices suggested normal mammalian hypoxia sensitivity (Hochachka et al., 1988), but more recent studies show that the cerebral hypoxia tolerance of these animals is due, in part, to intrinsic neuronal properties, because intracellularly recorded cortical pyramidal neurons of acute brain slices from hooded seals maintain near-normal resting membrane potential (Fig. 9) and the ability to generate action potentials when stimulated, even when subjected to severely hypoxic conditions that cause mouse neurons to rapidly depolarize (Folkow et al., 2008). Also, as in eider ducks (Ludvigsen and Folkow, 2009), isolated cerebellar slices from seals can have differential responses to hypoxia or chemical anoxia, in that some sites maintain spontaneous activity whereas others shut down but recover even after 1 h of insult (L.P.F., S. Ludvigsen and S. Geiseler, unpublished observations). This suggests that some neurons may enter into an inactive state while others remain active, which possibly reflects a reconfiguration at the organ level that would allow some networks to continue to control vital functions while others conserve energy by entering into a hypometabolic state (Ramirez et al., 2007). Studies of cellular processes that may underlie the unusual neural hypoxia tolerance of diving mammals and which could also explain their apparent high resistance towards post-dive oxidative stress and damage (e.g. studies of Ca^{2+} influx rates and NMDA receptor functions of neuroglobin and of cerebral antioxidant capacity) are under way, but at a pace that is set by the inherent logistic difficulties involved in accessing and studying these mammals from this perspective.

Buried alive! Arrested development and hypoxia tolerance in the naked mole-rat

In contrast to the other species discussed so far, fossorial animals experience chronic environmental hypoxia, rather than seasonal or occasional episodes of oxygen deprivation. African naked mole-rats (*Heterocephalus glaber*), are unusual even among other subterranean and other mole-rat species. Most notably, they are cold-blooded (Buffenstein and Yahav, 1991), they are the longest-lived rodent known – with lifespans exceeding 30 years (Buffenstein, 2008) – and they live in a eusocial structure similar to ants and bees (Jarvis, 1981). A key aspect of the naked mole-rat's lifestyle in the context of our investigations is that they live in colonies with a great many individuals, some colonies having more than 300 members (Brett, 1991). The combination of a large number of extremely

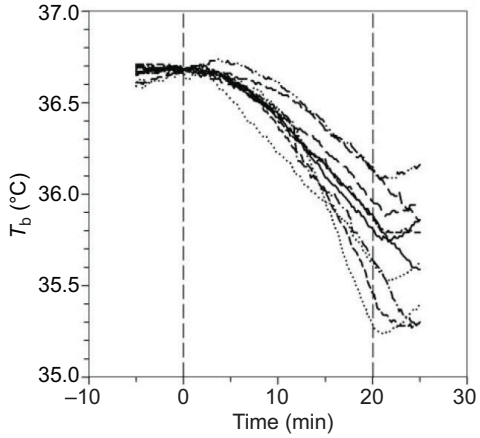

Fig. 8. Changes in brain temperature (T_{brain}; °C) of a hooded seal during 10 experimental dives lasting for 20 min (between vertical bars) and during the first 5 min of the recovery period. Lines for individual dives were normalized to fit the median brain temperature at the start of diving (t=0). [Reprinted from Blix et al. (Blix et al., 2010).]

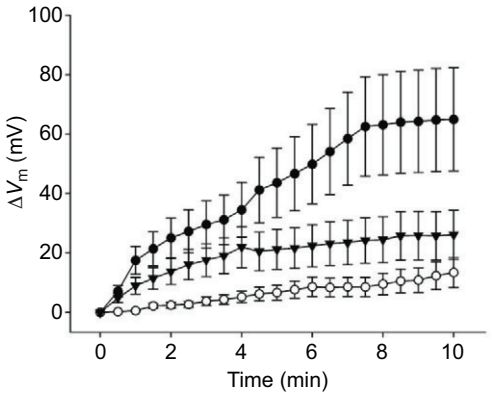

Fig. 9. Average membrane potential changes (ΔV_m) in cortical pyramidal neurons of hooded seals and mice, as evaluated every 30 s during the initial 10 min of severe hypoxia. Closed circles, adult mice (n=14); closed triangles, neonatal mice (n=10); open circles, adult hooded seals (n=7). Values are means ± s.e.m. [Reprinted from Folkow et al. (Folkow et al., 2008), with permission from Elsevier.]

social animals living in a crowded subterranean space where ventilation is poor means that naked mole-rats are exposed to chronically low levels of O_2 (and high levels of CO_2). Although gas concentrations have not been measured in naked mole-rat burrows in nature, in other fossorial species O_2 levels can be as low as 6–14% and CO_2 levels can be as high as 6–10% (Arieli, 1979; van Aardt et al., 2007). Because most of these measurements are for burrows of solitary animals or small colonies, levels in large colonies of naked mole-rats may reach even more extreme values. Consistent with living in an oxygen-deprived environment, naked mole-rats have high-O_2-affinity hemoglobin (Johansen et al., 1976), and a low resting metabolism (Buffenstein and Yahav, 1991).

In addition to the chronic environmental hypoxia of fossorial life, naked mole-rats also experience acute hypoxia during certain behaviors such as foraging and tunnel excavation. We studied the acute response of naked mole-rat brain tissue to hypoxic challenge in two ways using hippocampal slices maintained *in vitro* (Larson and Park, 2009). In the first, we measured the oxygen sensitivity of synaptic transmission in slices from naked mole-rats and mice. Slices were maintained in 'interface-style' chambers where the lower surface is exposed to the artificial cerebrospinal fluid perfusate and the upper surface is exposed to 100% O_2 (less 5% CO_2 to maintain pH with a bicarbonate buffer system). In this type of chamber, the slice draws O_2 directly from the chamber atmosphere and it is standard practice to use a 'carbogen' gas mixture containing enough CO_2 (5%) to buffer the pH of the artificial cerebrospinal fluid (ACSF) and the balance (95%) containing pure O_2. The situation regarding O_2 availability to the tissue is very different from that *in vivo*; however, it is worth noting that the timing of neuronal responses to hypoxia in interface slice chambers more closely models *in vivo* responses to ischemia than in slices submerged in artificial cerebrospinal fluid where the O_2 supply is limited to that dissolved in the medium (Croning and Haddad, 1998). After a baseline period, various portions of the oxygen in the atmosphere above the slice surfaces were replaced with N_2 for 30 min, and then returned to 100% O_2. Synaptic transmission was measured as the amplitude of field excitatory post-synaptic potentials evoked by stimulation of Schaffer-commissural fibers in field CA1. Slices from both mice and naked mole-rats tolerated replacement of half the oxygen atmosphere with nitrogen equally well. However, further reductions of the O_2 supply caused divergent effects on mouse and naked mole-rat slices. Fig. 10 shows example data from slices exposed to 15, 10 or 0% O_2 (Fig. 10A,B,E). In each case, the mouse slice showed a much more rapid and severe decline in function compared with the naked mole-rat slice. Summary data show that slices from naked mole-rats are much more resistant to hypoxia challenge (Fig. 10C), and are much more likely to recover after severe hypoxia (Fig. 10D) than slices from mice.

In a second set of experiments, we measured the time required to abolish all electrical activity in slices from mice and naked mole-rats after replacement of all O_2 in the slices' atmosphere with N_2 (nominal anoxia). In mice, removal of O_2 triggers a rapid (1–2 min) suppression of synaptic transmission, followed by a sudden loss of antidromic spikes and fiber volleys (presynaptic action potentials) and a spreading depression-like extracellular DC potential shift due to synchronized loss of membrane potentials and efflux of potassium. In mice, the anoxic depolarization occurs approximately 3.5 min after anoxia onset at 35°C. In slices from naked mole-rats, the suppression of synaptic transmission is delayed and progresses more slowly, with the anoxic depolarization occurring about 13 min after anoxia onset (Fig. 10F). All of these changes occurred more slowly at 30°C but the difference between mouse and mole-rat remained.

These results indicate that isolated brain slices from naked mole-rats are remarkably tolerant of acute hypoxic challenge. Anoxic depolarization is one step in a cascade of neuronal processes that occur during oxygen deprivation, including alterations in metabolic enzymes and ion channels, release of neurotransmitters (glutamate, adenosine) and activation of receptor-coupled signaling mechanisms (Erecińska and Silver, 2001; Lipton, 1999). A key element of the hypoxia cascade that determines whether the cellular response is reversible or leads to cell death is the accumulation of free intracellular calcium ions, which trigger cytotoxic mechanisms (Deshpande et al., 1987; Lee et al., 1991). In a study using the calcium indicator, fura-2, we found that calcium accumulation during hypoxia is very much lower in brain slices from naked mole-rats compared with age-matched mice (Peterson et al., 2012a). Fig. 11 shows change in calcium over time, before, during and after a 10 min exposure to hypoxia for neonatal and weanling (considered adult-like) mice (Fig. 11A) and naked mole-rats (Fig. 11B). The downward deflection in the curves corresponds to increasing levels of intracellular calcium. For both species there was significantly more calcium taken up by slices from older animals. However, the species differences at both ages are dramatic (Fig. 11C). In fact, the 10 min exposure had no appreciable effect on the neonatal naked mole-rats, so we had to test an additional group with a longer duration (Fig. 11D) to produce an effect.

The extreme tolerance of naked mole-rat brain to hypoxia calls to mind the well-known tolerance of mammals as neonates (Bickler, 2004) and led us to suggest that hypoxia tolerance in the naked mole-rat brain might result from retention of juvenile characteristics into the adult period (Larson and Park, 2009). The results from the calcium imaging experiments are consistent with this and, incidentally, the ability to load slice neurons from naked mole-rats with fura-2 far beyond weaning age is also highly suggestive (Peterson et al., 2012a). The 'neoteny hypothesis' for naked mole-rat brain also explains two other observations that we made in our initial studies of neuronal electrophysiology in hippocampal slices: a lack of synaptic (paired-pulse) facilitation and an insensitivity to exogenous adenosine – two features only observed in hippocampus of typical lab rodents very early in postnatal development (Larson and Park, 2009).

In order to pursue this hypothesis further, we examined the expression of NMDA receptor subunits in brains of neonatal and adult mice and naked mole-rats. NMDA receptors are important mediators of hypoxia-induced excitotoxicity and show dramatic shifts in subunit composition from the neonatal period to adulthood in rats and mice: most forebrain neurons express the GluN2B subunit at high levels in the neonatal period and high levels of GluN2A in adulthood. Moreover, Bickler and colleagues have shown that the GluN2D subunit expressed at higher levels in neonatal rat brain actually prevents calcium fluxes rather than mediating them in response to hypoxic conditions (Bickler et al., 2003). We used immunoblotting to compare NMDA receptor subunit expression changes from neonatal to adult periods in mice and naked mole-rats brain (Peterson et al., 2012b). Although expression levels between species could not be directly compared since the antibody may not have the same affinity for proteins in both, we could compare the relative decrease (or increase) in expression from the neonatal to adult periods within each species. GluN2A and GluN2B did not show significant between-species differences in relative change from neonate to adult. However, adult naked mole-rat brain retains a remarkably higher proportion of GluN2D (66% of neonate) compared with adult mouse brain (13% of neonate). This is highly significant since GluN2D was implicated

The Journal of Experimental Biology (2014) doi:10.1242/jeb.085381

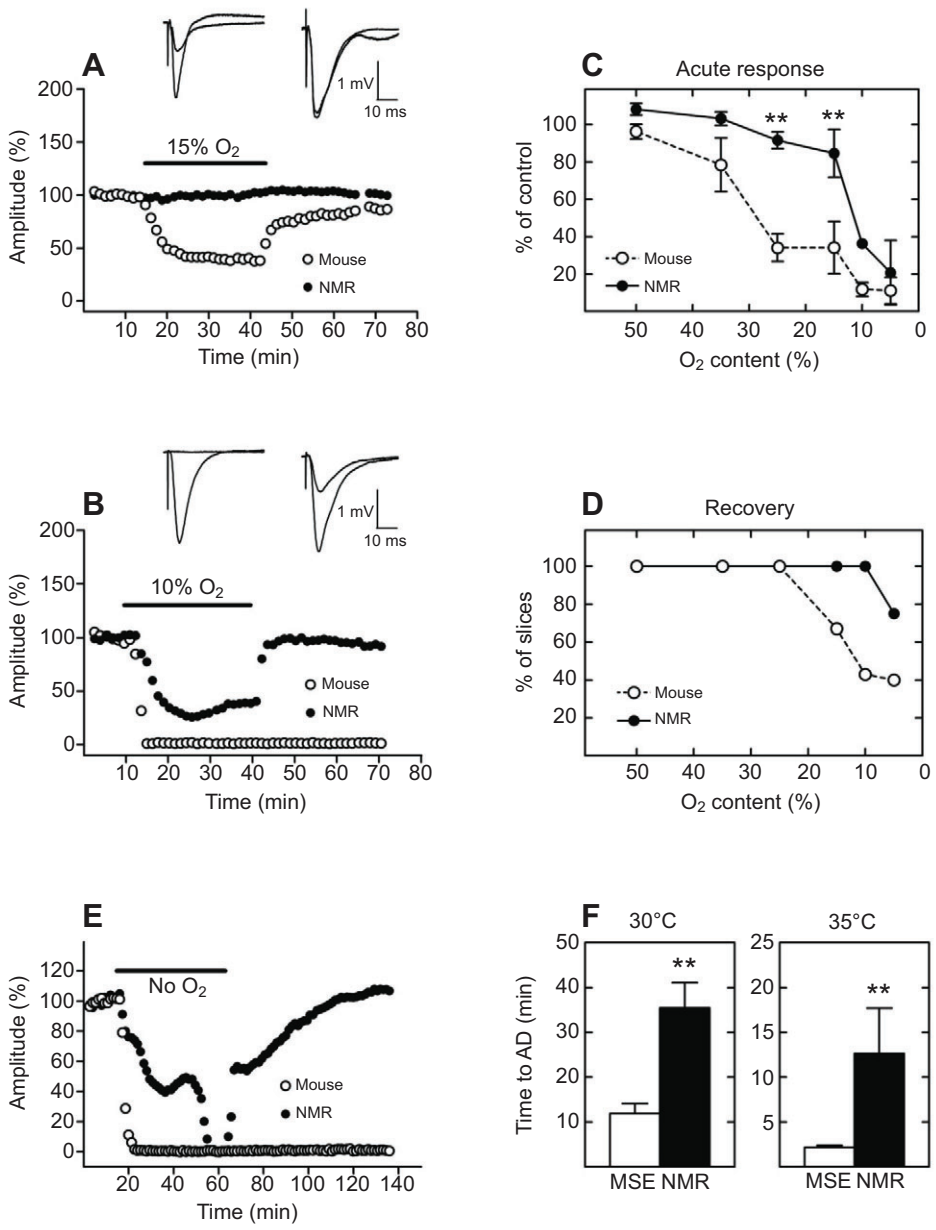

Fig. 10. Resistance of naked mole-rat (NMR) hippocampus to hypoxia. Field excitatory postsynaptic potential (EPSP) amplitude in hippocampal slices before, during (horizontal bar) and after replacement of 95% oxygen (O_2) in the slice chamber with 15% O_2/80% N_2 (A) or 10% O_2/85% N_2 (B) for 30 min. Inset traces show EPSPs recorded before and during hypoxia for mouse (left) and mole-rat (right). (C) Decrease in field EPSP amplitude in NMR (n=25) and mouse (n=48) slices at varying O_2 content (means ± s.e.m.). (D) Percentage of slices showing any functional recovery after re-oxygenation. (E) Response to removal of all O_2 from the chamber atmosphere. (F) Duration of exposure to O_2-free atmosphere needed to produce anoxic depolarization (AD) in slices from mice (MSE, n=19) and NMR (n=13) incubated at 30 or 35°C. All NMRs were at least 1 year old and mice were at least 2 months old. **P<0.01. [Adapted from Larson and Park (Larson and Park, 2009) and reprinted with permission.]

in hypoxia tolerance in neonatal rat brain (Bickler et al., 2003) and its expression in naked mole-rat brain shows retention of a neonatal feature into adulthood.

These findings provide partial support for the hypothesis that naked mole-rat brain is hypoxia tolerant because it has arrested development. Could this be a general mechanism that is used by many fossorial species or is it peculiar to mole-rats or even unique to *H. glaber*? Fig. 12 shows time to anoxic depolarization in slices from three species of African mole-rat (Bathyergidae), one species of European mole-rat (Spalacidae), two other families of terrestrial rodents (three murids and two cricetids), and three other mammalian orders (Marsupiala, Carnivora and Lagomorpha). Among the eutherians, the naked mole-rat and common mole-rat (*Cryptomys hottentotus*) stand out as hypoxia tolerant. The common mole-rat is more distantly related to the naked mole-rat than to the Damaraland mole-rat (*Cryptomys damarensis*). The latter, despite its close resemblance to naked mole-rats in habitat and social organization, did not show unusual hypoxia tolerance. It remains to be seen whether or not the common mole-rat shows other manifestations of arrested development. It would also be of interest to test fossorial species other than mole-rats under the same conditions. As noted above, hippocampal slices from arctic ground squirrels have significantly delayed electrophysiological responses to combined oxygen and glucose deprivation, compared to rats (Dave et al., 2009).

If the neoteny hypothesis for hypoxia tolerance in naked mole-rat brain holds up under further mechanistic and comparative scrutiny, it may explain some other, seemingly unrelated, unusual traits of these animals. For example, peripheral insensitivity to chemical irritants (LaVinka et al., 2009), lack of a functional substance P nociceptive pathway (Park et al., 2003), poor thermoregulation (Buffenstein and Yahav, 1991), absence of fur, and high-affinity hemoglobin (Johansen et al., 1976) may all be juvenile characteristics retained into adulthood. Slowed or arrested development might even contribute to the extraordinary lifespan (Buffenstein, 2008) of these remarkable animals. It is tempting to speculate that environmental conditions (fossorial) and patchy food resources (Bennett and Faulkes, 2000) might have driven a

The Journal of Experimental Biology (2014) doi:10.1242/jeb.085381

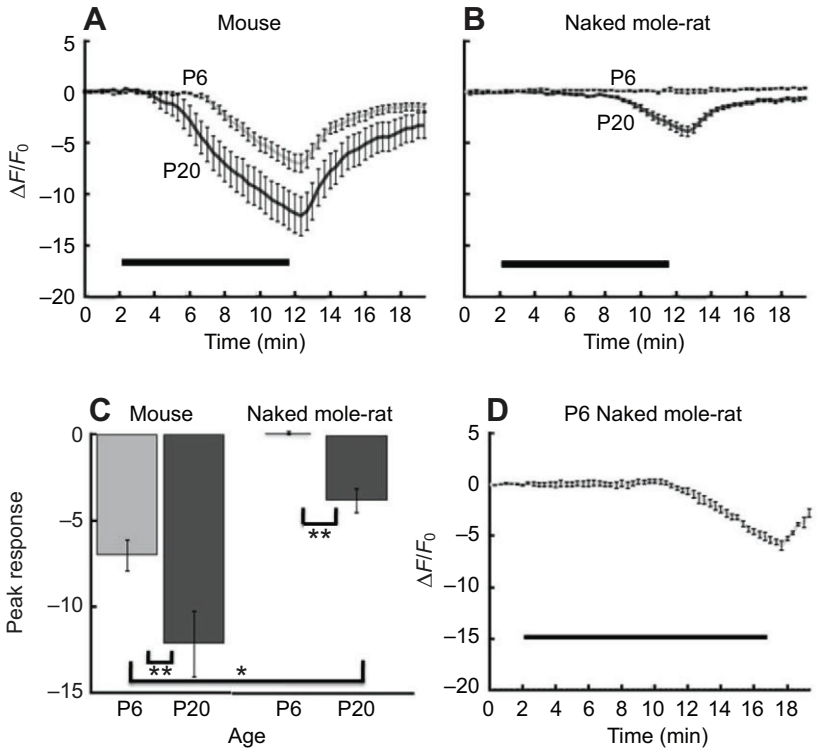

Fig. 11. Increase in internal calcium from exposure to hypoxic bath solution. (A) Data from postnatal day 6 (P6; 11 slices, 6 animals) and P20 (11 slices, 6 animals) mouse hippocampal slices. Values on the *y*-axis indicate the percentage change in calcium-mediated fluorescence within CA1 neurons in the field of interest with negative values corresponding to an increase in calcium (calcium decreases the fluorescent signal). Images were collected every 20 s over 20 min. The horizontal black bar indicates the 10 min when hypoxic bath solution was in the recording chamber. In these experiments, slices were superfused with artificial cerebrospinal fluid (ACSF) saturated with 95% O_2 and 5% CO_2 in the baseline and recovery periods; hypoxic solution was ACSF saturated with 95% N_2 and 5% CO_2. Error bars indicate ± s.e.m. (B) Data from P6 (14 slices, 5 animals) and P20 (10 slices, 3 animals) naked mole-rat slices. (C) Summary data showing the change in maximal calcium with age for mice and naked mole-rats for a 10 min exposure. **P*<0.05 and ***P*<0.01, according to the Newman–Keuls test. (D) Data from P6 (7 slices, 2 animals) naked mole-rat slices with an extended hypoxia exposure (15 min). Note that in all panels, animals in the P6 groups actually ranged in age from P5 to P7, and animals in the P20 groups actually ranged in age from P18 to P22. [Adapted from Peterson et al. (Peterson et al., 2012a) and reprinted with permission.]

(conceptually) simple ontogenetic timing change that allowed development of intrinsic brain tolerance to hypoxia, a communal lifestyle (eusociality), and extremely long life.

Discussion

Consideration of what is known about intrinsic brain tolerance to hypoxia in these different species seems to raise more questions than have yet been answered. For purposes of discussion and synthesis, we offer two dimensions along which the different organisms and their hypoxia tolerance mechanisms can be compared and contrasted. These dimensions are not really orthogonal but may capture a large part of the variance between species.

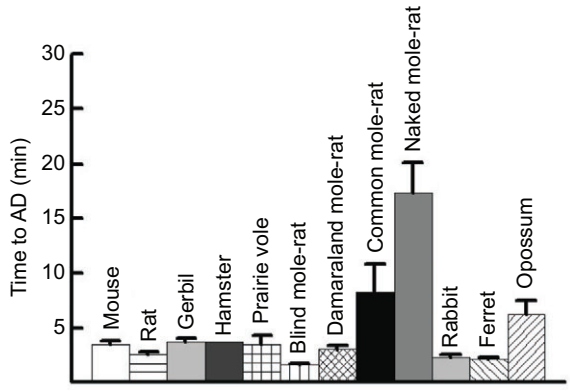

Fig. 12. Comparison of hypoxia sensitivity of hippocampal slices from diverse species of rodents and other mammalian orders. Histograms show average (means ± s.e.m.) time to induce anoxic depolarization (AD) in field CA1 after nominal anoxia (complete replacement of slice atmospheric O_2 with N_2). Brains from four common laboratory rodents were sampled (*Mus musculus*, Muridae, *n*=36; *Rattus norvegicus*, Muridae, *n*=4; *Meriones unguiculatus*, Cricetidae, *n*=2; and *Mesocricetus auratus*, Cricetidae, *n*=1), the prairie vole (*Microtus ochrogaster*, Cricetidae, *n*=5), the blind mole-rat (*Spalax sp.*, Spalacidae, *n*=3), three African mole-rats (*Cryptomys damarensis*, *n*=4; *Cryptomys hottentotus*, *n*=4; *Heterocephalus glaber*, *n*=11; all Bathyergidae), a lagomorph (*Oryctolagus cuniculus*, *n*=8), a carnivore (*Mustela putorius*, *n*=3), and a marsupial (*Monodelphis domestica*, *n*=3). (Unpublished data from J.L., S. Pawlowska and T.J.P.)

The first dimension has to do with the nature of the hypoxic threat imposed by the habitat and lifestyle of the animal. As was pointed out, a key mechanism to extend hypoxic survival is entrance into a deep but reversible hypo-metabolic state. The inducing conditions, duration and level of this hypoxia-tolerant state vary widely in the different species we have considered. It may be a lifelong adaptation to chronically low levels of ambient oxygen as in naked mole-rats; it may not be needed at all times but available for use during appetitive behavior patterns such as diving in seals and cetaceans; it may involve hibernation, a physiological state that is induced not by hypoxia per se but rather is entered as a means to conserve calories in seasons when food resources are scarce and requires flexibility in cerebral and systemic blood flow, as in arctic ground squirrels; or involve all three of these timescales and environmental and/or organismal inducers. It can be useful to consider chronic adaptations as distinct from those that are induced by a hypoxic challenge, whether the chronic adaptations are associated with chronic environmental hypoxia or merely the threat of unpredictable episodes. Thus we would distinguish chronic specializations that are preparatory and reduce the effects of hypoxia from specializations that are acute and reactive in nature.

The second dimension relates to the functional nature of the specialization. From the work presented here, we can distinguish a few categories: (1) dampening of the effect of systemic hypoxemia on the brain by improving O_2 delivery or using molecular O_2 buffers (e.g. neuroglobin); (2) reduction or restriction of energy consumption; (3) alterations to cellular metabolism (aerobic/anaerobic) in glia and neurons; (4) protection against excitotoxic damage; (5) protection against anoxic stress-induced necrosis and apoptosis; (6) prevention of oxidative stress during re-oxygenation; and (7) promotion of restorative processes.

1. Species-specific preparatory adaptations such as a particularly high capillary density in the brain have been described for diving mammals but do not seem to have been measured in the other species. This modification would bias the brain to receive a larger share of the O_2 supply when levels get low, given that brain blood flow appears to be well-maintained during diving (Blix et al., 1983; Zapol et al., 1979). Neuroglobin could serve to buffer O_2 levels as a preparatory mechanism. This seems to be the case with regard to cetaceans, although neuroglobin levels were not found to be higher in diving seals than in typical non-diving mammals, although its distribution is unusual. A reactive role for neuroglobin is suggested by its upregulation by hypoxia in turtles, possibly as a mechanism to buffer reactive oxygen species during re-oxygenation (see also below). Neuroglobin levels were found to be higher in the blind mole-rat (*Spalax*) brain under normoxic conditions, but downregulated during hypoxia (Avivi et al., 2010).

2. Low resting metabolism can be seen as a preparatory mechanism for energy conservation when hypoxic or ischemic episodes occur, at least in naked mole-rats and in hibernating arctic ground squirrels, although it does not explain intrinsic brain tolerance of hypoxia. Reactive mechanisms to reduce energy demand during hypoxic episodes are manifold and best described in the turtle: they include ‘channel arrest’, ‘spike arrest’, release of adenosine/inhibition of glutamate release, release of GABA, and inhibition of protein synthesis, among others. Such mechanisms may not be as significant in arctic ground squirrels or naked mole-rats, but may involve select populations of neurons in diving mammals.

3. A shift of cellular metabolism toward anaerobic pathways (in neurons or glia) would be a reactive adaptation to hypoxic episodes and may be important in seal brain, but not in arctic ground squirrels. A shift to glycolysis must be vital during very prolonged periods of anoxia in the turtle.

4. Protection against excitotoxic damage induced by hypoxic release of glutamate and its interaction with NMDA receptors is an important preparatory mechanism in turtles, arctic ground squirrels and naked mole-rats; it has not been assessed in diving mammals. In turtle, excitotoxicity is dampened indirectly by δ-opioid receptor-mediated suppression of NMDA receptor currents and may be subject to reactive regulation as well. In arctic ground squirrels, NMDA receptor expression is lower than in hypoxia-sensitive rats, whereas in naked mole-rats, NMDA receptor subunit expression (GluN2D) favors suppression of calcium fluxes in response to hypoxia.

5. Protection against hypoxia-induced apoptosis probably involves both protective and reactive mechanisms in turtles, through constitutive and induced changes in expression of heat shock proteins, other stress-associated proteins and apoptosis mediators. There are also some indications that protection of neurons from non-excitotoxic death may be important for hypoxia tolerance in the arctic ground squirrel as well. We know very little about the cell death pathways in naked mole-rats and diving seals.

6. The generation of reactive oxygen species during re-oxygenation (recovery) after an episode of acute hypoxia is a final aspect of the hypoxic catastrophe. The mechanisms by which ROS damage is avoided or ameliorated are beginning to be unraveled in freshwater turtles; as noted above, neuroglobin may be an important mediator, perhaps also in diving mammals. High levels of antioxidants in the brain of the arctic ground squirrel may help to alleviate ROS damage during recovery from hibernation.

7. Restorative processes including neurogenesis or synaptic remodeling may play a role in turtles and arctic ground squirrels, an aspect of the response to hypoxia that has not been studied in naked mole-rats and diving seals.

Hypothermia is a significant factor in hypoxia tolerance in most of the animals reviewed here. Freshwater turtles, being cold-blooded, are clearly subject to suppressed cellular metabolism when ponds freeze over; hibernation is associated with hypothermia in arctic ground squirrels. Naked mole-rats are the only mammals with significantly reduced body temperature (28°C) in their thermostable natural habitat; physiological thermoregulation is very poor in these animals (Buffenstein and Yahav, 1991; McNab, 1979). Aside from the effect on metabolic rate, the significance of hypothermia in naked mole-rats on brain hypoxia tolerance is less clear. Decreases in brain temperature may also be a reactive protection mechanism in diving seals.

Study of hypoxia-tolerant species has revealed many ways to mitigate the hypoxic catastrophe in neurons; however, one area that is yet to be addressed is the physiological cost. Presumably, deployment of special mechanisms for hypoxia tolerance must divert resources from other brain functions. As an example, synapses in naked mole-rat hippocampus do not show paired-pulse facilitation, a robust short-term synaptic plasticity mechanism normally present in many forebrain synapses in all other species that have been studied. Is this related to hypoxia tolerance? There has been little or no discussion of the potential behavioral or cognitive costs incurred by adaptations for hypoxia tolerance. Can they be measured? Are they significant? Meaningless? Or is there something unexpected yet to be learned from a comparative study of hypoxia tolerance in vertebrates?

Acknowledgements
We are grateful for the thoughtful comments and suggestions of two anonymous reviewers.

Competing interests
The authors declare no competing financial interests.

Author contributions
J.L. wrote the Introduction and Discussion sections, co-wrote (with T.J.P.) the section on hypoxia tolerance in the naked mole-rat, and revised the article. K.L.D. wrote the section on hypoxia tolerance in hibernating mammals, and revised the article. L.P.F. wrote the section on hypoxia tolerance in diving mammals, and revised the article. S.L.M. wrote the section on hypoxia tolerance in freshwater turtle brain, and revised the article. T.J.P. co-wrote (with J.L.) the section on hypoxia tolerance in the naked mole-rat, and revised the article.

Funding
J.L. was supported by grants from the National Science Foundation [grant number 744979]; and the US Army Medical Research and Materiel Command [grant number 10917352). S.L.M. was supported by the National Institutes of Health [grant number 1R15AG033374-01]; the American Heart Association; the American Federation of Aging Research; and the Florida Atlantic University Foundation. K.L.D. was supported by the US Army Research Office [grant number W911NF-05-1-0280]; The US Army Medical Research and Materiel Command [grant number 05178001]; the National Institute of Neurological Disorders and Stroke [grant numbers NS041069-06 and R15NS070779]; and Alaska IDeA Networks of Biomedical Research Excellence and Alaska Experimental Program to Stimulate Competitive Research. L.P.F. was supported by the Norwegian Research Council [grant number 164791/V40]; and the work on neuroglobin by grants from Deutsche Forschungsgemeinschaft to Dr Thorsten Burmester [grant numbers Bu956/10, Bu956/12; Ha2103/3]. T.J.P. was supported by the National Science Foundation [grant number 744979]; and a generous gift from a foundation that prefers to remain anonymous. Deposited in PMC for release after 12 months.

References

Anderson, T. R., Jarvis, C. R., Biedermann, A. J., Molnar, C. and Andrew, R. D. (2005). Blocking the anoxic depolarization protects without functional compromise following simulated stroke in cortical brain slices. *J. Neurophysiol.* **93**, 963-979.

Arieli, R. (1979). The atmospheric environment of the fossorial mole rat (*Spalax ehrenbergi*): effects of season, soil texture, rain, temperature and activity. *Comp. Biochem. Physiol.* **63A**, 569-575.

Avivi, A., Gerlach, F., Joel, A., Reuss, S., Burmester, T., Nevo, E. and Hankeln, T. (2010). Neuroglobin, cytoglobin, and myoglobin contribute to hypoxia adaptation of the subterranean mole rat *Spalax*. *Proc. Natl. Acad. Sci. USA* **107**, 21570-21575.

Beere, H. M. (2001). Stressed to death: regulation of apoptotic signaling pathways by the heat shock proteins. *Sci. STKE* **2001**, re1.
Bennett, N. C. and Faulkes, C. G. (2000). *African Mole-Rats: Ecology and Eusociality*. Cambridge: Cambridge University Press.
Bickler, P. E. (2004). Clinical perspectives: neuroprotection lessons from hypoxia-tolerant organisms. *J. Exp. Biol.* **207**, 3243-3249.
Bickler, P. E., Fahlman, C. S. and Taylor, D. M. (2003). Oxygen sensitivity of NMDA receptors: relationship to NR2 subunit composition and hypoxia tolerance of neonatal neurons. *Neuroscience* **118**, 25-35.
Biggar, K. K. and Storey, K. B. (2012). Evidence for cell cycle suppression and microRNA regulation of cyclin D1 during anoxia exposure in turtles. *Cell Cycle* **11**, 1705-1713.
Blix, A. S. and Folkow, B. (1983). Cardiovascular adjustments to diving in mammals and birds. In *Handbook of Physiology. The Cardiovascular System III. Peripheral Circulation and Organ Blood Flow* (ed. J. T. Shepherd and F. M. Abboud), pp. 917-945. Bethesda, MD: American Physiological Society.
Blix, A. S., Elsner, R. and Kjekshus, J. K. (1983). Cardiac output and its distribution through capillaries and A-V shunts in diving seals. *Acta Physiol. Scand.* **118**, 109-116.
Blix, A. S., Walløe, L., Messelt, E. B. and Folkow, L. P. (2010). Selective brain cooling and its vascular basis in diving seals. *J. Exp. Biol.* **213**, 2610-2616.
Brett, R. A. (1991). The population structure of naked mole-rat colonies. In *The Biology of the Naked Mole-Rat* (ed. P. W. Sherman, J. U. M. Jarvis and R. D. Alexander), pp. 97-136. Princeton, NJ: Princeton University Press.
Buck, L. T. and Bickler, P. E. (1998). Adenosine and anoxia reduce N-methyl-D-aspartate receptor open probability in turtle cerebrocortex. *J. Exp. Biol.* **201**, 289-297.
Buffenstein, R. (2008). Negligible senescence in the longest living rodent, the naked mole-rat: insights from a successfully aging species. *J. Comp. Physiol. B* **178**, 439-445.
Buffenstein, R. and Yahav, S. (1991). Is the naked mole-rat *Heterocephalus glaber* an endothermic yet poikilothermic mammal? *J. Therm. Biol.* **16**, 227-232.
Bullard, R. W., David, G. and Nichols, C. T. (1960). The mechanisms of hypoxic tolerance in hibernating and non-hibernating mammals. In *Bulletin of the Museum of Comparative Zoology at Harvard College*, Vol. 24 (ed. C. P. Lyman and A. R. Dawe), pp. 321-335. Cambridge, MA: Museum of Comparative Zoology at Harvard College.
Burmester, T. and Hankeln, T. (2009). What is the function of neuroglobin? *J. Exp. Biol.* **212**, 1423-1428.
Burmester, T., Weich, B., Reinhardt, S. and Hankeln, T. (2000). A vertebrate globin expressed in the brain. *Nature* **407**, 520-523.
Burns, J. M., Lestyk, K. C., Folkow, L. P., Hammill, M. O. and Blix, A. S. (2007). Size and distribution of oxygen stores in harp and hooded seals from birth to maturity. *J. Comp. Physiol. B* **177**, 687-700.
Chen, Y., Cantrell, A. R., Messing, R. O., Scheuer, T. and Catterall, W. A. (2005). Specific modulation of Na+ channels in hippocampal neurons by protein kinase C epsilon. *J. Neurosci.* **25**, 507-513.
Christian, S. L., Ross, A. P., Zhao, H. W., Kristenson, H. J., Zhan, X., Rasley, B. T., Bickler, P. E. and Drew, K. L. (2008). Arctic ground squirrel (*Spermophilus parryii*) hippocampal neurons tolerate prolonged oxygen-glucose deprivation and maintain baseline ERK1/2 and JNK activation despite drastic ATP loss. *J. Cereb. Blood Flow Metab.* **28**, 1307-1319.
Croning, M. D. and Haddad, G. G. (1998). Comparison of brain slice chamber designs for investigations of oxygen deprivation *in vitro*. *J. Neurosci. Methods* **81**, 103-111.
D'Alecy, L. G., Lundy, E. F., Kluger, M. J., Harker, C. T., LeMay, D. R. and Shlafer, M. (1990). Beta-hydroxybutyrate and response to hypoxia in the ground squirrel, *Spermophilus tridecimlineatus*. *Comp. Biochem. Physiol.* **96B**, 189-193.
Dausmann, K. H., Glos, J., Ganzhorn, J. U. and Heldmaier, G. (2004). Physiology: hibernation in a tropical primate. *Nature* **429**, 825-826.
Dave, K. R., Prado, R., Raval, A. P., Drew, K. L. and Pérez-Pinzón, M. A. (2006). The arctic ground squirrel brain is resistant to injury from cardiac arrest during euthermia. *Stroke* **37**, 1261-1265.
Dave, K. R., Anthony Defazio, R., Raval, A. P., Dashkin, O., Saul, I., Iceman, K. E., Pérez-Pinzón, M. A. and Drew, K. L. (2009). Protein kinase C epsilon activation delays neuronal depolarization during cardiac arrest in the euthermic arctic ground squirrel. *J. Neurochem.* **110**, 1170-1179.
Deshpande, J. K., Siesjö, B. K. and Wieloch, T. (1987). Calcium accumulation and neuronal damage in the rat hippocampus following cerebral ischemia. *J. Cereb. Blood Flow Metab.* **7**, 89-95.
Drew, K. L., Rice, M. E., Kuhn, T. B. and Smith, M. A. (2001). Neuroprotective adaptations in hibernation: therapeutic implications for ischemia-reperfusion, traumatic brain injury and neurodegenerative diseases. *Free Radic. Biol. Med.* **31**, 563-573.
Drew, K. L., Harris, M. B., LaManna, J. C., Smith, M. A., Zhu, X. W. and Ma, Y. L. (2004). Hypoxia tolerance in mammalian heterotherms. *J. Exp. Biol.* **207**, 3155-3162.
Drew, K. L., McGee, R. C., Wells, M. S. and Kelleher-Andersson, J. A. (2011). Growth and differentiation of adult hippocampal arctic ground squirrel neural stem cells. *J. Vis. Exp.* **47**, 2199.
Drew, K. L., Zuckerman, J. A., Shenk, P. E., Bogren, L. K., Jinka, T. R. and Moore, J. T. (2012). Hibernation: a natural model of tolerance to cerebral ischemia/reperfusion. In *Innate Neuroprotection for Stroke* (ed. J. Gidday and M. Pérez-Pinzón), pp. 37-50. New York, NY: Springer.
Elsner, R., Shurley, J. T., Hammond, D. D. and Brooks, R. E. (1970). Cerebral tolerance to hypoxemia in asphyxiated Weddell seals. *Respir. Physiol.* **9**, 287-297.
Erecińska, M. and Silver, I. A. (2001). Tissue oxygen tension and brain sensitivity to hypoxia. *Respir. Physiol.* **128**, 263-276.
Feldenberg, L. R., Thevananther, S., del Rio, M., de Leon, M. and Devarajan, P. (1999). Partial ATP depletion induces Fas- and caspase-mediated apoptosis in MDCK cells. *Am. J. Physiol.* **276**, F837-F846.
Fernandes, J. A., Lutz, P. L., Tannenbaum, A., Todorov, A. T., Liebovitch, L. and Vertes, R. (1997). Electroencephalogram activity in the anoxic turtle brain. *Am. J. Physiol.* **273**, R911-R919.
Folkow, L. P. and Blix, A. S. (2010). Air breathers under water: diving mammals and birds. In *Respiratory Physiology of Vertebrates. Life With and Without Oxygen* (ed. G. E. Nilsson), pp. 222-264. Cambridge: Cambridge University Press.
Folkow, L. P., Ramirez, J. M., Ludvigsen, S., Ramirez, N. and Blix, A. S. (2008). Remarkable neuronal hypoxia tolerance in the deep-diving adult hooded seal (*Cystophora cristata*). *Neurosci. Lett.* **446**, 147-150.
Fraser, K. P., Houlihan, D. F., Lutz, P. L., Leone-Kabler, S., Manuel, L. and Brechin, J. G. (2001). Complete suppression of protein synthesis during anoxia with no post-anoxia protein synthesis debt in the red-eared slider turtle *Trachemys scripta elegans*. *J. Exp. Biol.* **204**, 4353-4360.
Frerichs, K. U. and Hallenbeck, J. M. (1998). Hibernation in ground squirrels induces state and species-specific tolerance to hypoxia and aglycemia: an in vitro study in hippocampal slices. *J. Cereb. Blood Flow Metab.* **18**, 168-175.
Frerichs, K. U., Kennedy, C., Sokoloff, L. and Hallenbeck, J. M. (1994). Local cerebral blood flow during hibernation, a model of natural tolerance to 'cerebral ischemia'. *J. Cereb. Blood Flow Metab.* **14**, 193-205.
Geiser, F. (2004). Metabolic rate and body temperature reduction during hibernation and daily torpor. *Annu. Rev. Physiol.* **66**, 239-274.
Geiser, F. and Ruf, T. (1995). Hibernation versus daily torpor in mammals and birds: physiological variables and classification of torpor patterns. *Physiol. Zool.* **68**, 935-966.
Giffard, R. G., Han, R. Q., Emery, J. F., Duan, M. and Pittet, J. F. (2008). Regulation of apoptotic and inflammatory cell signaling in cerebral ischemia: the complex roles of heat shock protein 70. *Anesthesiology* **109**, 339-348.
Glezer, I. I., Jacobs, M. S. and Morgane, P. J. (1987). Ultrastructure of the blood-brain barrier in the dolphin (*Stenella coeruleoalba*). *Brain Res.* **414**, 205-218.
Guppy, M., Hill, R. D., Schneider, R. C., Qvist, J., Liggins, G. C., Zapol, W. M. and Hochachka, P. W. (1986). Microcomputer-assisted metabolic studies of voluntary diving of Weddell seals. *Am. J. Physiol.* **250**, R175-R187.
Harris, J. J., Jolivet, R. and Attwell, D. (2012). Synaptic energy use and supply. *Neuron* **75**, 762-777.
Hashimoto, T., Yonetani, M. and Nakamura, H. (2003). Selective brain hypothermia protects against hypoxic-ischemic injury in newborn rats by reducing hydroxyl radical production. *Kobe J. Med. Sci.* **49**, 83-91.
Hindell, M. A., Slip, D. J. and Burton, H. R. (1991). The diving behaviour of adult male and female southern elephant seals, *Mirounga leonina* (Pinnipedia: Phocidae). *Aust. J. Zool.* **39**, 595-619.
Hochachka, P. W. (1981). Brain, lung, and heart functions during diving and recovery. *Science* **212**, 509-514.
Hochachka, P. W., Castellini, J. M., Hill, R. D., Schneider, R. C., Bengtson, J. L., Hill, S. E., Liggins, G. C. and Zapol, W. M. (1988). Protective metabolic mechanisms during liver ischemia: transferable lessons from long-diving animals. *Mol. Cell. Biochem.* **84**, 77-85.
Hong, S. K., Ashwell-Erickson, S., Gigliotti, P. and Elsner, R. (1982). Effects of anoxia and low pH on organic ion transport and electrolyte distribution in harbour seal (*Phoca vitulina*) kidney slices. *J. Comp. Physiol. B* **149**, 19-24.
Hylland, P., Nilsson, G. E. and Lutz, P. L. (1994). Time course of anoxia-induced increase in cerebral blood flow rate in turtles: evidence for a role of adenosine. *J. Cereb. Blood Flow Metab.* **14**, 877-881.
Jackson, D. C. (2004). Acid-base balance during hypoxic hypometabolism: selected vertebrate strategies. *Respir. Physiol. Neurobiol.* **141**, 273-283.
Jackson, D. C. and Ultsch, G. R. (2010). Physiology of hibernation under the ice by turtles and frogs. *J. Exp. Zool. A* **313**, 311-327.
Jarvis, J. U. (1981). Eusociality in a mammal: cooperative breeding in naked mole-rat colonies. *Science* **212**, 571-573.
Johansen, K., Lykkeboe, G., Weber, R. E. and Maloiy, G. M. (1976). Blood respiratory properties in the naked mole rat *Heterocephalus glaber*, a mammal of low body temperature. *Respir. Physiol.* **28**, 303-314.
Kerem, D. and Elsner, R. (1973). Cerebral tolerance to asphyxial hypoxia in the harbor seal. *Respir. Physiol.* **19**, 188-200.
Kerem, D., Hammond, D. D. and Elsner, R. (1973). Tissue glycogen levels in the Weddell seal, *Leptonychotes weddelli*: a possible adaptation to asphyxial hypoxia. *Comp. Biochem. Physiol.* **45A**, 731-736.
Kesaraju, S. and Milton, S. L. (2009). Preliminary evidence of neuronal regeneration in the anoxia tolerant vertebrate brain. *Exp. Neurol.* **215**, 401-403.
Kesaraju, S., Schmidt-Kastner, R., Prentice, H. M. and Milton, S. L. (2009). Modulation of stress proteins and apoptotic regulators in the anoxia tolerant turtle brain. *J. Neurochem.* **109**, 1413-1426.
Krivoruchko, A. and Storey, K. B. (2010a). Epigenetics in anoxia tolerance: a role for histone deacetylases. *Mol. Cell. Biochem.* **342**, 151-161.
Krivoruchko, A. and Storey, K. B. (2010b). Regulation of the heat shock response under anoxia in the turtle, *Trachemys scripta elegans*. *J. Comp. Physiol. B* **180**, 403-414.
Kurtz, C. C., Lindell, S. L., Mangino, M. J. and Carey, H. V. (2006). Hibernation confers resistance to intestinal ischemia-reperfusion injury. *Am. J. Physiol.* **291**, G895-G901.
Ladelfa, M. F., Toledo, M. F., Laiseca, J. E. and Monte, M. (2011). Interaction of p53 with tumor suppressive and oncogenic signaling pathways to control cellular reactive oxygen species production. *Antioxid. Redox Signal.* **15**, 1749-1761.

Lanneau, D., Brunet, M., Frisan, E., Solary, E., Fontenay, M. and Garrido, C. (2008). Heat shock proteins: essential proteins for apoptosis regulation. *J. Cell. Mol. Med.* **12**, 743-761.
Larson, J. and Park, T. J. (2009). Extreme hypoxia tolerance of naked mole-rat brain. *Neuroreport* **20**, 1634-1637.
LaVinka, P. C., Brand, A., Landau, V. J., Wirtshafter, D. and Park, T. J. (2009). Extreme tolerance to ammonia fumes in African naked mole-rats: animals that naturally lack neuropeptides from trigeminal chemosensory nerve fibers. *J. Comp. Physiol. A* **195**, 419-427.
Lee, K. S., Frank, S., Vanderklish, P., Arai, A. and Lynch, G. (1991). Inhibition of proteolysis protects hippocampal neurons from ischemia. *Proc. Natl. Acad. Sci. USA* **88**, 7233-7237.
Lee, M., Hyun, D. H., Marshall, K. A., Ellerby, L. M., Bredesen, D. E., Jenner, P. and Halliwell, B. (2001). Effect of overexpression of BCL-2 on cellular oxidative damage, nitric oxide production, antioxidant defenses, and the proteasome. *Free Radic. Biol. Med.* **31**, 1550-1559.
Lenfant, C., Johansen, K. and Torrance, J. D. (1970). Gas transport and oxygen storage capacity in some pinnipeds and the sea otter. *Respir. Physiol.* **9**, 277-286.
Lindell, S. L., Klahn, S. L., Piazza, T. M., Mangino, M. J., Torrealba, J. R., Southard, J. H. and Carey, H. V. (2005). Natural resistance to liver cold ischemia-reperfusion injury associated with the hibernation phenotype. *Am. J. Physiol.* **288**, G473-G480.
Lipton, P. (1999). Ischemic cell death in brain neurons. *Physiol. Rev.* **79**, 1431-1568.
Ludvigsen, S. and Folkow, L. P. (2009). Differences in *in vitro* cerebellar neuronal responses to hypoxia in eider ducks, chicken and rats. *J. Comp. Physiol. A* **195**, 1021-1030.
Lutz, P. L. and Manuel, L. (1999). Maintenance of adenosine A1 receptor function during long-term anoxia in the turtle brain. *Am. J. Physiol.* **276**, R633-R636.
Lutz, P. L. and Milton, S. L. (2004). Negotiating brain anoxia survival in the turtle. *J. Exp. Biol.* **207**, 3141-3147.
Ma, Y. L., Zhu, X., Rivera, P. M., Tøien, Ø., Barnes, B. M., LaManna, J. C., Smith, M. A. and Drew, K. L. (2005). Absence of cellular stress in brain after hypoxia induced by arousal from hibernation in Arctic ground squirrels. *Am. J. Physiol.* **289**, R1297-R1306.
McGee, R. C., Drew, K. L., Wells, M. S. and Kelleher-Andersson, J. A. (2008). Neurons derived from Arctic ground squirrel neural stem cells tolerate oxygen-glucose deprivation by enhanced capacity for anaerobic metabolism and neurogenesis. *Soc. Neurosci. Abstracts* **2008**, 151.113.
McNab, B. K. (1979). The influence of body size on the energetics and distribution of fossorial and burrowing mammals. *Ecology* **60**, 1010-1021.
Meir, J. U., Champagne, C. D., Costa, D. P., Williams, C. L. and Ponganis, P. J. (2009). Extreme hypoxemic tolerance and blood oxygen depletion in diving elephant seals. *Am. J. Physiol.* **297**, R927-R939.
Messelt, E. B. and Blix, A. S. (1976). The LDH of the frequently asphyxiated beaver (*Castor fiber*). *Comp. Biochem. Physiol.* **53B**, 77-80.
Milton, S. L. and Lutz, P. L. (1998). Low extracellular dopamine levels are maintained in the anoxic turtle (*Trachemys scripta*) striatum. *J. Cereb. Blood Flow Metab.* **18**, 803-807.
Milton, S. L. and Lutz, P. L. (2005). Adenosine and ATP-sensitive potassium channels modulate dopamine release in the anoxic turtle (*Trachemys scripta*) striatum. *Am. J. Physiol.* **289**, R77-R83.
Milton, S. L., Thompson, J. W. and Lutz, P. L. (2002). Mechanisms for maintaining extracellular glutamate levels in the anoxic turtle striatum. *Am. J. Physiol.* **282**, R1317-R1323.
Milton, S. L., Nayak, G., Lutz, P. L. and Prentice, H. M. (2006). Gene transcription of neuroglobin is upregulated by hypoxia and anoxia in the brain of the anoxia-tolerant turtle *Trachemys scripta*. *J. Biomed. Sci.* **13**, 509-514.
Milton, S. L., Nayak, G., Kesaraju, S., Kara, L. and Prentice, H. M. (2007). Suppression of reactive oxygen species production enhances neuronal survival in vitro and in vivo in the anoxia-tolerant turtle *Trachemys scripta*. *J. Neurochem.* **101**, 993-1001.
Milton, S. L., Dirk, L. J., Kara, L. F. and Prentice, H. M. (2008). Adenosine modulates ERK1/2, PI3K/Akt, and p38MAPK activation in the brain of the anoxia-tolerant turtle *Trachemys scripta*. *J. Cereb. Blood Flow Metab.* **28**, 1469-1477.
Mitz, S. A., Reuss, S., Folkow, L. P., Blix, A. S., Ramirez, J. M., Hankeln, T. and Burmester, T. (2009). When the brain goes diving: glial oxidative metabolism may confer hypoxia tolerance to the seal brain. *Neuroscience* **163**, 552-560.
Murphy, B., Zapol, W. M. and Hochachka, P. W. (1980). Metabolic activities of heart, lung, and brain during diving and recovery in the Weddell seal. *J. Appl. Physiol.* **48**, 596-605.
Nayak, G., Prentice, H. M. and Milton, S. L. (2009). Role of neuroglobin in regulating reactive oxygen species in the brain of the anoxia-tolerant turtle *Trachemys scripta*. *J. Neurochem.* **110**, 603-612.
Nayak, G. H., Prentice, H. M. and Milton, S. L. (2011). Neuroprotective signaling pathways are modulated by adenosine in the anoxia tolerant turtle. *J. Cereb. Blood Flow Metab.* **31**, 467-475.
Nilsson, G. E. and Lutz, P. L. (1991). Release of inhibitory neurotransmitters in response to anoxia in turtle brain. *Am. J. Physiol.* **261**, R32-R37.
Nilsson, G. E. and Lutz, P. L. (1992). Adenosine release in the anoxic turtle brain as a mechanism for anoxic survival. *J. Exp. Biol.* **162**, 345-351.
Nowak, G., Bakajsova, D. and Clifton, G. L. (2004). Protein kinase C-epsilon modulates mitochondrial function and active Na+ transport after oxidant injury in renal cells. *Am. J. Physiol.* **286**, 307F-316F.
Obrenovitch, T. P. (2008). Molecular physiology of preconditioning-induced brain tolerance to ischemia. *Physiol. Rev.* **88**, 211-247.
Odden, A., Folkow, L. P., Caputa, M., Hotvedt, R. and Blix, A. S. (1999). Brain cooling in diving seals. *Acta Physiol. Scand.* **166**, 77-78.
Osborne, P. G., Sato, J., Shuke, N. and Hashimoto, M. (2005). Sympathetic alpha-adrenergic regulation of blood flow and volume in hamsters arousing from hibernation. *Am. J. Physiol.* **289**, R554-R562.
Packard, G. C. and Packard, M. J. (2003). Natural freeze-tolerance in hatchling painted turtles? *Comp. Biochem. Physiol.* **134A**, 233-246.
Pamenter, M. E. and Buck, L. T. (2008). delta-Opioid receptor antagonism induces NMDA receptor-dependent excitotoxicity in anoxic turtle cortex. *J. Exp. Biol.* **211**, 3512-3517.
Pamenter, M. E., Richards, M. D. and Buck, L. T. (2007). Anoxia-induced changes in reactive oxygen species and cyclic nucleotides in the painted turtle. *J. Comp. Physiol. B* **177**, 473-481.
Pamenter, M. E., Hogg, D. W., Gu, X. Q., Buck, L. T. and Haddad, G. G. (2012). Painted turtle cortex is resistant to an in vitro mimic of the ischemic mammalian penumbra. *J. Cereb. Blood Flow Metab.* **32**, 2033-2043.
Park, T. J., Comer, C., Carol, A., Lu, Y., Hong, H. S. and Rice, F. L. (2003). Somatosensory organization and behavior in naked mole-rats: II. Peripheral structures, innervation, and selective lack of neuropeptides associated with thermoregulation and pain. *J. Comp. Neurol.* **465**, 104-120.
Pék, M. and Lutz, P. L. (1997). Role for adenosine in channel arrest in the anoxic turtle brain. *J. Exp. Biol.* **200**, 1913-1917.
Pérez-Pinzón, M. A. and Rice, M. E. (1995). Seasonal- and temperature-dependent variation in CNS ascorbate and glutathione levels in anoxia-tolerant turtles. *Brain Res.* **705**, 45-52.
Pérez-Pinzón, M. A., Lutz, P. L., Sick, T. J. and Rosenthal, M. (1993). Adenosine, a 'retaliatory' metabolite, promotes anoxia tolerance in turtle brain. *J. Cereb. Blood Flow Metab.* **13**, 728-732.
Peterson, B. L., Larson, J., Buffenstein, R., Park, T. J. and Fall, C. P. (2012a). Blunted neuronal calcium response to hypoxia in naked mole-rat hippocampus. *PLoS ONE* **7**, e31568.
Peterson, B. L., Park, T. J. and Larson, J. (2012b). Adult naked mole-rat brain retains the NMDA receptor subunit GluN2D associated with hypoxia tolerance in neonatal mammals. *Neurosci. Lett.* **506**, 342-345.
Ponganis, P. J., Meir, J. U. and Williams, C. L. (2011). In pursuit of Irving and Scholander: a review of oxygen store management in seals and penguins. *J. Exp. Biol.* **214**, 3325-3339.
Popov, V. I., Kraev, I. V., Ignat'ev, D. A. and Stewart, M. G. (2011). Suspension of mitotic activity in dentate gyrus of the hibernating ground squirrel. *Neural Plast.* **2011**, 867525.
Prentice, H. M., Milton, S. L., Scheurle, D. and Lutz, P. L. (2004). The upregulation of cognate and inducible heat shock proteins in the anoxic turtle brain. *J. Cereb. Blood Flow Metab.* **24**, 826-828.
Qvist, J., Hill, R. D., Schneider, R. C., Falke, K. J., Liggins, G. C., Guppy, M., Elliot, R. L., Hochachka, P. W. and Zapol, W. M. (1986). Hemoglobin concentrations and blood gas tensions of free-diving Weddell seals. *J. Appl. Physiol.* **61**, 1560-1569.
Ramirez, J. M., Folkow, L. P. and Blix, A. S. (2007). Hypoxia tolerance in mammals and birds: from the wilderness to the clinic. *Annu. Rev. Physiol.* **69**, 113-143.
Ramirez, J. M., Folkow, L. P., Ludvigsen, S., Ramirez, P. N. and Blix, A. S. (2011). Slow intrinsic oscillations in thick neocortical slices of hypoxia tolerant deep diving seals. *Neuroscience* **177**, 35-42.
Reese, S. A., Stewart, E. R., Crocker, C. E., Jackson, D. C. and Ultsch, G. R. (2004). Geographic variation of the physiological response to overwintering in the painted turtle (*Chrysemys picta*). *Physiol. Biochem. Zool.* **77**, 619-630.
Rice, M. E., Lee, E. J. and Choy, Y. (1995). High levels of ascorbic acid, not glutathione, in the CNS of anoxia-tolerant reptiles contrasted with levels in anoxia-intolerant species. *J. Neurochem.* **64**, 1790-1799.
Rider, M. H., Hussain, N., Dilworth, S. M. and Storey, K. B. (2009). Phosphorylation of translation factors in response to anoxia in turtles, *Trachemys scripta elegans*: role of the AMP-activated protein kinase and target of rapamycin signalling pathways. *Mol. Cell. Biochem.* **332**, 207-213.
Roesner, A., Mitz, S. A., Hankeln, T. and Burmester, T. (2008). Globins and hypoxia adaptation in the goldfish, *Carassius auratus*. *FEBS J.* **275**, 3633-3643.
Ross, A. P., Christian, S. L., Zhao, H. W. and Drew, K. L. (2006). Persistent tolerance to oxygen and nutrient deprivation and N-methyl-D-aspartate in cultured hippocampal slices from hibernating Arctic ground squirrel. *J. Cereb. Blood Flow Metab.* **26**, 1148-1156.
Schneuer, M., Flachsbarth, S., Czech-Damal, N. U., Folkow, L. P., Siebert, U. and Burmester, T. (2012). Neuroglobin of seals and whales: evidence for a divergent role in the diving brain. *Neuroscience* **223**, 35-44.
Scholander, P. F. (1940). Experimental investigations on the respiratory functions in diving mammals and birds. *Hvalradets Skrifter* **22**, 1-131.
Shoubridge, E. A., Carscadden, J. E. and Leggett, W. C. (1976). LDH isozyme patterns in cetaceans: evidence for a biochemical adaptation to diving. *Comp. Biochem. Physiol.* **53B**, 357-359.
Snoeckx, L. H., Cornelussen, R. N., Van Nieuwenhoven, F. A., Reneman, R. S. and Van Der Vusse, G. J. (2001). Heat shock proteins and cardiovascular pathophysiology. *Physiol. Rev.* **81**, 1461-1497.
Stecyk, J. A., Couturier, C. S., Fagernes, C. E., Ellefsen, S. and Nilsson, G. E. (2012). Quantification of heat shock protein mRNA expression in warm and cold anoxic turtles (*Trachemys scripta*) using an external RNA control for normalization. *Comp. Biochem. Physiol.* **7D**, 59-72.
Storey, K. B. (2006). Reptile freeze tolerance: metabolism and gene expression. *Cryobiology* **52**, 1-16.
Takeda, Y., Namba, K., Higuchi, T., Hagioka, S., Takata, K., Hirakawa, M. and Morita, K. (2003). Quantitative evaluation of the neuroprotective effects of hypothermia ranging from 34 degrees C to 31 degrees C on brain ischemia in gerbils

and determination of the mechanism of neuroprotection. *Crit. Care Med.* **31**, 255-260.

Thompson, J. W., Prentice, H. M. and Lutz, P. L. (2007). Regulation of extracellular glutamate levels in the long-term anoxic turtle striatum: coordinated activity of glutamate transporters, adenosine, K (ATP) (+) channels and GABA. *J. Biomed. Sci.* **14**, 809-817.

Ultsch, G. R. (2006). The ecology of overwintering among turtles: where turtles overwinter and its consequences. *Biol. Rev. Camb. Philos. Soc.* **81**, 339-367.

van Aardt, W. J., Bronner, G. and Buffenstein, R. (2007). Hemoglobin-oxygen-affinity and acid-base properties of blood from the fossorial mole-rat, *Cryptomys hottentotus pretoriae*. *Comp. Biochem. Physiol.* **147A**, 50-56.

von der Ohe, C. G., Darian-Smith, C., Garner, C. C. and Heller, H. C. (2006). Ubiquitous and temperature-dependent neural plasticity in hibernators. *J. Neurosci.* **26**, 10590-10598.

Vousden, K. H. and Ryan, K. M. (2009). p53 and metabolism. *Nat. Rev. Cancer* **9**, 691-700.

Wang, X. T., Pei, D. S., Xu, J., Guan, Q. H., Sun, Y. F., Liu, X. M. and Zhang, G. Y. (2007). Opposing effects of Bad phosphorylation at two distinct sites by Akt1 and JNK1/2 on ischemic brain injury. *Cell. Signal.* **19**, 1844-1856.

Wanka, C., Steinbach, J. P. and Rieger, J. (2012). Tp53-induced glycolysis and apoptosis regulator (TIGAR) protects glioma cells from starvation-induced cell death by up-regulating respiration and improving cellular redox homeostasis. *J. Biol. Chem.* **287**, 33436-33446.

Watkins, W. A., Moore, K. E. and Tyack, P. (1985). Investigations of sperm whale acoustic behaviours in the southeast Caribbean. *Cetology* **49**, 1-15.

Weltzin, M. M., Zhao, H. W., Drew, K. L. and Bucci, D. J. (2006). Arousal from hibernation alters contextual learning and memory. *Behav. Brain Res.* **167**, 128-133.

Willmore, W. G. and Storey, K. B. (1997). Antioxidant systems and anoxia tolerance in a freshwater turtle *Trachemys scripta elegans*. *Mol. Cell. Biochem.* **170**, 177-185.

Willmore, W. G. and Storey, K. B. (2007). Purification and properties of glutathione reductase from liver of the anoxia-tolerant turtle, *Trachemys scripta elegans*. *Mol. Cell. Biochem.* **297**, 139-149.

Wittenberg, J. B. and Wittenberg, B. A. (2003). Myoglobin function reassessed. *J. Exp. Biol.* **206**, 2011-2020.

Xia, Y. and Haddad, G. G. (2001). Major difference in the expression of delta- and mu-opioid receptors between turtle and rat brain. *J. Comp. Neurol.* **436**, 202-210.

Yenari, M. A. and Han, H. S. (2012). Neuroprotective mechanisms of hypothermia in brain ischaemia. *Nat. Rev. Neurosci.* **13**, 267-278.

Zapol, W. M., Liggins, G. C., Schneider, R. C., Qvist, J., Snider, M. T., Creasy, R. K. and Hochachka, P. W. (1979). Regional blood flow during simulated diving in the conscious Weddell seal. *J. Appl. Physiol.* **47**, 968-973.

Zenteno-Savín, T., Clayton-Hernández, E. and Elsner, R. (2002). Diving seals: are they a model for coping with oxidative stress? *Comp. Biochem. Physiol.* **133C**, 527-536.

Zhang, J., Haddad, G. G. and Xia, Y. (2000). delta-, but not mu- and kappa-, opioid receptor activation protects neocortical neurons from glutamate-induced excitotoxic injury. *Brain Res.* **885**, 143-153.

Zhang, X. D., Qin, Z. H. and Wang, J. (2010). The role of p53 in cell metabolism. *Acta Pharmacol. Sin.* **31**, 1208-1212.

Zhang, J., Biggar, K. K. and Storey, K. B. (2013). Regulation of p53 by reversible post-transcriptional and post-translational mechanisms in liver and skeletal muscle of an anoxia tolerant turtle, *Trachemys scripta elegans*. *Gene* **513**, 147-155.

Zhao, H. W., Ross, A. P., Christian, S. L., Buchholz, J. N. and Drew, K. L. (2006). Decreased NR1 phosphorylation and decreased NMDAR function in hibernating Arctic ground squirrels. *J. Neurosci. Res.* **84**, 291-298.

Zhou, F., Zhu, X., Castellani, R. J., Stimmelmayr, R., Perry, G., Smith, M. A. and Drew, K. L. (2001). Hibernation, a model of neuroprotection. *Am. J. Pathol.* **158**, 2145-2151.

Zhu, X., Smith, M. A., Perry, G., Wang, Y., Ross, A. P., Zhao, H. W., LaManna, J. C. and Drew, K. L. (2005). The MAPK's are differentially modulated in AGS during hibernation. *J. Neuroscience Research* **80**, 862-868.

Zivkovic, G. and Buck, L. T. (2010). Regulation of AMPA receptor currents by mitochondrial ATP-sensitive K+ channels in anoxic turtle neurons. *J. Neurophysiol.* **104**, 1913-1922.

APPENDIX 5

BRAIN RESEARCH ▮ (▮▮▮▮) ▮▮▮–▮▮▮

Available online at www.sciencedirect.com

ScienceDirect

www.elsevier.com/locate/brainres

Research Report

Theta-burst LTP

John Larson[a,*], *Erin Munkácsy*[b]

[a]*Psychiatric Institute, Department of Psychiatry, University of Illinois College of Medicine, Chicago, IL 60612, United States*

[b]*Barshop Institute for Longevity and Aging Studies, Department of Cell and Structural Biology, University of Texas Health Science Center at San Antonio, San Antonio, TX 78245, United States*

ARTICLE INFO

Article history:
Accepted 18 October 2014

Keywords:
Long-term potentiation
LTP
Theta burst stimulation
NMDA
AMPA
GABA
Hippocampus
CA1

ABSTRACT

This review covers the spatial and temporal rules governing induction of hippocampal long-term potentiation (LTP) by theta-burst stimulation. Induction of LTP in field CA1 by high frequency stimulation bursts that resemble the burst discharges (complex-spikes) of hippocampal pyramidal neurons involves a multiple-step mechanism. A single burst is insufficient for LTP induction because it evokes both excitatory and inhibitory currents that partially cancel and limit postsynaptic depolarization. Bursts repeated at the frequency (~5 Hz) of the endogenous theta rhythm induce maximal LTP, primarily because this frequency disables feed-forward inhibition and allows sufficient postsynaptic depolarization to activate voltage-sensitive NMDA receptors. The disinhibitory process, referred to as "priming", involves presynaptic GABA autoreceptors that inhibit GABA release. Activation of NMDA receptors allows a calcium flux into dendritic spines that serves as the proximal trigger for LTP. We include new data showing that theta-burst stimulation is more efficient than other forms of stimulation for LTP induction. In addition, we demonstrate that associative interactions between synapses activated during theta-bursts are limited to major dendritic domains since such interactions occur within apical or basal dendritic trees but not between them. We review evidence that recordings of electrophysiological responses during theta burst stimulation can help to determine if experimental manipulations that affect LTP do so by affecting events antecedent to the induction process, such as NMDA receptor activation, or downstream signaling cascades that result from postsynaptic calcium fluxes. Finally, we argue that theta-burst LTP represents a minimal model for stable, non-decremental LTP that is more sensitive to a variety of experimental manipulations than is LTP induced by other stimulation paradigms.

This article is part of a Special Issue entitled SI: Brain and Memory.

*Corresponding author.
E-mail address: jrlarson@uic.edu (J. Larson).

http://dx.doi.org/10.1016/j.brainres.2014.10.034
0006-8993/

Please cite this article as: Larson, J., Munkácsy, E., Theta-burst LTP. Brain Research (2014), http://dx.doi.org/10.1016/j.brainres.2014.10.034

Contents

1. Introduction

During the first decade after the discovery of long-term potentiation (LTP) was announced (Bliss and Gardner-Medwin, 1973; Bliss and Lomo, 1973), there was some skepticism that it could serve as a memory mechanism, given the conditions that seemed necessary to induce the effect. At the same time, it seemed too many that memory could only be studied neurobiologically in simple nervous systems in which stimulus and response could be traced directly. In this time period (the first decade after 1973), there were 49 papers published on LTP; in the same interval, Eric Kandel's lab alone published 77 papers on mechanisms of learning in *Aplysia*. Of course, there were many factors that contributed to the lag in appreciation of LTP (and the decline in popularity of the invertebrate model system approach), but an important one was the question of whether or not LTP could be produced by physiological processes during learning.

The discovery that "theta-burst stimulation" (TBS) was an effective stimulus for LTP (Larson et al., 1986) was significant for three reasons: *first*, it showed that patterns of neuronal firing (complex-spikes) that occurred spontaneously during behavior could, if appropriately timed, induce LTP; *second*, the optimal repetition rate corresponded to the frequency of the hippocampal theta rhythm, an EEG pattern previously related indirectly to memory storage processes; and *third*, patterned stimulation paradigms allowed the uncovering of multiple events that contribute to LTP induction.

We will begin with a historical review, then present some original data pertaining to a few unresolved issues, and conclude with a discussion of some theoretical and practical implications. LTP can be divided into two sets of processes which we will refer to as *induction* and *expression*. The induction events are transient and very brief (<1 s), involve both presynaptic and postsynaptic responses to unusual patterns of activation, and are modulated by local circuit mechanisms. Expression refers to the synapse-specific and enduring (>1 hour) enhancement of synaptic transmission. In addition, persistence of expression requires mechanisms for stabilization or continued maintenance. This review will focus on the mechanisms by which theta burst stimulation induces LTP and will not say much about the cellular events downstream from the induction events. The post-induction events are most likely common to LTP induced by TBS and other stimulation paradigms; i.e., they are not particular to theta-burst LTP.

The theta-burst paradigm mimics two characteristics of hippocampal physiology: complex-spike discharges of the pyramidal neurons (Ranck Jr., 1973) and the rhythmic modulation of excitability of those cells during theta rhythm (Rudell et al., 1980). Hippocampal theta was originally described as the hippocampal "arousal rhythm" (Green and Arduini, 1954) since it was correlated with the neocortical desynchronization characteristic of awake, attentive states. Follow-up studies attempted to relate theta to specific psychological concepts such as attention, learning, memory encoding, etc.; however, Vanderwolf (1969), in a very influential paper, argued effectively that theta should be considered as a hippocampal correlate of voluntary movement. This conclusion invites the question: why is the hippocampus concerned with movement? One explanation is that movement in space necessitates updating cognitive maps of the environment and the spatial activity of hippocampal place cells (O'Keefe and Nadel, 1978). A second explanation is that much of voluntary movement is exploratory in nature, involving the gathering of both spatial and non-spatial information relevant to goal-directed behaviors. Perhaps one of the most impressive examples of the coupling of behavior to neural activity in mammals occurs during exploratory sniffing in rodents: rhythmic respiration is coupled to theta rhythm throughout the "olfactory–hippocampal circuit" (olfactory bulb, piriform cortex, entorhinal cortex, dentate gyrus, and hippocampus) both at the gross behavioral level and with synchronization of the behavioral rhythm with the EEG pattern on a cycle-by-cycle basis (Macrides, 1975; Macrides et al., 1982; Rojas-Líbano et al., 2014; Tsanov et al., 2014). This suggests that a stimulus sampling pattern organizes neuronal activity throughout a brain circuit that processes the information obtained by the sampling behavior. The synchronization of olfactory sampling with hippocampal theta may be only the most direct and striking example of this: sniffing in rodents is also synchronized with active tactile sensation using the mystacial vibrissae (Deschenes et al., 2012; Welker, 1964), although the pathways for somatosensory information to reach the hippocampus are far less direct than those for olfaction. It is also intriguing that visual saccades in humans and non-human primates occur at frequencies in the theta range and may be coupled to hippocampal theta (Hoffman et al., 2013).

The efficacy of stimulation patterns mimicking complex-spike discharges was first tested in the *in vivo* dentate gyrus (Douglas and Goddard, 1975; Douglas, 1977) and eight-pulse,

Please cite this article as: Larson, J., Munkácsy, E., Theta-burst LTP. Brain Research (2014), http://dx.doi.org/10.1016/j.brainres.2014.10.034

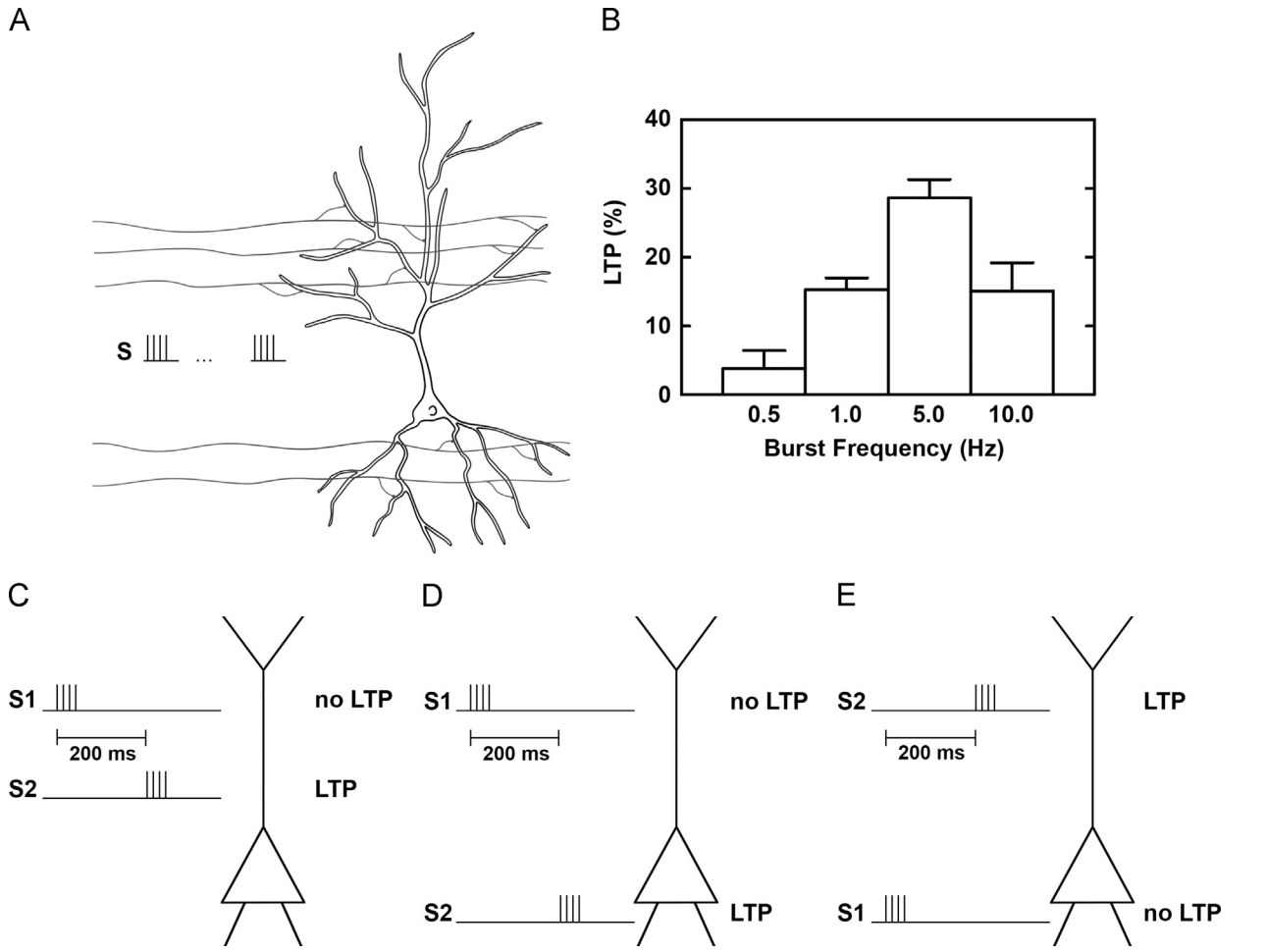

Fig. 1 – Timing rules for theta-burst LTP. (A) CA1 pyramidal neuron with apical and basal dendritic trees that receive excitatory synaptic connections from CA3 via Schaffer collaterals and commissural inputs to both apical and basal dendritic trees. Bursts of high frequency stimulation (S) are used to simulate complex-spike discharges in the afferent neurons. Timing rules are established by varying inter-burst frequency and spatial location of the activated synapses. (B) At apical dendritic synapses, bursts repeated at 5 Hz produce optimal LTP. Histogram plots the magnitude of LTP induced by 5–20 bursts repeated at the frequencies indicated on the abscissa. Figure modified from Larson et al. (1986). A similar frequency dependence is seen at basal dendritic synapses (Capocchi et al., 1992). (C) A burst to one apical dendritic input (S1) does not itself produce LTP at those synapses, but primes the cell so that a second burst to a separate input (S2) 200 ms later triggers LTP at only the synapses activated by the second burst. (D) A burst to an apical dendritic input (S1) can prime LTP induction at a basal dendritic input (S2). (E) A burst to a basal dendritic input (S1) can prime LTP induction at an apical dendritic input (S2). Results depicted in panels C–E are from Larson and Lynch (1986).

400 Hz bursts for LTP induction became common in studies of this structure. In this system, each burst was thought to induce an increment of LTP; repetition served only to summate these increments and little regard was placed on the repetition rate (Douglas, 1977). However, due to limited effectiveness, this pattern never caught on for studies of CA1 in hippocampal slices, where the most common induction pattern was a 1–2 s-long 100 Hz train (tetanus). Combining the complex-spike pattern with a theta frequency repetition rate produced a robust, reliable, and stable LTP in the CA1 field of hippocampal slices (Larson et al., 1986). These experiments used a four-pulse burst at 100 Hz to mimic the complex-spike burst and repeated it ten times at five bursts per second to approximate the theta rhythm frequency. The significance of LTP induced by this pattern was not immediately apparent until it was found that burst repetition frequencies lower or higher that 5 Hz were significantly less effective for LTP induction. The frequency-dependence of burst-induced LTP is reproduced in Fig. 1A, B.

2. Multiple-step induction mechanism and peculiarity of the theta frequency

What accounts for this frequency-dependence? Many mechanisms contribute. The first clue was that either a single burst or multiple bursts repeated at long intervals (≥ 2 s) were almost always ineffective (Larson and Lynch, 1986; Rose and Dunwiddie, 1986). However, a burst to one input could "prime" the circuit so that a second burst to a separate input 200 ms

Please cite this article as: Larson, J., Munkácsy, E., Theta-burst LTP. Brain Research (2014), http://dx.doi.org/10.1016/j.brainres.2014.10.034

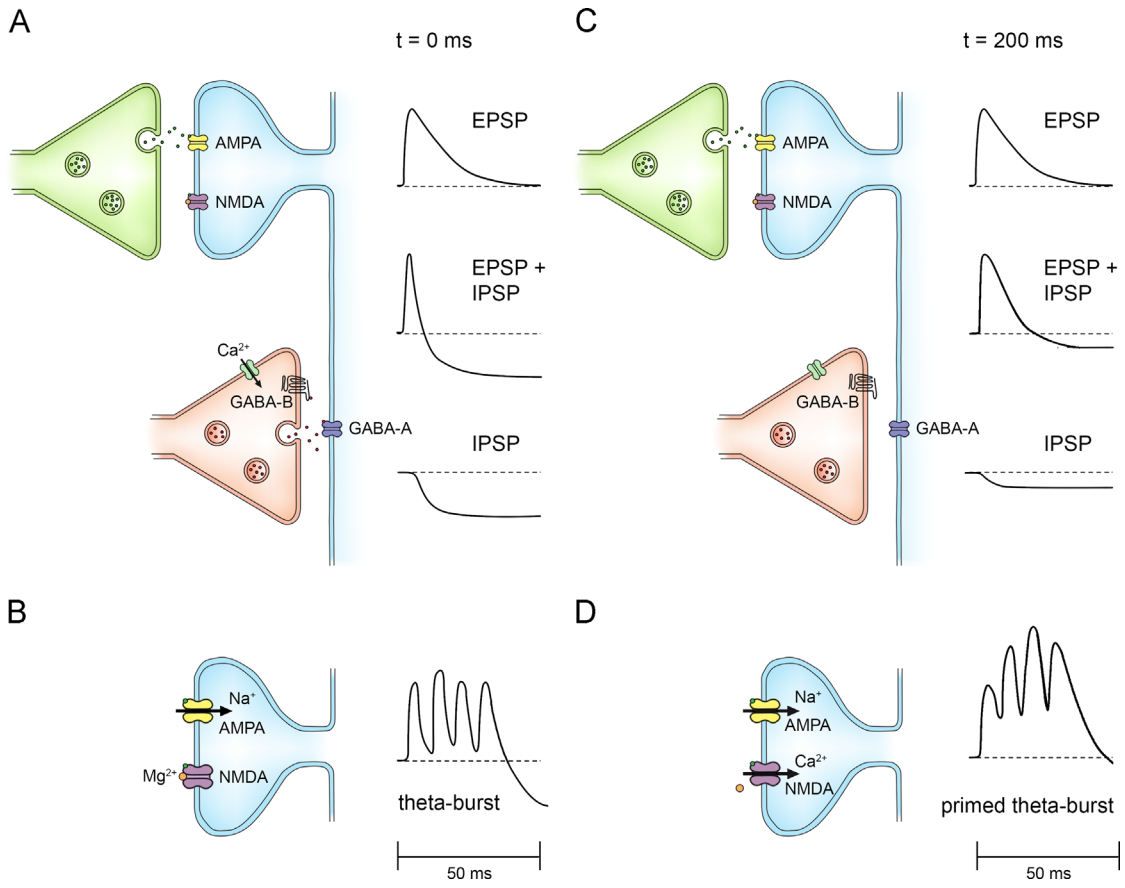

Fig. 2 – Multiple-step induction mechanism for theta-burst LTP in field CA1 of hippocampus. (A) In the "unprimed" state ($t=0$ ms), afferent stimulation activates a monosynaptic glutamatergic (excitatory) axo-spinous synapse and a disynaptic GABAergic (inhibitory) axo-dendritic synapse on the same pyramidal neuron. Glutamate activates postsynaptic AMPA receptors to depolarize the pyramidal neuron (EPSP) while co-expressed NMDA receptors are blocked by Mg^{2+}. GABA activates postsynaptic $GABA_A$ receptors that hyperpolarize the neuron (IPSP). The IPSP curtails the depolarization evoked by the EPSP (EPSP+IPSP). The GABA released at the inhibitory synapse also activates a slow, metabotropic $GABA_B$ receptor on the presynaptic inhibitory terminal. (B) A high frequency burst (theta-burst) under these conditions results in poor temporal summation of the depolarization due to the feed-forward inhibition. (C) In the "primed" state ($t=200$ ms), there is little change in the synaptic action at the excitatory synapse, but the action of the presynaptic $GABA_B$ receptor produces a use-dependent suppression of GABA release. The diminished IPSP causes the EPSP to have a prolonged depolarizing effect (EPSP+IPSP). (D) A high frequency burst in the primed state (primed theta-burst) shows enhanced temporal summation of excitation; the enhanced depolarization allows relief of the Mg^{2+} channel block and a calcium influx through the NMDA receptor.

later would reliably induce LTP, but only on the synapses activated by the second burst (Fig. 1C). A single burst activates a feed-forward inhibitory postsynaptic potential (IPSP) that truncates the excitatory postsynaptic potentials (EPSPs) evoked by that burst or a subsequent burst within 100–150 ms. The key to the theta frequency optimum is that the feed-forward inhibition becomes suppressed after its own activation and does not recover for about a second (Davies et al., 1990; McCarren and Alger, 1985). Because of this disinhibition, a second burst at 200 ms after the first burst evokes maximal postsynaptic depolarization in the pyramidal neuron. Bursts that occur too early are shunted by the already-present IPSP; bursts that are delayed too long encounter a recovering IPSP. We initially referred to the IPSP suppression as "priming" the circuit and showed that it could be effectuated by a single pulse (no burst required) and that it was spatially widespread since priming of apical synapses could be induced by basal dendritic stimulation and vice-versa (Fig. 1D, E) (Larson and Lynch, 1986). The IPSP suppression was verified (Pacelli et al., 1989, 1991) and shown to be mediated by metabotropic $GABA_B$ autoreceptors that result in diminished GABA release (Davies et al., 1991; Mott and Lewis, 1991, 1992). The enhanced burst-evoked depolarization of "primed" bursts allows measurable NMDA receptor-dependent currents to be activated (Larson and Lynch, 1988). There is evidence that the IPSP suppression is restricted to the feed-forward inhibitory circuit and absent in the feedback (recurrent) circuit, but this needs to be more firmly established (Arai et al., 1995). Interestingly, this may explain how theta rhythm is sustained if the GABAergic inhibitory interneurons ("theta" cells) are mainly the feedback rather than feed-forward interneurons. The main contributors to LTP induction by TBS are diagramed in Fig. 2.

Please cite this article as: Larson, J., Munkácsy, E., Theta-burst LTP. Brain Research (2014), http://dx.doi.org/10.1016/j.brainres.2014.10.034

Other factors that contribute to the pattern of dendritic depolarization and synaptic NMDA receptor activation are agents that enhance AMPA receptor activity by enhancing glutamate release or by allosteric modulation of AMPA receptors (ampakines): the latter drugs magnify the depolarization without changing the temporal pattern of burst response enhancement. Consequently, ampakines magnify the LTP induced by suboptimal burst repetitions (i.e., after 5 bursts) but do not alter the maximal LTP expressed (Arai and Lynch, 1992). In contrast, an agent such as forskolin that antagonizes the calcium-dependent AHP between theta bursts elevates the LTP "ceiling" without changing the fractional increment produced by suboptimal bursts (Arai and Lynch, 1992), possibly by extending the duration of NMDA receptor currents.

A four-pulse burst was used in these experiments because it is within the common range of hippocampal complex-spikes and because three-pulse bursts are rarely sufficient – see also Arai et al. (2004) and Diamond et al. (1988). We have used 100 Hz as the intra-burst frequency because it allows resolution of responses to the individual pulses. Other variations on pulse number and intra-burst frequency have not been studied systematically. It is likely that intra-burst frequency effects such as presynaptic facilitation and depletion (Pan and Zucker, 2009) interact with pulse number to determine the synaptic cleft glutamate concentration available to interact with postsynaptic NMDA receptors.

The theta frequency optimum has been questioned by Grover and colleagues who tested the efficacy of four-pulse bursts repeated 20 times at frequencies from 0.05 to 10.0 Hz, with maximal LTP induced at 2–3 Hz (Grover et al., 2009), making the interesting point that the lower frequency maximum may correspond more closely to the delta waves that are present in the hippocampal EEG during slow-wave sleep rather than the theta waves of behavioral arousal and REM sleep. It is an intriguing possibility to consider that the frequency–plasticity relationship may be altered by changes in "circuit kinetics", perhaps dictated by brainstem modulatory systems, associated with different behavioral states. On the other hand, the frequency–plasticity relationship may also be distorted during regular repetition of bursts to a single input. A pair of appropriately timed bursts is much more likely to occur naturally during behavior than a series of 10–20 bursts repeated at regular intervals. Studies using the primed-burst paradigm (homosynaptic priming) or the two-input paradigm showed significant LTP maxima at 140 ms (~7 Hz) (Diamond et al., 1988) and 100–200 ms (5–10 Hz), respectively (Larson, 1987). Since a single (primed) burst is sufficient to induce a small increment of stable LTP that is additive (Larson and Lynch, 1986), this frequency-dependence seems more likely to reflect the conditions *in vivo* than those that obtain when many bursts are repeated in a long series. In chronic single-unit recording studies, Otto and Eichenbaum observed that complex-spike burst discharges of CA1 pyramidal cells were often preceded by spike or burst activity at theta periodicity during odor discrimination or spatial learning (Otto et al., 1991), validating the occurrence of theta-burst activity in freely-behaving animals.

Theta-burst LTP exhibits three other canonical features of LTP: cooperativity (associativity), saturation, and stability. The requirement for adequate postsynaptic depolarization to activate voltage-sensitive NMDA receptors was discussed above; normally, this is provided by simultaneous stimulation of many afferents (cooperativity). How realistic is this? It is comforting perhaps that detectable and stable LTP is induced by a single appropriately-primed four-pulse burst (Larson and Lynch, 1986; Rose and Dunwiddie, 1986). In situ, some of the necessary depolarization may be provided by the theta rhythm itself: experiments show that single bursts *in vivo* can be effective when timed to occur at the peak depolarization of endogenous theta waves and are ineffective when evoked at the trough (Holscher et al., 1997; Hyman et al., 2003; McCartney et al., 2004; Orr et al., 2001; Pavlides et al., 1988). Thus, LTP induction may not require unrealistically massive synchronization of many bursting inputs to a cell. We will return to the spatial limits of within-burst spatial summation in a later section. With regard to saturation, LTP resulting from a single episode of TBS seems to reach a maximum after about 10 bursts (Larson et al., 1986); however, this limit may be exceeded with widely-spaced episodes (Kramar et al., 2012), suggesting that synapses may differ in LTP threshold, with later episodes recruiting less susceptible synapses (Lynch et al., 2013). Finally, theta-burst LTP in slice preparations typically is non-decremental after the first 15 min. This also appears to be true *in vivo*, where the potentiation is maintained at a stable level for weeks (Staubli and Lynch, 1987).

3. "Economy" of theta-burst stimulation

It seems evident from the frequency-dependence of patterned burst-induced LTP that long continuous trains (tetanic stimulation) would be less efficient than TBS in the sense that each stimulus pulse would contribute less to the LTP effect. However,

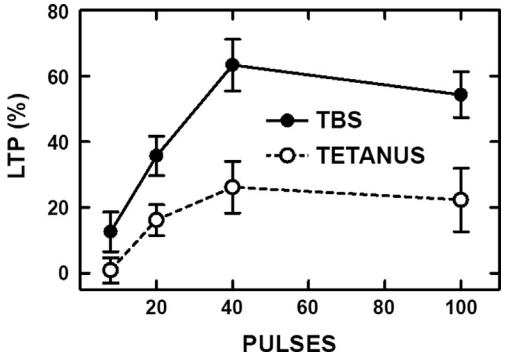

Fig. 3 – Theta-burst stimulation is more efficient than continuous high frequency stimulation for LTP induction in hippocampal field CA1. LTP at apical dendritic synapses was measured as the percent increase in field EPSP slope 60 min after LTP induction by stimulation of Schaffer-commissural fibers with either a continuous, 100 Hz train consisting of 8–100 pulses (TETANUS) or the same total number of pulses given as bursts of four repeated at 200 ms intervals (TBS). Significantly greater LTP was evoked by TBS with 20 pulses (5 bursts, $p<0.05$), 40 pulses (10 bursts, $p<0.01$), and 100 pulses (25 bursts, $p<0.01$) than tetani consisting of the corresponding number of pulses. Results are from unpublished data by J. Larson and J. Crouch.

Please cite this article as: Larson, J., Munkácsy, E., Theta-burst LTP. Brain Research (2014), http://dx.doi.org/10.1016/j.brainres.2014.10.034

this has received little systematic study. One study of field CA1 in rat hippocampal slices (Hernandez et al., 2005) reported no statistically-significant differences between the amounts of LTP induced by tetani and theta-bursts containing the same total stimulation pulses. The minimal TBS stimulus consisted of ten theta bursts in that study, so the submaximal stimulation range was not investigated. Furthermore, the pulse number-LTP magnitude curves for both TBS and tetanic stimulation were fairly flat, suggesting that a ceiling effect may have obtained with the minimal conditions used.

We re-examined this issue using a two-input paradigm in field CA1 of male adult (2–3 months) mouse (CD-1) hippocampal slices. Slices were prepared as described (Larson et al., 1999) and maintained at the interface between perfused (1 mL/min) aCSF (in mM: NaCl 124, KCl 3, KH_2PO_4 1.2, $NaHCO_3$ 26, $MgSO_4$ 2.5, $CaCl_2$ 3.4, D-glucose 10, Na-L-ascorbate 2) and an atmosphere of 95%O_2/5% CO_2, at 34±1 °C. Stimulation electrodes (bipolar twisted nichrome wires) were placed in *stratum radiatum* of CA1a and CA1c and field potentials recorded via a glass microelectrode (2 M NaCl) in *s. radiatum* of CA1b. Test pulse intensity was set to evoke a 2.0 mV field EPSP using a stimulus pulse duration of 0.1 ms. Each slice tested was given a theta-burst stimulus on one pathway and a tetanus (continuous 100 Hz train) consisting of the same total number of stimulus pulses on the other pathway (in random order and with position counter-balanced) with at least 30 min delay between LTP induction episodes. Pulse duration was increased to 0.2 ms during the induction stimuli. The degree of LTP induced was quantified at 60 min post-stimulation for each pathway. The total number of induction pulses used in different slices was 8 (2 theta-bursts or an 80 ms long tetanus), 20 (5 theta-bursts or a 200 ms tetanus), 40 (10 theta-bursts or a 400 ms tetanus), or 100 (25 theta-bursts or a 1 s tetanus). As shown in Fig. 3, no significant LTP was induced by the shortest tetanus, although significant LTP was induced by the same number of pulses (8) given as two theta-bursts (however, due to large variances, the direct comparison of TBS to tetanus was not significant). For greater numbers of pulses, theta-bursts yielded more LTP than the same number of pulses given as a single tetanus. A two-way ANOVA on the percent change persisting at 60 min post LTP stimulation showed significant main effects of stimulus pattern ($F_{1,124}=25.65$, $p<0.0001$) and pulse number ($F_{3,124}=11.39$, $p<0.0001$) but no significant interaction between the two independent variables ($F_{3,124}=1.37$, $p>0.25$). These results confirm that TBS is indeed more economical for LTP induction than un-patterned stimulation. In fact, the 100-pulse tetanus yielded somewhat less LTP than a theta-burst pattern of only 20 pulses. More is not necessarily better! A possible explanation for the weaker effect of tetanic stimulation is that depletion of glutamate available for release occurs during continuous trains, thus reducing NMDA receptor activation.

4. Spatial limits of associative theta-burst LTP

Classic "associative LTP" experiments in the CA1 *s. radiatum* (apical dendritic layer) showed that a single stimulus train of intensity or duration too weak to induce LTP on its own can do so if simultaneously paired with a stronger train to a separate input (Barrionuevo and Brown, 1983; Gustafsson and Wigstrom, 1986; Kelso and Brown, 1986; Kelso et al., 1986). Further studies provided evidence that these associative interactions are most effective when the two inputs terminate in spatially-overlapping regions of the dendritic tree (Hardie and Spruston, 2009; White et al., 1988, 1990) or individual branches (Govindarajan et al., 2011), although there is one report that strong stimulation of a basal dendritic (*s. oriens*) input can facilitate LTP in a simultaneously-stimulated apical dendritic input (Gustafsson and Wigstrom, 1986).

We investigated associative interactions between basal and apical dendritic synapses using TBS in field CA1 of hippocampal slices from adult male CD-1 mice, prepared and maintained as described above. Two stimulating electrodes were used: one was designated as the test electrode (S1; weak) and positioned either in *s. radiatum* (apical dendrite) or *stratum oriens* (basal dendrite) of CA1c; the other electrode was designated the conditioning electrode (S2; strong) and was positioned either in *s. radiatum* or *s. oriens* of CA1a. The recording electrode was positioned in CA1b in the same lamina as the test electrode. Stimulus intensity for the S1 (weak) electrode was always set to evoke a fEPSP about 1 mV in amplitude (typically about 20–25% of the maximal population spike-free fEPSP) while the S2 (strong) intensity was always set to evoke a population spike. In the first set of experiments (see Fig. 4A–D), S1 was positioned in *s. radiatum*. After establishing a baseline, two episodes of five theta-bursts (4 pulses at 100 Hz with 200 ms between the bursts) separated by 5 s were given to the test electrode (S1) alone. Recording was continued for 30 min to monitor the LTP induced. The conditioning (S2) stimulation electrode was then placed in *s. oriens* and S1 responses monitored for a 10 min baseline before both test (S1) and conditioning (S2) electrodes were given the same theta-bursts simultaneously. After an additional 30 min of recording, the conditioning (S2) electrode was moved to *s. radiatum*, the combined theta-burst stimulation (S1+S2) repeated, and LTP monitored on S1 for an additional 30 min. Stimulus pulse duration was *never* increased during TBS. In the second set of experiments (see Fig. 4E–H), S1 was located in *s. oriens* and S2 was first in *s. radiatum* and subsequently in *s. oriens*.

Conditioning stimulation of an apical dendritic input effectively facilitated LTP in the apical dendritic test input. In contrast, no associative LTP was induced in the apical test input when the conditioning stimulation was a basal dendritic input. Likewise, the basal dendritic test input was facilitated by a basal conditioning stimulus, but not by an apical input.

These results suggest that associative interactions during LTP induction by theta-bursts are limited to dendritic compartments. Weak and strong synaptic inputs can cooperate for LTP induction within the same dendritic tree but not between dendrites separated by the soma. The conventional interpretation of such interactions is that they require spatial summation of depolarization to allow activation of synaptic NMDA receptors. This suggests that the spatial summation can occur within apical or basal dendritic trees but not between them. One possibility is that shunting inhibition at the soma limits the spread of depolarization from apical to basal dendrites and vice-versa. While feed-forward IPSPs are suppressed during theta-bursts, these may be preferentially

Please cite this article as: Larson, J., Munkácsy, E., Theta-burst LTP. Brain Research (2014), http://dx.doi.org/10.1016/j.brainres.2014.10.034

located in the dendrites (Alger and Nicoll, 1982); somatic feedback IPSPs, $GABA_B$-dependent postsynaptic IPSPs, and calcium-activated after-hyperpolarizations appear to be intact during theta-bursts. The only experiment in which associative interactions between apical and basal dendritic synapses were found was conducted with $GABA_A$ receptors blocked pharmacologically (Gustafsson and Wigstrom, 1986). Alternatively, if associative LTP depends on diffusion and summation of chemical signals, this process also appears to be compartment specific (Govindarajan et al., 2011). In any case, it appears that the conditions of our experiment allow effective summation of synaptic signals within branches of the apical or basal dendritic trees, but not between the apical and basal compartments.

5. A within-burst timing effect

The possible role of asynchrony within theta-bursts was studied using a three-input paradigm in field CA1 of hippocampal slices (Larson and Lynch, 1989). The paradigm and results are summarized in Fig. 5. Three separate apical

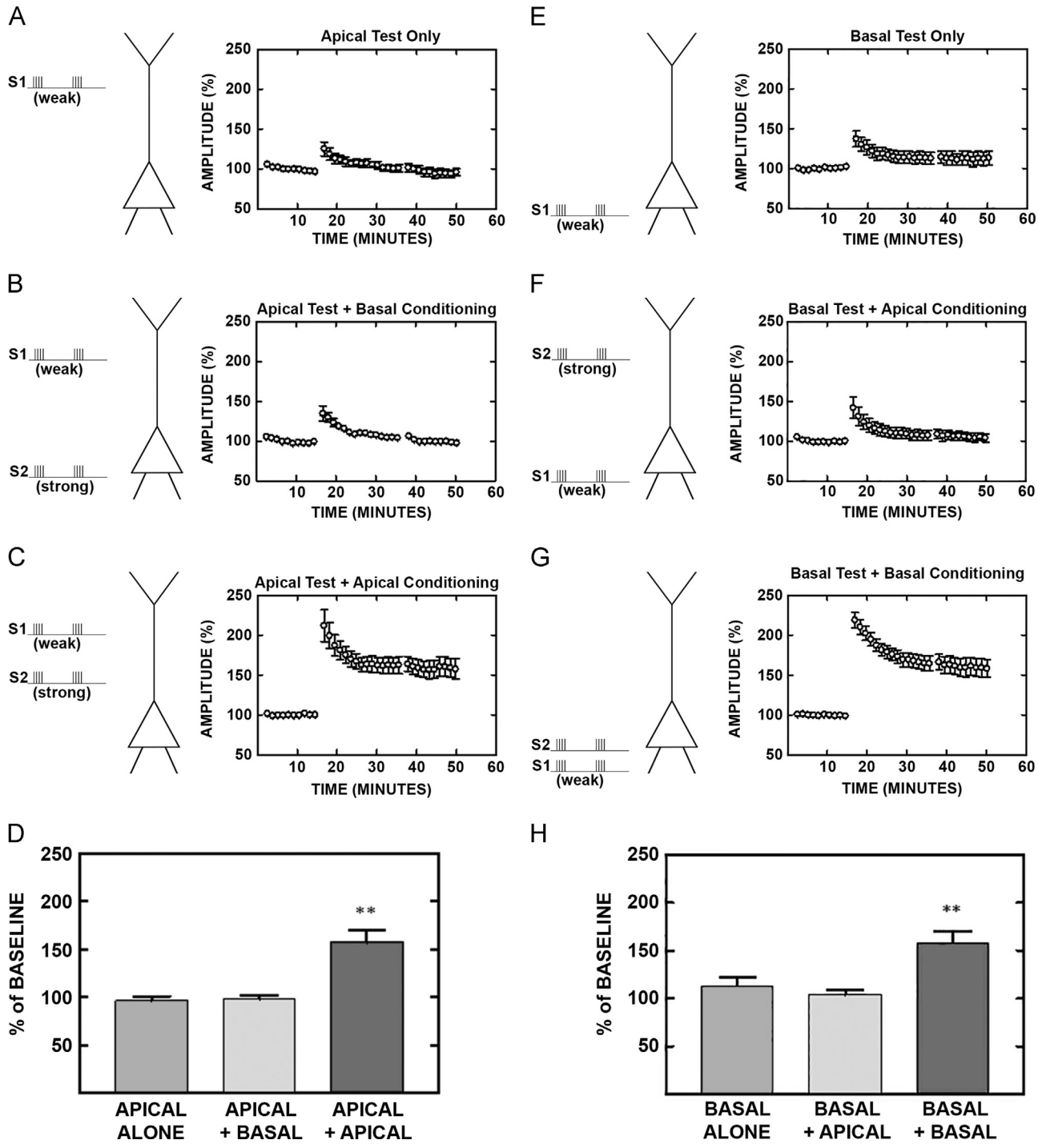

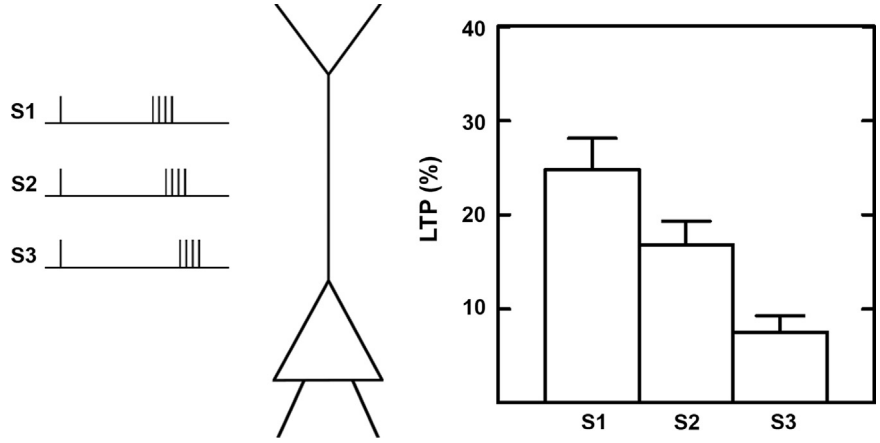

Fig. 5 – Within-burst timing and LTP. Hippocampal slices were prepared with a recoding electrode and three stimulating electrodes in *s. radiatum* of CA1. After a baseline period of recording responses to all three inputs, patterned stimulation was applied as depicted at left. All three inputs received a priming pulse followed by asynchronous bursts. The first pulse in the burst (4 pulses, 100 Hz) to S1 occurred 180 ms after the priming pulse, the first pulse to S2 coincided with the third pulse in the S1 burst, and the first pulse in the S3 burst coincided with the third pulse in the S2 burst. The pattern was repeated ten times at 5 s. intervals. The LTP induced at all three sets of synapses were statistically different from each other ($p<0.05$). Modified from Larson and Lynch (1989).

dendritic inputs were stimulated using stimulus intensity too low for any one input to be potentiated by TBS independently. For LTP induction, each input was stimulated with a simultaneous "priming" pulse followed by a 4-pulse burst to each input in a staggered but partially overlapping sequence. The spatial position of the inputs was counter-balanced *vis a vis* the timing pattern in different slices. The pulse-burst pattern was repeated ten times at five-second intervals. The degree of LTP induced was significantly related to the position of the input in the temporal sequence, with the synapses stimulated first in the sequence showing the most potentiation and the last-stimulated input being potentiated the least. One explanation for this timing effect is that the later arriving bursts can maintain depolarization longer at the synapses activated first and sustain NMDA channel activity at those synapses (Larson and Lynch, 1989). There is some similarity between this within-burst rule and the rules that govern spike timing-dependent plasticity (Feldman, 2012). The functional significance of the within-burst timing rule was investigated in network models; this work indicated that it contributes to encoding and recall of cues consisting of temporal sequences (Granger et al., 1994).

6. Theta-burst responses as diagnostics

Measuring postsynaptic responses to theta-bursts can be used to determine if experimental manipulations such as drugs or mutations affect LTP by interfering with the electrophysiological responses of the circuit to TBS or, alternatively,

Fig. 4 – Associative LTP induced by theta-burst stimulation is restricted to major dendritic domains. (A) A test electrode (S1) placed in the *s. radiatum* of field CA1 was used to study the spatial rules governing associative LTP induced by theta-burst stimulation. Stimulus intensity was set to evoke a field EPSP too weak (~1 mV in amplitude) to induce LTP when stimulated with TBS alone (see text for details). Graph shows field EPSP amplitude measured at 20 s intervals for 15 min before and 35 min. after TBS (each point is the mean ± S.E.M. of 4 consecutive trials) in seven different slices, each from a different mouse. (B) The same test input (S1) was then given TBS simultaneous with TBS to a strong input (S2) to the basal dendrites. The graph shows the S1 response amplitude (as in A) before and after TBS to S1 and S2 ($n=7$). (C) The test input was then given TBS simultaneous with stimulation of a strong input to the apical dendritic field (S2). This resulted in robust LTP to the S1 input ($n=6$, one slice rejected from analysis due to instability). (D) Histograms show field EPSP amplitude measured 30 min after TBS, relative to the pre-TBS baseline, in the three stimulation conditions. LTP was significantly greater after the apical-apical pairing than in the other two conditions ($p<0.01$). (E) as in (A), except that the test input (S1) was to the basal dendrites ($n=6$ experiments in slices from different mice). Weak stimulation to the basal dendritic input did not induce LTP when stimulated alone (E) or in combination with an apical dendritic input (F), but did show robust LTP after combined stimulation of a strong (S2) basal dendritic input (G). Histograms (H) show that significantly greater LTP was induced after combined basal-basal stimulation than in the other two conditions (**$p<0.01$). One slice in (E) was rejected from analysis due to instability. In both (C) and (G), the physical location of weak (S1) and strong (S2) electrodes were in subfields CA1c and CA1a, respectively (recording electrode in CA1b), and paired-pulse tests confirmed that the activated fibers were independent. In all other cases, the stimulation electrodes were in CA1c (i.e., the subfield closest to CA3). Results are from unpublished experiments by E. Munkácsy, N. Bartolotti, and J. Larson.**

Please cite this article as: Larson, J., Munkácsy, E., Theta-burst LTP. Brain Research (2014), http://dx.doi.org/10.1016/j.brainres.2014.10.034

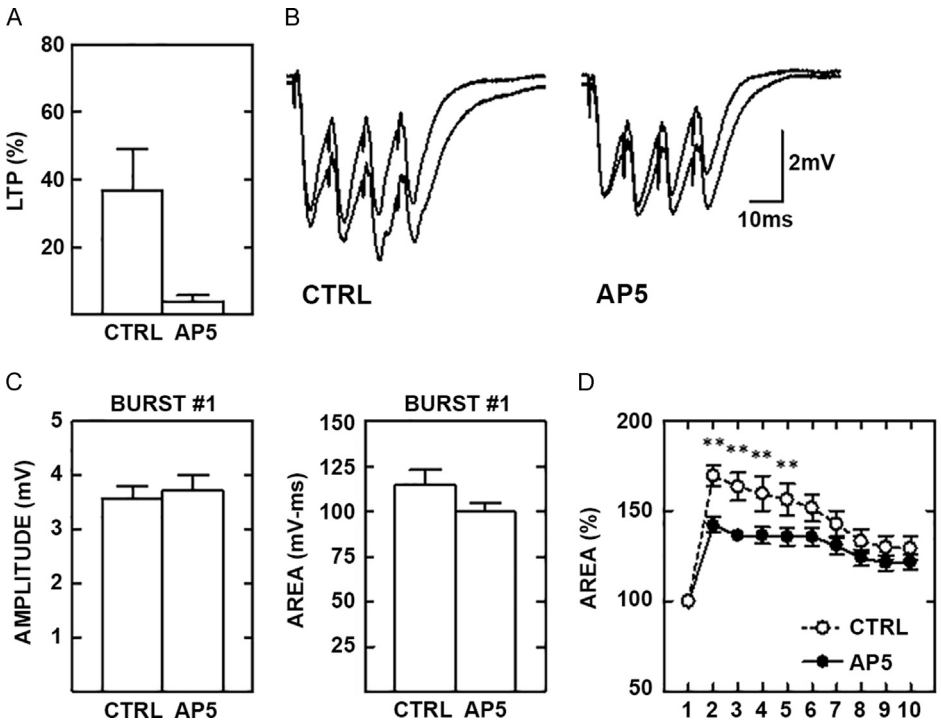

Fig. 6 – Activation of NMDA receptors during theta-burst stimulation. (A) The NMDA receptor antagonist, D-AP5 (50 μM) blocks LTP induction by TBS consisting of ten bursts (4 pulses, 100 Hz) repeated at 5 Hz. LTP was measured as the percent increase in field EPSP slope 60 min after TBS in the absence of D-AP5 (CTRL) or 60 min after TBS given in the presence of the drug (AP5). Data are means+S.E.M. ($n=7$). (B) Field EPSP waveforms evoked by the first two bursts in the TBS under control conditions (CTRL) and in the presence of the antagonist (AP5). The second burst response is larger than the first in both conditions. (C) Measurements of the amplitude of the first response within the first burst (left panel) and the total area under the response to the first burst (right panel) were not significantly affected by AP5. (D) The areas of bursts 2–10 were calculated and expressed as a percentage of the area of the first burst in both the AP5 condition and the control condition. The NMDA receptor antagonist significantly reduced the area of responses to second through fifth bursts of the TBS ($p<0.01$). Unpublished data from J. Larson and J. Crouch.**

affect downstream signaling cascades. The activation of NMDA receptors by theta patterned stimulation was first demonstrated using a two-input paradigm (Larson and Lynch, 1988), but is also evident in the standard TBS paradigm, as shown in Fig. 6. Mouse hippocampal slices were prepared as described above with two stimulation electrodes and an extracellular recording electrode in *s. radiatum* of field CA1. Slices were first stimulated with 10 theta-bursts on one pathway and synaptic transmission was monitored for 60 min. post-TBS. Slices were then perfused with the competitive NMDA receptor antagonist, D-AP5 (50 μM), and stimulated with an identical TBS on the second pathway. Synaptic transmission was again monitored for one hour post-TBS. Field potentials evoked by the theta bursts were recorded and measured (see Fig. 6 legend for details). The NMDA antagonist, while blocking LTP, had very little effect on the response to the first ("unprimed") burst, but reduced the envelope of depolarization evoked by several of the succeeding bursts. With repeated theta-bursts, synaptic facilitation and depletion probably contribute to the inverted U shape of the burst response enhancement curves.

Other conditions in which alterations of LTP are associated with altered burst responses include suppressed LTP in transgenic mouse models for Alzheimer's disease (Larson et al., 1999), suppressed LTP by diazepam (del Cerro et al., 1992), reduced LTP after neonatal lesions of contralateral hippocampus (van Praag et al., 1998), reduced LTP after inhibition of matrix metalloproteinases (Meighan et al., 2007), enhanced LTP in mice overexpressing brain protease nexin-1 (Luthi et al., 1997), facilitated LTP by an M1 muscarinic antagonist (Boddeke et al., 1992), and enhanced LTP after environmental enrichment (Malik and Chattarji, 2012), among others. Recording and analyzing the burst response pattern can help to provide a first-pass evaluation of whether an experimental manipulation affects events before or after the NMDA receptor-mediated influx of calcium that serves as the essential trigger for LTP induction.

7. Sensitivity of theta-burst LTP to various experimental manipulations

There is considerable overlap between the downstream molecular events triggered by TBS and other high-frequency tetanic stimulation methods; however, there are many conditions in which theta-burst LTP is more sensitive to experimental manipulations than is the LTP induced by long trains of 100 Hz stimulation. For example, theta-burst LTP is more

Please cite this article as: Larson, J., Munkácsy, E., Theta-burst LTP. Brain Research (2014), http://dx.doi.org/10.1016/j.brainres.2014.10.034

vulnerable to aging (Moore et al., 1993; Rex et al., 2005) and experimentally-induced stress (Diamond et al., 1989, 1992, 1994) than is tetanus-induced LTP and appears to be more sensitive to manipulations that affect BDNF (Chen et al., 1999, 2010; Kang et al., 1997; Pang et al., 2004; Patterson et al., 2001; Skucas et al., 2011), serotonin (Corradetti et al., 1992), endocannabinoid (Pan et al., 2011), or adenosine receptor-dependent (Costenla et al., 1999) signaling mechanisms. Experiments on a number of mutant mouse models show selective or larger disruptions of LTP induced by theta-bursts than of LTP induced by tetanic stimulation (Evers et al., 2002; Gong et al., 2009; Jedlicka et al., 2009; Luthi et al., 1997; Shalin et al., 2006). Many of these experimental conditions also affect learning and/or memory processes, suggesting that theta-burst LTP may be a better model for the memory effects than tetanus-induced LTP.

Few of the manipulations described above have been resolved into effects on events antecedent or consequent to the LTP induction triggering event. The preponderance of evidence suggests that theta-burst LTP represents a minimalist model for stable (non-decremental) LTP. If so, then we might expect that theta-burst LTP would be more sensitive to perturbations of events antecedent to LTP induction. Theta-burst stimulation exploits the endogenous circuit properties to maximize NMDA receptor activation with the least amount of afferent stimulation. Under some circumstances, long trains may simply be less efficient for triggering LTP (Fig. 3). However, this inefficiency may be overcome by high intensity trains or multiple repetitions at short (<1 min) intervals. Some paradigms may even engage mechanisms in addition to those minimally essential for stable LTP. For example, trains of 200 Hz stimulation are reported to activate voltage-dependent calcium channels as well as synaptic NMDA receptor-mediated calcium fluxes (Grover and Teyler, 1990). Clearly, manipulations that alter the circuit dynamics exploited by theta-bursts, such as blockade of inhibition, have a major effect on the sensitivity of theta-burst LTP as compared to tetanus-induced LTP (Pacelli et al., 1989).

If we consider the events consequent to the minimal trigger for LTP – NMDA receptor-mediated calcium flux into the dendritic spine – the situation is more complex. The biochemical mechanisms for insertion of AMPA receptors (LTP expression) and cytoskeletal reorganization essential for LTP stabilization must be common to all stimulation paradigms that produce a stable effect. Under the mild induction conditions of TBS, these mechanisms may be more sensitive to disruption by experimental manipulations. On the other hand, more intense or protracted stimulation patterns may engage additional pathways that would be sensitive to disruptions that have little effect on theta-burst LTP (Smith et al., 2009).

8. Conclusions

The forty-odd years of LTP research have been filled with debates, even arguments, about its cellular mechanism and significance for learning and memory. We have reviewed here one aspect of this history: the relationship between naturally-occurring cell activity patterns and LTP induction. The traditions that have influenced attitudes about synaptic plasticity have been argued elsewhere (Larson et al., 1991) and will not be elaborated here except to say that one approach considers all manifestations of plasticity to be potential participants in brain substrates of experience, or at least worthy of study in their own right, whereas a second approach emphasizes the plastic changes that are triggered by neuronal activity patterns that actually occur during learning events. Theta-burst LTP emerged from the latter tradition. The former tradition has its own merits; indeed, the discovery of LTP arose from an exploration of the frequency-dependence of synaptic transmission (Andersen, 1991).

Most of the work reviewed here has used the field CA1 of hippocampus as a model system. However, theta-bursts induce LTP in other cortical networks, including the dentate gyrus (Greenstein et al., 1988; Yeckel and Berger, 1998), subiculum (Commins et al., 1999), perirhinal cortex (Cousens and Otto, 1998), piriform cortex (Jung et al., 1990; Kanter and Haberly, 1990), entorhinal cortex (de Curtis and Llinas, 1993; Yun et al., 2002), as well as visual (Heynen and Bear, 2001; Kirkwood et al., 1995), somatosensory (Castro-Alamancos and Connors, 1996; Hardingham et al., 2003), auditory (Hogsden et al., 2011), anterior cingulate (Liu and Zhuo, 2014), prefrontal (Maroun and Richter-Levin, 2003; Vickery et al., 1997), and insular (Liu et al., 2013) neocortices. Whether or not theta-burst LTP in these areas reflects resonance with local circuit operation and the same cellular mechanisms as in CA1 is not clear. Neocortical neurons show intrinsic rhythmogenesis (Silva et al., 1991) and circuit resonance (Castro-Alamancos, 2013) in the theta frequency range. Furthermore, there is now a large literature of studies using transcranial magnetic stimulation protocols based on theta burst stimulation for therapeutic purposes in neurological disease in which long-term enhancement of cortical function is indicated (Huang et al., 2005; Nettekoven et al., 2014).

We have presented a model for the means by which theta burst stimulation leads to NMDA receptor activation for LTP induction, tested the efficiency of theta-burst LTP, described the limitations of spatial summation of synaptic activity during theta bursts, and discussed the special sensitivity of theta-burst LTP to a variety of experimental manipulations. We argued that theta-burst LTP represents a minimal model for the LTP process. The discussion has emphasized cellular mechanisms and has omitted detailed consideration of the role of theta and bursting in learning and memory. A few studies have reported parallel effects of experimental manipulations on spontaneous theta rhythm *in vivo* and theta-burst LTP (Maren et al., 1994; Staubli and Xu, 1995). An alternative approach, showing that theta-burst stimulation *in vivo* produces synaptic potentiation as its behavioral significance is learned (Roman et al., 1987) was instrumental in the development of the theta-burst LTP paradigm.

Acknowledgments

We thank Nancy Long Bartolotti and Joel Crouch for assistance with some of the experiments reported here. JL was supported by grants from the NIH (DC005793) and Department of Defense (USAMRMC 10917352). EM was supported by the UIC Honors College, UIC College of Liberal Arts and

Sciences, the Glenn Foundation for Medical Research, and NIH (T32 AG021890).

REFERENCES

Alger, B.E., Nicoll, R.A., 1982. Feed-forward dendritic inhibition in rat hippocampal pyramidal cells studied in vitro. J. Physiol. 328, 105–123.

Andersen, P., 1991. Foreword: LTP—an exciting and continuing saga. In: Baudry, M., Davis, J.L. (Eds.), Long-term Potentiation: A Debate of Current Issues. MIT Press, Cambridge, MA, pp. xiii–xvii.

Arai, A., Lynch, G., 1992. Factors regulating the magnitude of long-term potentiation induced by theta pattern stimulation. Brain Res. 598, 173–184.

Arai, A., Silberg, J., Lynch, G., 1995. Differences in the refractory properties of two distinct inhibitory circuitries in field CA1 of the hippocampus. Brain Res. 704, 298–306.

Arai, A.C., Xia, Y.F., Suzuki, E., 2004. Modulation of AMPA receptor kinetics differentially influences synaptic plasticity in the hippocampus. Neuroscience 123, 1011–1024.

Barrionuevo, G., Brown, T.H., 1983. Associative long-term potentiation in hippocampal slices. Proc. Natl. Acad. Sci. USA 80, 7347–7351.

Bliss, T.V., Gardner-Medwin, A.R., 1973. Long-lasting potentiation of synaptic transmission in the dentate area of the unanaestetized rabbit following stimulation of the perforant path. J. Physiol. 232, 357–374.

Bliss, T.V., Lomo, T., 1973. Long-lasting potentiation of synaptic transmission in the dentate area of the anaesthetized rabbit following stimulation of the perforant path. J. Physiol. 232, 331–356.

Boddeke, E.W.G.M., Enz, A., Shapiro, G., 1992. SDZ ENS 163, a selective muscarinic M1 receptor agonist, facilitates the induction of long-term potentiation in rat hippocampal slices. Eur. J. Pharmacol. 222, 21–25.

Capocchi, G., Zampolini, M., Larson, J., 1992. Theta burst stimulation is optimal for induction of LTP at both apical and basal dendritic synapses on hippocampal CA1 neurons. Brain Res. 591, 332–336.

Castro-Alamancos, M.A., Connors, B.W., 1996. Short-term synaptic enhancement and long-term potentiation in neocortex. Proc. Natl. Acad. Sci. USA 93, 1335–1339.

Castro-Alamancos, M.A., 2013. The motor cortex: a network tuned to 7–14 Hz. Front. Neural Circuits 7, 21.

Chen, G., et al., 1999. Relative contribution of endogenous neurotrophins in hippocampal long-term potentiation. J. Neurosci. 19, 7983–7990.

Chen, L.Y., et al., 2010. Learning induces neurotrophin signaling at hippocampal synapses. Proc. Natl. Acad. Sci. USA 107, 7030–7035.

Commins, S., et al., 1999. The effects of single and multiple episodes of theta patterned or high frequency stimulation on synaptic transmission from hippocampal area CA1 to the subiculum in rats. Neurosci. Lett. 270, 99–102.

Corradetti, R., et al., 1992. Serotonin blocks the long-term potentiation induced by primed burst stimulation in the CA1 region of rat hippocampal slices. Neuroscience 46, 511–518.

Costenla, A.R., de Mendonca, A., Ribeiro, J.A., 1999. Adenosine modulates synaptic plasticity in hippocampal slices from aged rats. Brain Res. 851, 228–234.

Cousens, G., Otto, T.A., 1998. Induction and transient suppression of long-term potentiation in the peri- and postrhinal cortices following theta-related stimulation of hippocampal field CA1. Brain Res. 780, 95–101.

Davies, C.H., Davies, S.N., Collingridge, G.L., 1990. Paired-pulse depression of monosynaptic GABA-mediated inhibitory postsynaptic responses in rat hippocampus. J. Physiol. 424, 513–531.

Davies, C.H., et al., 1991. GABA autoreceptors regulate the induction of LTP. Nature 349, 609–611.

de Curtis, M., Llinas, R.R., 1993. Entorhinal cortex long-term potentiation evoked by theta-patterned stimulation of associative fibers in the isolated in vitro guinea pig brain. Brain Res. 600, 327–330.

del Cerro, S., Jung, M., Lynch, G., 1992. Benzodiazepines block long-term potentiation in slices of hippocampus and piriform cortex. Neuroscience 49, 1–6.

Deschenes, M., Moore, J., Kleinfeld, D., 2012. Sniffing and whisking in rodents. Curr. Opin. Neurobiol. 22, 243–250.

Diamond, D.M., Dunwiddie, T.V., Rose, G.M., 1988. Characteristics of hippocampal primed burst potentiation in vitro and in the awake rat. J. Neurosci. 8, 4079–4088.

Diamond, D.M., et al., 1989. Adrenalectomy reduces the threshold for hippocampal primed burst potentiation in the anesthetized rat. Brain Res. 492, 356–360.

Diamond, D.M., et al., 1992. Inverted-U relationship between the level of peripheral corticosterone and the magnitude of hippocampal primed burst potentiation. Hippocampus 2, 421–430.

Diamond, D.M., Fleshner, M., Rose, G.M., 1994. Psychological stress repeatedly blocks hippocampal primed burst potentiation in behaving rats. Behav. Brain Res. 62, 1–9.

Douglas, R.M., Goddard, G.V., 1975. Long-term potentiation of the perforant path-granule cell synapse in the rat hippocampus. Brain Res. 86, 205–215.

Douglas, R.M., 1977. Long lasting synaptic potentiation in the rat dentate gyrus following brief high frequency stimulation. Brain Res. 126, 361–365.

Evers, M.R., et al., 2002. Impairment of L-type Ca^{2+} channel-dependent forms of hippocampal synaptic plasticity in mice deficient in the extracellular matrix glycoprotein tenascin-C. J. Neurosci. 22, 7177–7194.

Feldman, Daniel E., 2012. The spike-timing dependence of plasticity. Neuron 75, 556–571.

Gong, N., et al., 2009. GABA transporter-1 activity modulates hippocampal theta oscillation and theta burst stimulation-induced long-term potentiation. J. Neurosci. 29, 15836–15845.

Govindarajan, A., et al., 2011. The dendritic branch is the preferred integrative unit for protein synthesis-dependent LTP. Neuron 69, 132–146.

Granger, R., et al., 1994. Non-Hebbian properties of long-term potentiation enable high-capacity encoding of temporal sequences. Proc. Natl. Acad. Sci. USA 91, 10104–10108.

Green, J.D., Arduini, A., 1954. Hippocampal electrical activity in arousal. J. Neurophysiol. 17, 533–557.

Greenstein, Y.J., Pavlides, C., Winson, J., 1988. Long-term potentiation in the dentate gyrus is preferentially induced at theta rhythm periodicity. Brain Res. 438, 331–334.

Grover, L.M., Teyler, T.J., 1990. Two components of long-term potentiation induced by different patterns of afferent activation. Nature 347, 477–479.

Grover, L.M., et al., 2009. LTP in hippocampal area CA1 is induced by burst stimulation over a broad frequency range centered around delta. Learn. Mem. 16, 69–81.

Gustafsson, B., Wigstrom, H., 1986. Hippocampal long-lasting potentiation produced by pairing single volleys and brief conditioning tetani evoked in separate afferents. J. Neurosci. 6, 1575–1582.

Hardie, J., Spruston, N., 2009. Synaptic depolarization is more effective than back-propagating action potentials during induction of associative long-term potentiation in hippocampal pyramidal neurons. J. Neurosci. 29, 3233–3241.

Hardingham, N., et al., 2003. Neocortical long-term potentiation and experience-dependent synaptic plasticity require alpha-

calcium/calmodulin-dependent protein kinase II autophosphorylation. J. Neurosci. 23, 4428–4436.
Hernandez, R.V., et al., 2005. Differences in the magnitude of long-term potentiation produced by theta burst and high frequency stimulation protocols matched in stimulus number. Brain Res. Brain Res. Protoc. 15, 6–13.
Heynen, A.J., Bear, M.F., 2001. Long-term potentiation of thalamocortical transmission in the adult visual cortex in vivo. J. Neurosci. 21, 9801–9813.
Hoffman, K.L., et al., 2013. Saccades during visual exploration align hippocampal 3–8 Hz rhythms in human and non-human primates. Front. Syst. Neurosci. 7, 1–10 (Article 43).
Hogsden, J.L., Rosen, L.G., Dringenberg, H.C., 2011. Pharmacological and deprivation-induced reinstatement of juvenile-like long-term potentiation in the primary auditory cortex of adult rats. Neuroscience 186, 208–219.
Holscher, C., Anwyl, R., Rowan, M.J., 1997. Stimulation on the positive phase of hippocampal theta rhythm induces long-term potentiation that can be depotentiated by stimulation on the negative phase in area CA1 in vivo. J. Neurosci. 17, 6470–6477.
Huang, Y.Z., et al., 2005. Theta burst stimulation of the human motor cortex. Neuron 45, 201–206.
Hyman, J.M., et al., 2003. Stimulation in hippocampal region CA1 in behaving rats yields long-term potentiation when delivered to the peak of theta and long-term depression when delivered to the trough. J. Neurosci. 23, 11725–11731.
Jedlicka, P., et al., 2009. Impairment of in vivo theta-burst long-term potentiation and network excitability in the dentate gyrus of synaptopodin-deficient mice lacking the spine apparatus and the cisternal organelle. Hippocampus 19, 130–140.
Jung, M.W., Larson, J., Lynch, G., 1990. Long-term potentiation of monosynaptic EPSPs in rat piriform cortex in vitro. Synapse 6, 279–283.
Kang, H., et al., 1997. Neurotrophins and time: different roles for TrkB signaling in hippocampal long-term potentiation. Neuron 19, 653–664.
Kanter, E.D., Haberly, L.B., 1990. NMDA-dependent induction of long-term potentiation in afferent and association fiber systems of piriform cortex in vitro. Brain Res. 525, 175–179.
Kelso, S.R., Brown, T.H., 1986. Differential conditioning of associative synaptic enhancement in hippocampal brain slices. Science 232, 85–87.
Kelso, S.R., Ganong, A.H., Brown, T.H., 1986. Hebbian synapses in hippocampus. Proc. Natl. Acad. Sci. USA 83, 5326–5330.
Kirkwood, A., Lee, H.K., Bear, M.F., 1995. Co-regulation of long-term potentiation and experience-dependent synaptic plasticity in visual cortex by age and experience. Nature 375, 328–331.
Kramar, E.A., et al., 2012. Synaptic evidence for the efficacy of spaced learning. Proc. Natl. Acad. Sci. USA 109, 5121–5126.
Larson, J., Lynch, G., 1986. Induction of synaptic potentiation in hippocampus by patterned stimulation involves two events. Science 232, 985–988.
Larson, J., Wong, D., Lynch, G., 1986. Patterned stimulation at the theta frequency is optimal for the induction of hippocampal long-term potentiation. Brain Res. 368, 347–350.
Larson, J., Lynch, G., 1988. Role of N-methyl-D-aspartate receptors in the induction of synaptic potentiation by burst stimulation patterned after the hippocampal theta-rhythm. Brain Res. 441, 111–118.
Larson, J., Lynch, G., 1989. Theta pattern stimulation and the induction of LTP: the sequence in which synapses are stimulated determines the degree to which they potentiate. Brain Res. 489, 49–58.
Larson, J., Ambros-Ingerson, J., Lynch, G., 1991. Sites and mechanisms for expression of long-term potentiation. In: Baudry, M., Davis, J.L. (Eds.), Long-Term Potentiation: A Debate of Current Issues. MIT Press, Cambridge, MA, pp. 121–139.
Larson, J., et al., 1999. Alterations in synaptic transmission and long-term potentiation in hippocampal slices from young and aged PDAPP mice. Brain Res. 840, 23–35.
Larson, J.R., 1987. Activity Patterns, Postsynaptic Events, and the Induction of Synaptic Plasticity in the Hippocampus. University of California, Irvine, Irvine, CA152.
Liu, M.G., et al., 2013. Long-term potentiation of synaptic transmission in the adult mouse insular cortex: multielectrode array recordings. J. Neurophysiol. 110, 505–521.
Liu, M.G., Zhuo, M., 2014. No requirement of TRPV1 in long-term potentiation or long-term depression in the anterior cingulate cortex. Mol. Brain 7, 27.
Luthi, A., et al., 1997. Endogenous serine protease inhibitor modulates epileptic activity and hippocampal long-term potentiation. J. Neurosci. 17, 4688–4699.
Lynch, G., et al., 2013. Differences between synaptic plasticity thresholds result in new timing rules for maximizing long-term potentiation. Neuropharmacology 64, 27–36.
Macrides, F., 1975. Temporal relations between hippocampal slow waves and exploratory sniffing in hamsters. Behav. Biol. 14, 295–308.
Macrides, F., Eichenbaum, H.B., Forbes, W.B., 1982. Temporal relationship between sniffing and the limbic theta rhythm during odor discrimination reversal learning. J. Neurosci. 2, 1705–1717.
Malik, R., Chattarji, S., 2012. Enhanced intrinsic excitability and EPSP-spike coupling accompany enriched environment-induced facilitation of LTP in hippocampal CA1 pyramidal neurons. J. Neurophysiol. 107, 1366–1378.
Maren, S., et al., 1994. Parallel augmentation of hippocampal long-term potentiation, theta rhythm, and contextual fear conditioning in water-deprived rats. Behav. Neurosci. 108, 44–56.
Maroun, M., Richter-Levin, G., 2003. Exposure to acute stress blocks the induction of long-term potentiation of the amygdala-prefrontal cortex pathway in vivo. J. Neurosci. 23, 4406–4409.
McCarren, M., Alger, B.E., 1985. Use-dependent depression of IPSPs in rat hippocampal pyramidal cells in vitro. J. Neurophysiol. 53, 557–571.
McCartney, H., et al., 2004. Theta reset produces optimal conditions for long-term potentiation. Hippocampus 14, 684–687.
Meighan, P.C., et al., 2007. Effects of matrix metalloproteinase inhibition on short- and long-term plasticity of schaffer collateral/CA1 synapses. J. Neurochem. 102, 2085–2096.
Moore, C.I., Browning, M.D., Rose, G.M., 1993. Hippocampal plasticity induced by primed burst, but not long-term potentiation, stimulation is impaired in area CA1 of aged Fischer 344 rats. Hippocampus 3, 57–66.
Mott, D.D., Lewis, D.V., 1991. Facilitation of the induction of long-term potentiation by GABAB receptors. Science 252, 1718–1720.
Mott, D.D., Lewis, D.V., 1992. GABAB receptors mediate disinhibition and facilitate long-term potentiation in the dentate gyrus. Epilepsy Res. Suppl. 7, 119–134.
Nettekoven, C., et al., 2014. Dose-dependent effects of theta burst rTMS on cortical excitability and resting-state connectivity of the human motor system. J. Neurosci. 34, 6849–6859.
O'Keefe, J., Nadel, L., 1978. In: The Hippocampus as a Cognitive Map. Oxford University Press, New York.
Orr, G., et al., 2001. Hippocampal synaptic plasticity is modulated by theta rhythm in the fascia dentata of adult and aged freely behaving rats. Hippocampus 11, 647–654.
Otto, T., et al., 1991. Learning-related patterns of CA1 spike trains parallel stimulation parameters optimal for inducing hippocampal long-term potentiation. Hippocampus 1, 181–192.

Please cite this article as: Larson, J., Munkácsy, E., Theta-burst LTP. Brain Research (2014), http://dx.doi.org/10.1016/j.brainres.2014.10.034

Pacelli, G.J., Su, W., Kelso, S.R., 1989. Activity-induced depression of synaptic inhibition during LTP-inducing patterned stimulation. Brain Res. 486, 26–32.

Pacelli, G.J., Su, W., Kelso, S.R., 1991. Activity-induced decrease in early and late inhibitory synaptic conductances in hippocampus. Synapse 7, 1–13.

Pan, B., Zucker, R.S., 2009. A general model of synaptic transmission and short-term plasticity. Neuron 62, 539–554.

Pan, B., et al., 2011. Alterations of endocannabinoid signaling, synaptic plasticity, learning, and memory in monoacylglycerol lipase knock-out mice. J. Neurosci. 31, 13420–13430.

Pang, P.T., et al., 2004. Cleavage of proBDNF by tPA/plasmin is essential for long-term hippocampal plasticity. Science 306, 487–491.

Patterson, S.L., et al., 2001. Some forms of cAMP-mediated long-lasting potentiation are associated with release of BDNF and nuclear translocation of phospho-MAP kinase. Neuron 32, 123–140.

Pavlides, C., et al., 1988. Long-term potentiation in the dentate gyrus is induced preferentially on the positive phase of theta-rhythm. Brain Res. 439, 383–387.

Ranck Jr., J.B., 1973. Studies on single neurons in dorsal hippocampal formation and septum in unrestrained rats. I. Behavioral correlates and firing repertoires. Exp. Neurol. 41, 461–531.

Rex, C.S., et al., 2005. Long-term potentiation is impaired in middle-aged rats: regional specificity and reversal by adenosine receptor antagonists. J. Neurosci. 25, 5956–5966.

Rojas-Líbano, D., et al., 2014. The olfactory bulb theta rhythm follows all frequencies of diaphragmatic respiration in the freely behaving rat. Front. Behav. Neurosci. 8, 1–12 (Article 214).

Roman, F., Staubli, U., Lynch, G., 1987. Evidence for synaptic potentiation in a cortical network during learning. Brain Res. 418, 221–226.

Rose, G.M., Dunwiddie, T.V., 1986. Induction of hippocampal long-term potentiation using physiologically patterned stimulation. Neurosci. Lett. 69, 244–248.

Rudell, A.P., Fox, S.E., Ranck Jr., J.B., 1980. Hippocampal excitability phase-locked to the theta rhythm in walking rats. Exp. Neurol. 68, 87–96.

Shalin, S.C., et al., 2006. Kinase suppressor of Ras1 compartmentalizes hippocampal signal transduction and subserves synaptic plasticity and memory formation. Neuron 50, 765–779.

Silva, L.R., Amitai, Y., Connors, B.W., 1991. Intrinsic oscillations of neocortex generated by layer 5 pyramidal neurons. Science 251, 432–435.

Skucas, V.A., et al., 2011. Impairment of select forms of spatial memory and neurotrophin-dependent synaptic plasticity by deletion of glial aquaporin-4. J. Neurosci. 31, 6392–6397.

Smith, J.P., et al., 2009. Stimulus pattern dependence of the Alzheimer's disease amyloid-beta 42 peptide's inhibition of long term potentiation in mouse hippocampal slices. Brain Res. 1269, 176–184.

Staubli, U., Lynch, G., 1987. Stable hippocampal long-term potentiation elicited by 'theta' pattern stimulation. Brain Res. 435, 227–234.

Staubli, U., Xu, F.B., 1995. Effects of 5-HT3 receptor antagonism on hippocampal theta rhythm, memory, and LTP induction in the freely moving rat. J. Neurosci. 15, 2445–2452.

Tsanov, M., et al., 2014. Respiratory cycle entrainment of septal neurons mediates the fast coupling of sniffing rate and hippocampal theta rhythm. Eur. J. Neurosci. 39, 957–974.

van Praag, H., et al., 1998. Unilateral hippocampal ablation at birth causes a reduction in contralateral LTP. Brain Res. 795, 170–178.

Vanderwolf, C.H., 1969. Hippocampal electrical activity and voluntary movement in the rat. Electroencephalogr. Clin. Neurophysiol. 26, 407–418.

Vickery, R.M., Morris, S.H., Bindman, L.J., 1997. Metabotropic glutamate receptors are involved in long-term potentiation in isolated slices of rat medial frontal cortex. J. Neurophysiol. 78, 3039–3046.

Welker, W.I., 1964. Analysis of sniffing of the albino rat. Behaviour 22, 223–244.

White, G., Levy, W.B., Steward, O., 1988. Evidence that associative interactions between synapses during the induction of long-term potentiation occur within local dendritic domains. Proc. Natl. Acad. Sci. USA 85, 2368–2372.

White, G., Levy, W.B., Steward, O., 1990. Spatial overlap between populations of synapses determines the extent of their associative interaction during the induction of long-term potentiation and depression. J. Neurophysiol. 64, 1186–1198.

Yeckel, M.F., Berger, T.W., 1998. Spatial distribution of potentiated synapses in hippocampus: dependence on cellular mechanisms and network properties. J. Neurosci. 18, 438–450.

Yun, S.H., Mook-Jung, I., Jung, M.W., 2002. Variation in effective stimulus patterns for induction of long-term potentiation across different layers of rat entorhinal cortex. J. Neurosci. 22, RC214.

Please cite this article as: Larson, J., Munkácsy, E., Theta-burst LTP. Brain Research (2014), http://dx.doi.org/10.1016/j.brainres.2014.10.034

APPENDIX Figure 1

Neurogenesis appears to be unaffected in subventricular zone of *Fmr1*-KO mice. Adult WT (n = 5) and *Fmr1*-KO (n = 5) mice were injected with the thymidine analog, bromodeoxyuridine (BrdU), twice a day for three days, one month before sacrifice, and then processed for immunohistochemistry. Figure 1A shows that the numbers of immature neurons and glial cells were not significantly different in Fmr1-KO and WT mice. Figure 1B provides examples of BrdU staining in the SVZ of representative *Fmr1*-KO and WT mice.

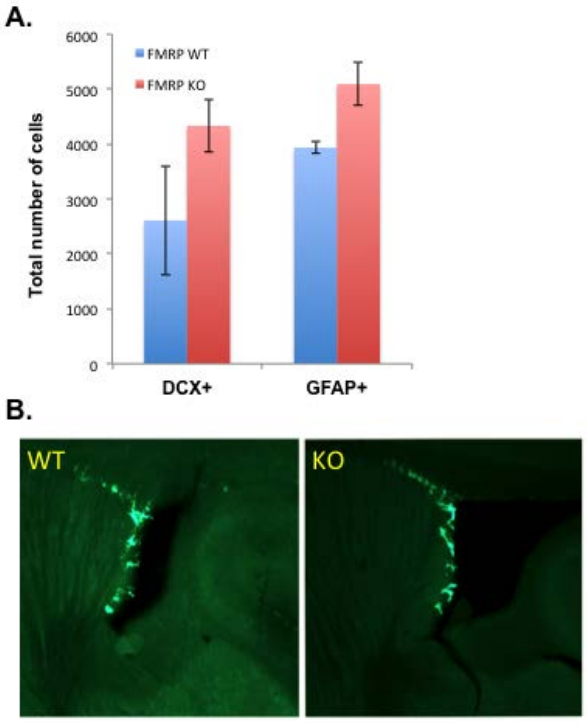

Figure 1. Quantification of neuroblasts and astrocytes in the subventricular zone of *Fmr1*-KO and WT mice. **A).** Quantitative analysis of DCX+ neuroblasts and GFAP+ astrocytes in the SVZ of *Fmr1*-KO (n = 5) and WT (n = 5) shows no significant difference between the mouse groups. **B)**. Representative confocal images of the SVZ of *Fmr1*-KO and WT mice (scale=250 μm).

Methods

Mice were perfused with 4% paraformaldehyde (PFA) and brains isolated and maintained in 4% PFA at 4°C for 48 hours, followed by 48 hours in 30% sucrose, then sagitally sectioned (50 μm) by microtome. Labeled cells were identified using fluorophore-conjugated secondary antibodies (Jackson Immunologicals) and visualized by fluorescent upright Axio Imager A1 (Zeiss, Thornwood, NY). Quantification of singly- and doubly-labeled cells was done as before (Lazarov et al., 2006) using the optical fractionator procedure for design-based stereology, using Stereo Investigator 7.0 software (MicroBrightField). Counting of cells was made at predetermined intervals (*x*= 100 μm, *y*= 100 μm) with a counting frame (75 μm x 75 μm) superimposed on the tissue section image. Section thickness was measured directly at each site with the optical dissector counting frame height (*h* = 22 μm) set at approximately 75% of mean section thickness.

APPENDIX Figure 2

Neurogenesis in subgranular layer of dentate gyrus is stimulated when Bax expression is suppressed in immature adult-generated neurons.

In NestinCreER$^{T2/+}$/Bax$^{f/+}$ mice, the survival of NPCs is enhanced by knocking down Bax in these cells exclusively by tamoxifen- regulatable recombinase CreER^{T2} that is expressed under the control of a rat 5.26 Kb nestin promoter fragment and induces the recombination of floxed-*Bax* selectively in NPC. Nestin CreER^{T2} dependent recombination is observed in type I neural stem cells (NSC) and type II NPC and their progeny in the DG of adult mice following treatment with tamoxifen, thus enhancing NPC survival. This significant increase in the survival of NPC and neurons ultimately increases neurogenesis and improves pattern separation (Sahay et al., 2011). Our preliminary results using APPswePS1ΔE9$^{DM/+}$ /nestinCreER$^{T2/+}$/Bax$^{lox/lox}$ mice treated with tamoxifen support these observations. These mice show an increase of about 2.5 fold in the number of proliferating (BrdU+) cells and a similar increase in the number of new neurons (BrdU+NeuN+) compared to vehicle-treated APPswePS1ΔE9$^{DM/+}$ /nestinCreER$^{T2/+}$/Bax$^{lox/lox}$ mice. We tested enhanced neurogenesis by conditionally ablating Bax expression in NPC. In these mice, floxed-Bax (Bax$^{lox/lox}$) and the tamoxifen regulatable nestin promoter-driven recombinase CreER^{T2} are co-expressed (nestin-CreER^{T2}/Bax$^{lox/lox}$). To make sure that these mice will breed with mice that exhibit cognitive deficits, we first bred them with mouse model of familial Alzheimer's disease (APPswePS1ΔE9/nestin-CreER^{T2}/Bax$^{lox/lox}$ mice). Our preliminary data show that nestin-CreER^{T2}/Bax$^{lox/lox}$ -induced enhanced neurogenesis in these mice (Figure 2).

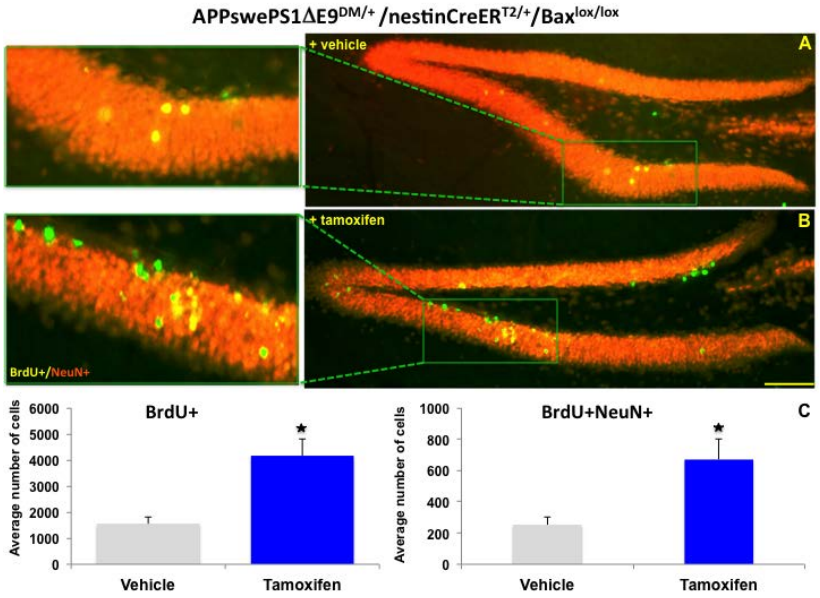

Figure 2. More new granule neurons in the dentate gyrus of tamoxifen-treated APPswePS1ΔE9$^{DM/+}$/nestinCreER$^{T2/+}$/Bax$^{lox/lox}$ mice. **A)**, **B)** Confocal images of BrdU+ cells in the dentate gyrus of vehicle (A) or tamoxifen (B)-treated APPswePS1ΔE9$^{DM/+}$ /nestinCreER$^{T2/+}$/Bax$^{lox/lox}$ mice one month following BrdU injection. Areas with relatively higher number of BrdU+ cells in each animal are enlarged as an insert [BrdU+ cells (green), NeuN+ neurons (orange), BrdU+NeuN+ new neurons (yellow)]. **C)** Quantitative analysis (N=3) of the survival rate of proliferating cells (BrdU+) and new neurons (BrdU+NeuN+) in these vehicle- and tamoxifen- treated mice (*t*-test, **p*<0.05). Scale bar in B: 125 μm.

APPENDIX Figure 3

Stimulation of hippocampal neurogenesis improves memory in an object recognition task.

Our preliminary data show that nestin-CreER^{T2}/Bax$^{lox/lox}$ -induced enhanced neurogenesis rescued learning and memory impairments in the novel object recognition task in tamoxifen-treated APPswePS1ΔE9/nestin-CreER^{T2}/Bax$^{lox/lox}$ mice. Specifically, examination of exploratory preference of mice in the Novel Object Recognition test showed that APPswePS1ΔE9 alone exhibit impaired preference of the novel object (Figure 3). Intriguingly, tamoxifen-treated APPswePS1ΔE9$^{DM/+}$/nestinCreER$^{T2/+}$/ Bax$^{lox/lox}$ mice that show increased neurogenesis exhibit clear preference for the novel object.

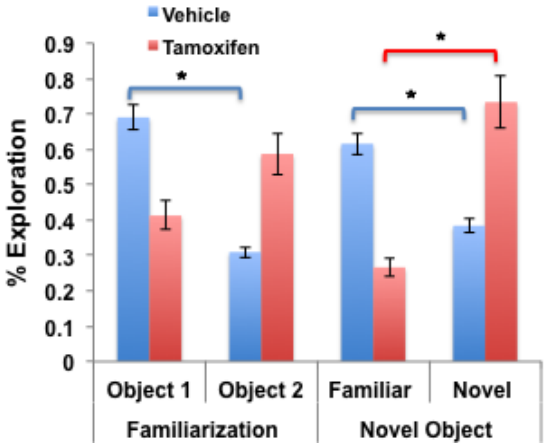

Figure 3. Association between extent of neurogenesis and exploratory preference. Vehicle- or tamoxifen-treated APPswePS1ΔE9$^{DM/+}$/nestin-CreER$^{T2/+}$/ Bax$^{lox/lox}$ mice were subject to novel object recognition test. Mice with enhanced neurogenesis exhibit clear preference for the novel object, suggesting that enhanced neurogenesis rescues impaired exploratory preference (n = 3, ANOVA, p<.05).

APPENDIX Figure 4

Comparison of LTP induced by high frequency bursts repeated at theta frequency (5 Hz) and a non-theta frequency (1 Hz) in hippocampal field CA1 of WT and *Fmr1*-KO mice
(P. Dykas, S. Corwin, & J. Larson, unpublished data).

Hippocampal slices were prepared from WT (n = 11) and *Fmr1*-KO (n = 7) mice and a recording electrode placed in stratum radiatum of Field CA1b to monitor field excitatory postsynaptic potentials (fEPSPs). Stimulation electrodes were placed in stratum radiatum of field CA1a and CA1c to activate separate sets of afferent synapses. The two synaptic pathways were stimulated alternately at 10 sec intervals for 13 minutes before and 70 minutes after episodes of LTP-inducing stimulation. One of the two pathways in each slice was randomly selected to receive high frequency bursts at 5 Hz (theta-burst stimulation); the other was stimulated with the same number of bursts at 1 Hz. At least 30 min separated the 5 Hz and 1 Hz stimulation episodes. LTP was quantified as the degree of potentiation of fEPSP slope 60 minutes after burst stimulation. The average results from all slices are plotted in Figure 4.

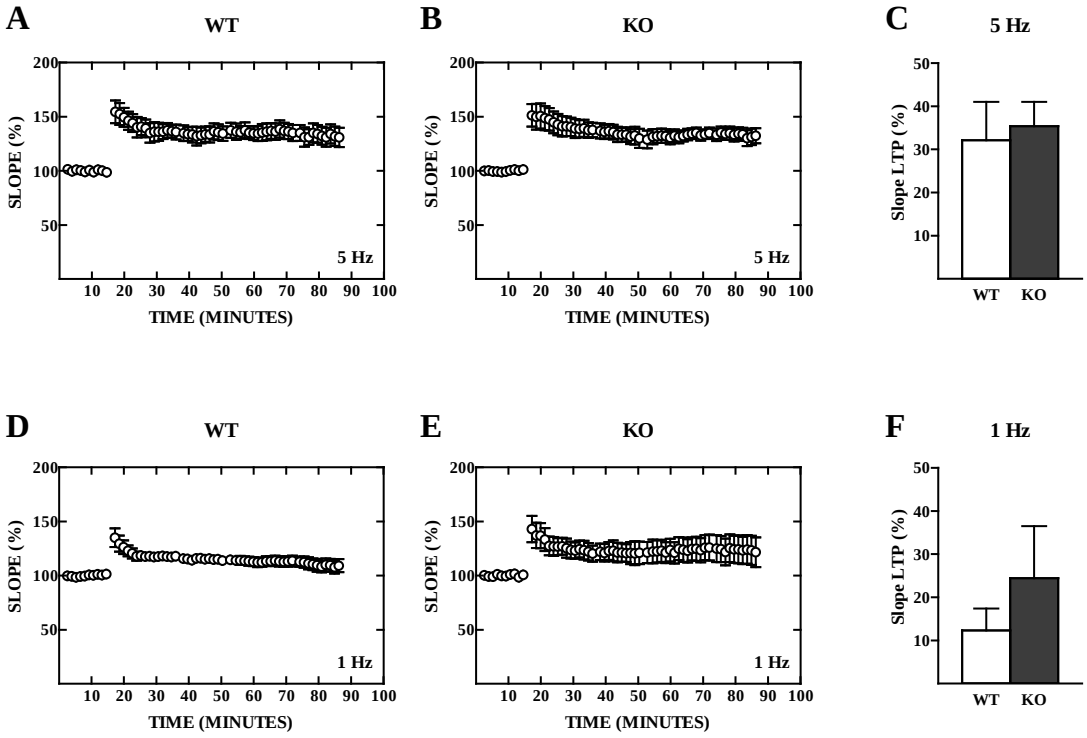

Figure 4. LTP after ten high frequency bursts repeated at 5 Hz (standard theta-burst stimulation) or 1 Hz in WT and *Fmr1*-KO mice. **A)** fEPSP slope recorded before and after 5 Hz bursts in slices from WT mice (n = 11). The graph shows mean (± s.e.m.) for 11 experiments, each for a different mouse. **B)** As in (A), for 7 experiments, each from a different *Fmr1*-KO mouse. **C)** Histograms show mean (+ s.e.m.) potentiation measured 60 minutes after burst stimulation at 5 Hz. There was no significant difference in LTP in WT and KO mice (t_{16} = 0.35, p>.70). **D)** As in (A), but for bursts repeated at 1 Hz in the same WT slices shown in (A). **E)** As in (D), but for 1 Hz bursts in the same *Fmr1*-KO slices shown in (B). **F)** Histograms show mean (+ s.e.m.) potentiation measured 60 minutes after burst stimulation. The difference between WT and KO was not statistically significant (t_{16} = 1.06, p>.30).

APPENDIX Figure 5

Olfactory learning up-regulates NMDA receptor expression in hippocampus.
(J. Sotto, A. Kirchner, G. Lugli, N.R. Smalheiser, & J. Larson, unpublished data)

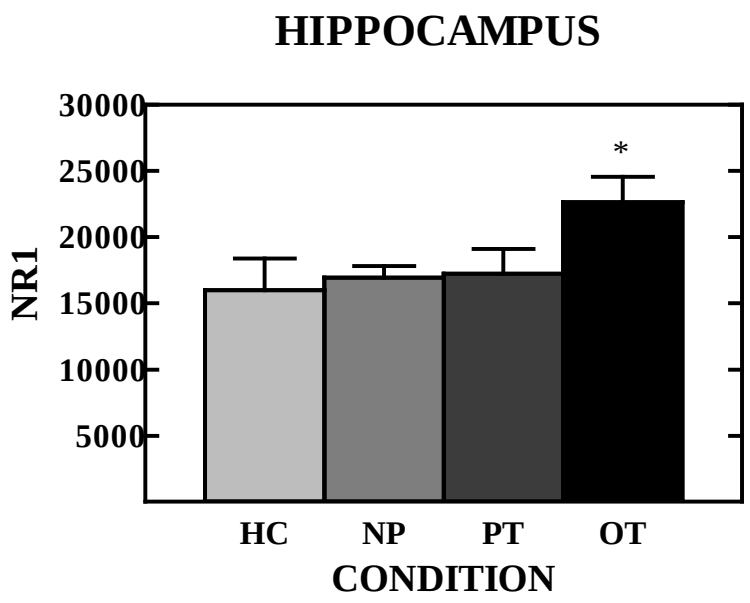

Figure 5. NMDA receptor expression in hippocampus is elevated after olfactory discrimination training in WT mice. Immunoblots using GluN1 antibody were quantified densitometrically for eight mice in each training group (mean + s.e.m.). The odor discrimination training group (OT) showed higher average GluN1 (NR1, arbitrary units) expression than the other three groups. The data were analyzed by analysis of variance, showing a significant main effect of training condition ($\mathbf{F}_{3,21} = 3.11$, $p<.05$). Post-hoc test using Dunnett's method showed that odor discrimination training (OT) resulted in higher GluN1 expression than the home cage (HC) control group (*: $p<.05$), but that the other control groups (nose poke, NP and pseudo-training, PT) did not differ from HC.